Search for Soft Unclustered Energy Patterns with muons at the LHC and studies of radiation damage in plastic scintillators

Christos Papageorgakis (University of Maryland)

SLAC FPD experimental seminar

12/18/2025

U.S. DEPARTMENT OF ENERGY | Office of Science

Work partially supported by DOE HEP under award DE-SC0010072

Outline of this talk

- **Part 0:** Introduction to Standard Model, LHC, and CMS
- **Part I:** Detector R&D.

  Studies of radiation damage in plastic scintillators.
- **Part II:** Search for Beyond the Standard Model (BSM) physics.

  Search for Soft Unclustered Energy Patterns at the LHC.

The Standard Model of Particle Physics

Or, why is it interesting to collide subatomic particles at high energies?

The Standard Model of particle physics

- Ordinary matter consists particles with **spin-$\frac{1}{2}$ (fermions)**.
- The 24 fermions consist of:
  - 6 **quarks** (u, d, s, c, b, t),
  - 6 **leptons** (e, μ, τ, and their neutrinos),
  - And their 12 **anti-particle** partners.
- The three forces are facilitated by particles with **spin-1 (bosons)**:
  - **Strong force:** gluons (g)
  - **Weak force:** $W^{\pm}$, Z bosons
  - **Electromagnetic force:** photons (γ)
- Plus, one bonus particle:
  - a spin-0 boson (scalar)
    → the **Higgs boson**!

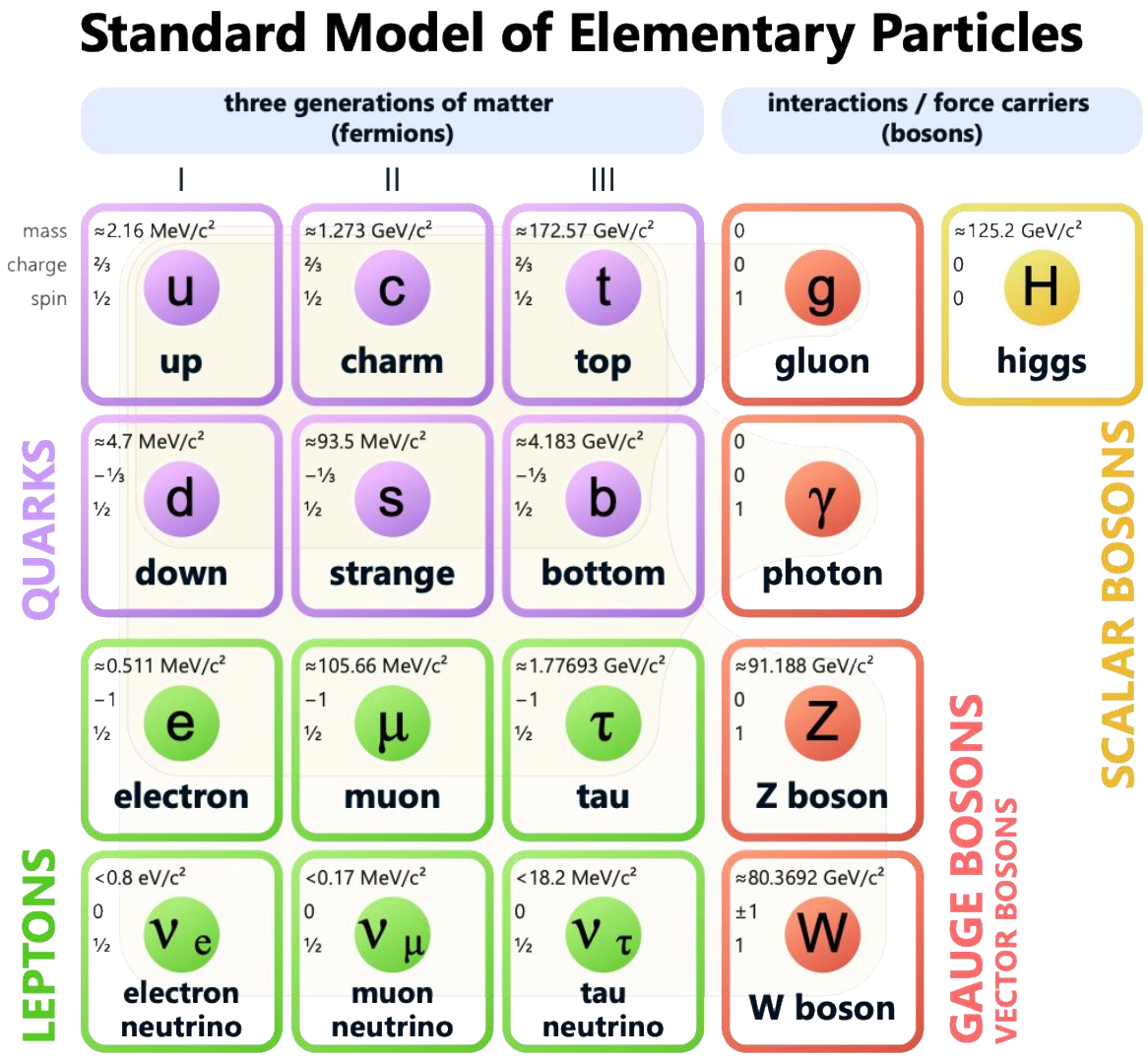

Is this the end?

Spoiler alert: not quite…

The Standard Model doesn't explain everything

Various open questions:

- What's the nature of **gravity** at the *quantum level*?
- **Hierarchy problem**: Why is the weak force so stronger than gravity?
- **Matter-antimatter asymmetry**: Why matter dominates this world?

But we also have **experimental anomalies**:

- We have observed that **neutrinos oscillate** between their flavors.
- This could be explained by a **neutrino mass**.
- However, the SM can't accommodate this…
- Yukawa couplings require both left and right-handed chiral components to assign a mass.
- We have discovered only left-handed neutrinos thus far…

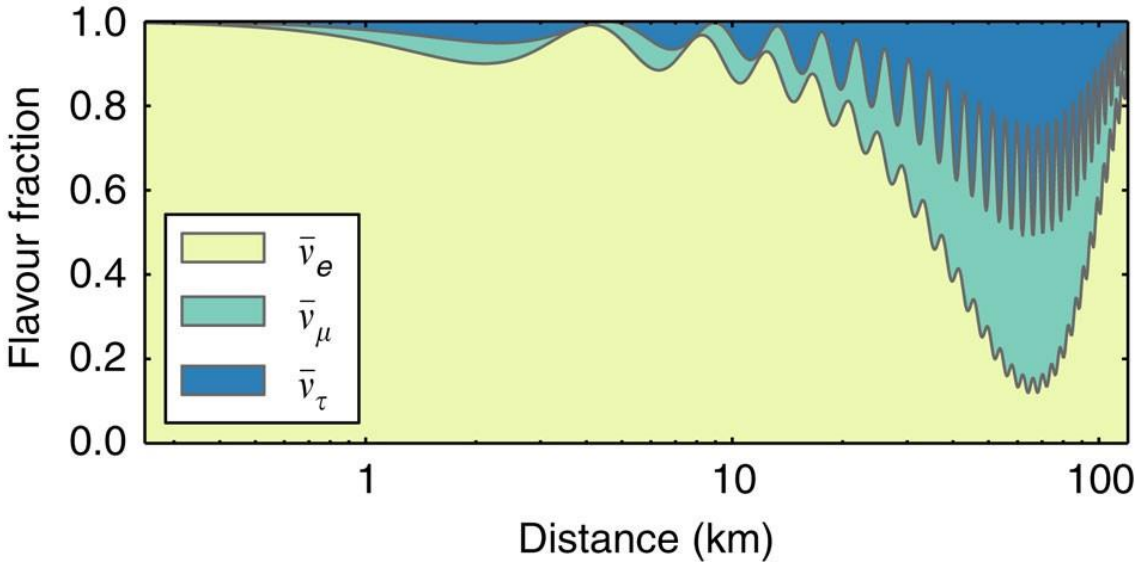

Dark matter

Numerous experimental results point to unknown matter:

- Anomalous galaxy rotation curves
- Gravitational lensing (i.e., Bullet Cluster)
- CMB anisotropies → **best explained by ΛCDM**

Predicts that 27% of the universe is cold dark matter!

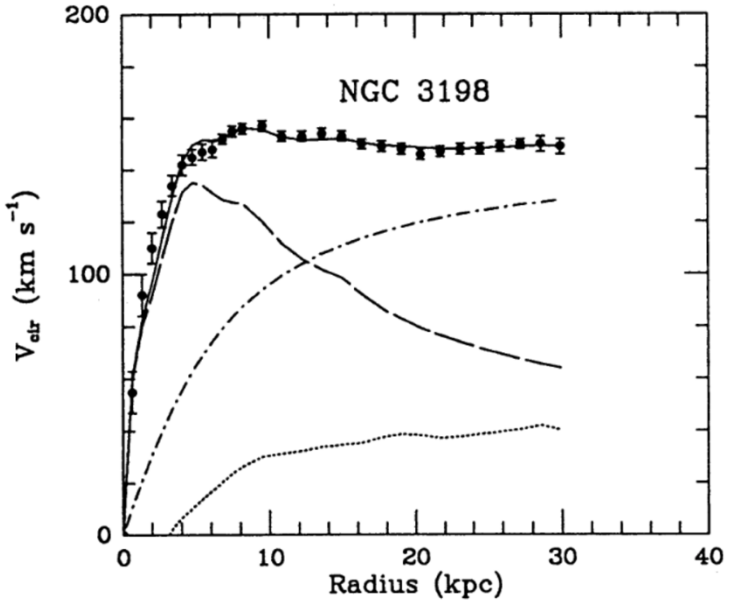

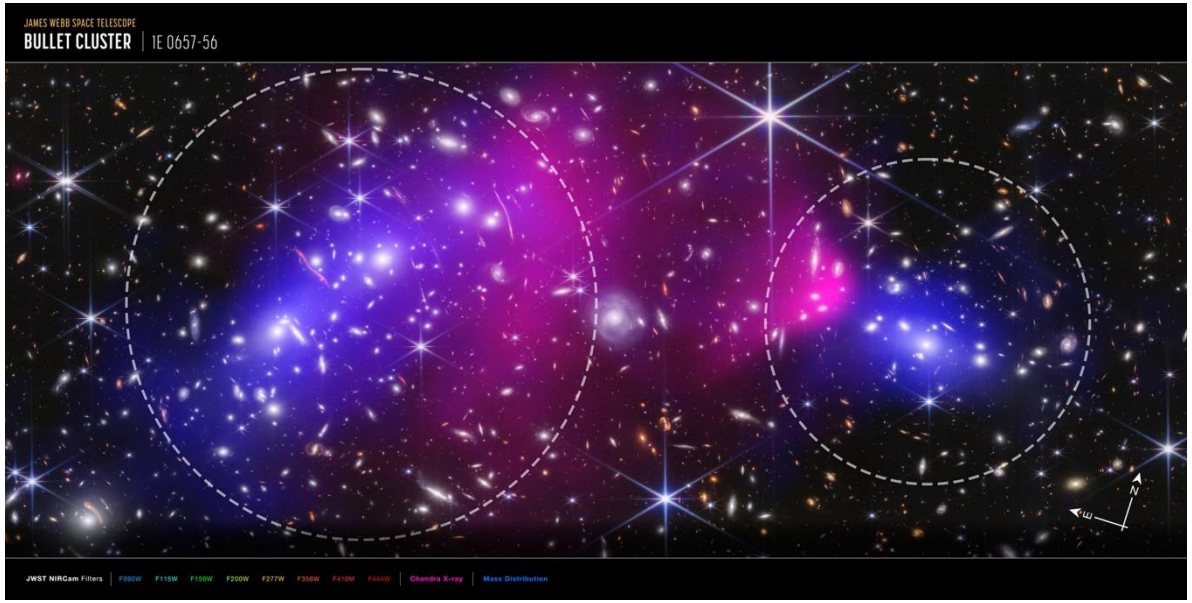

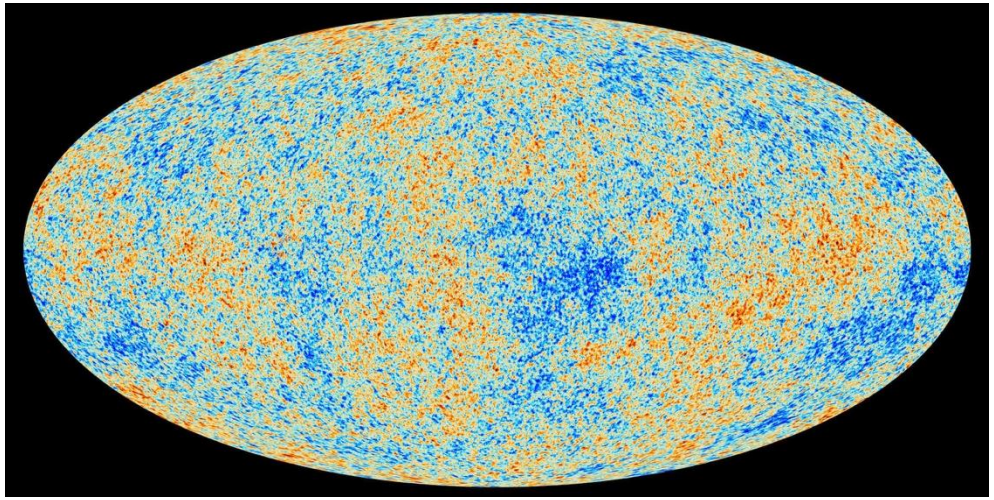

How do we test the SM and search for new physics?

The Large Hadron Collider

The work I will present today is related to the **Large Hadron Collider (LHC)**:

- most powerful particle collider in operation,
- underground ring at ~ 100 m depth,
- perimeter 26.7 km,
- 4 Interaction Points (IP) hosting physics experiments:

  ATLAS, ALICE, CMS, and LHCb
- charged particles collide heads-on at unprecedented energies.

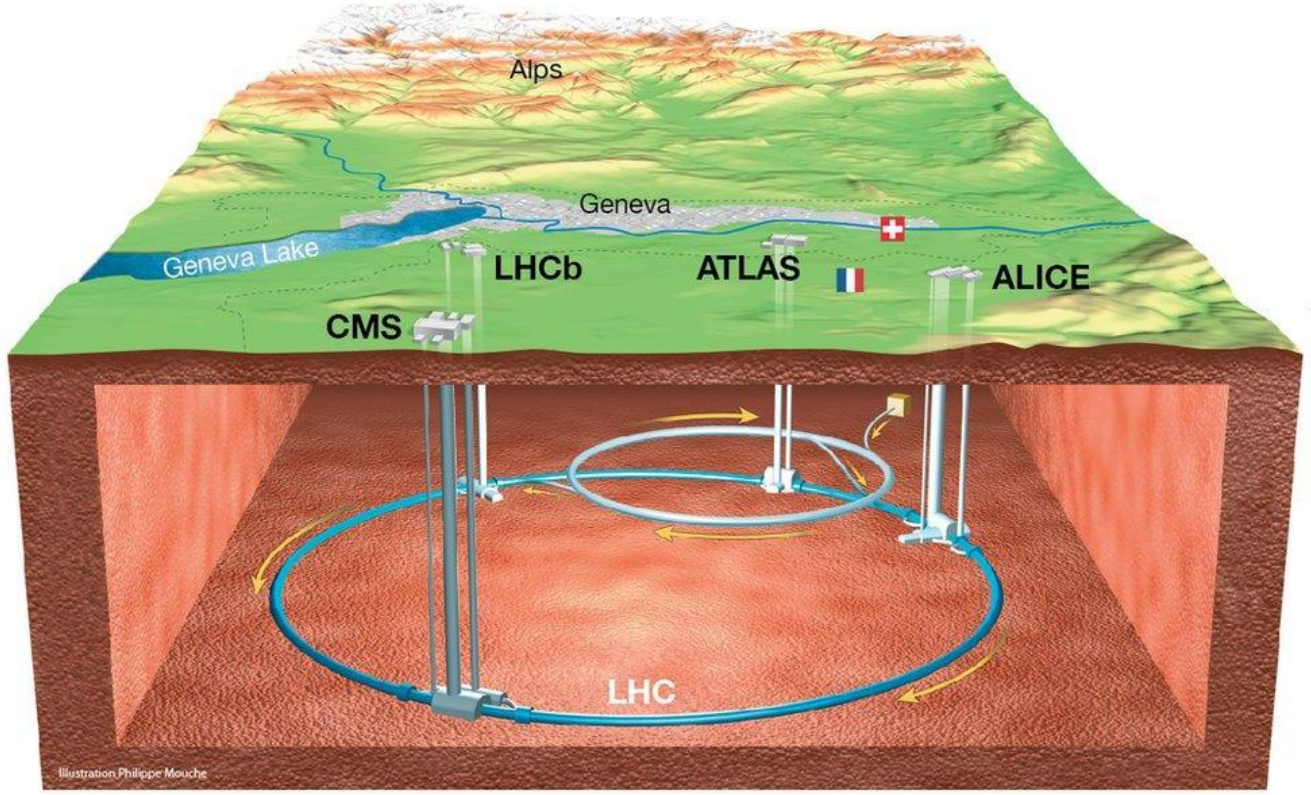

The Compact Muon Solenoid experiment

- Particle detection can be separated into two broad categories:
  - **Trackers:** Record the particle trajectories.
  - **Calorimeters:** Measure their energies.
- CMS has two trackers:
  - the **inner tracking system**
  - the **muon system**
- and two calorimeters:
  - the **Hadron Calorimeter (HCAL)**
  - the **Electromagnetic calorimeter (ECAL)**

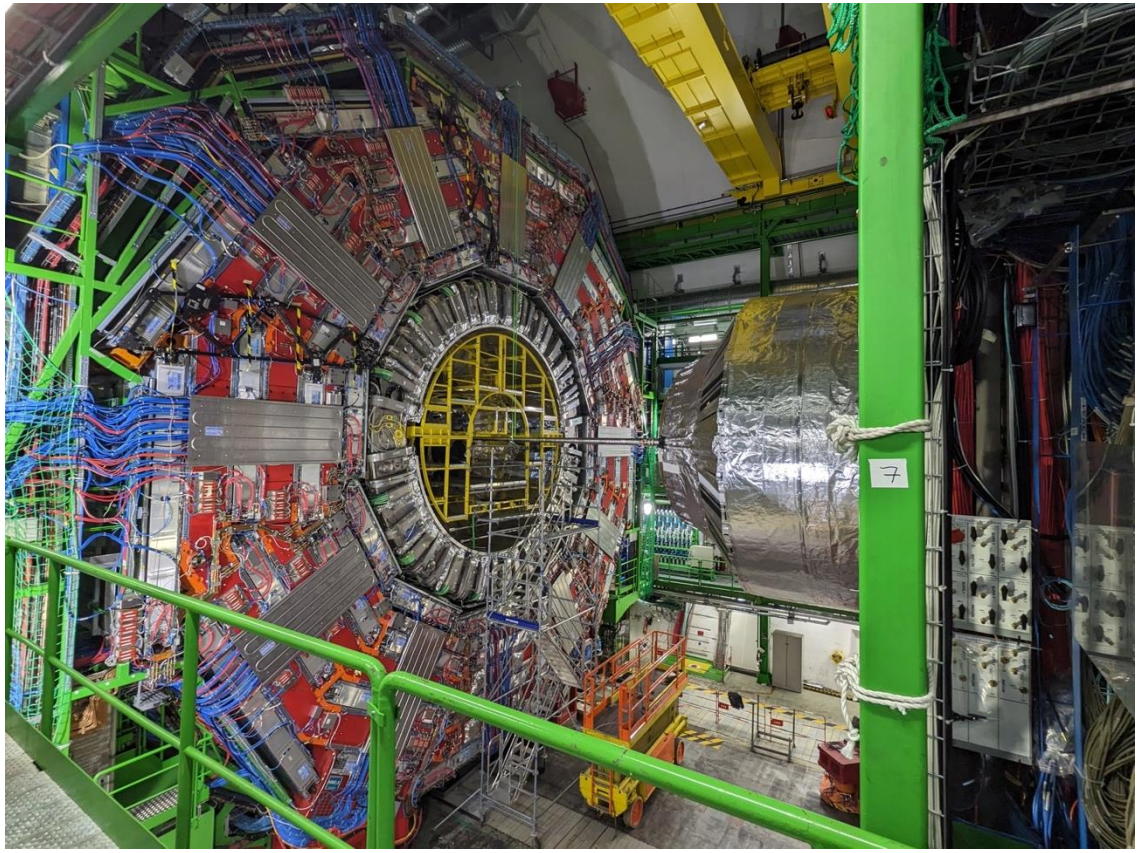

Picture was taken from the visitor balcony on 01/19/2023 during the YETS.

Tracking

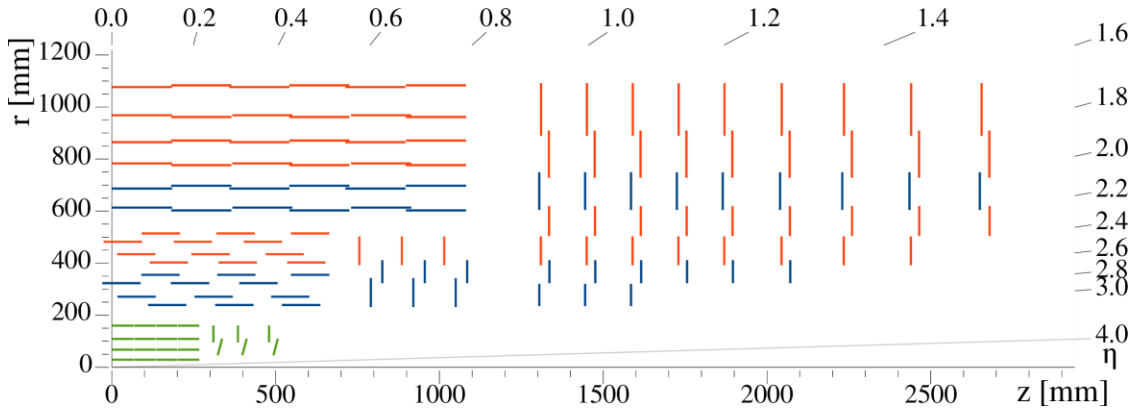

- The **tracker** and the **pixel detector**.
- Made entirely out of silicon.

- The **muon tracking system**.
- Consists of four subsystems:
  - **DT**
  - **CSC**
  - **RPC**
  - **GEM**

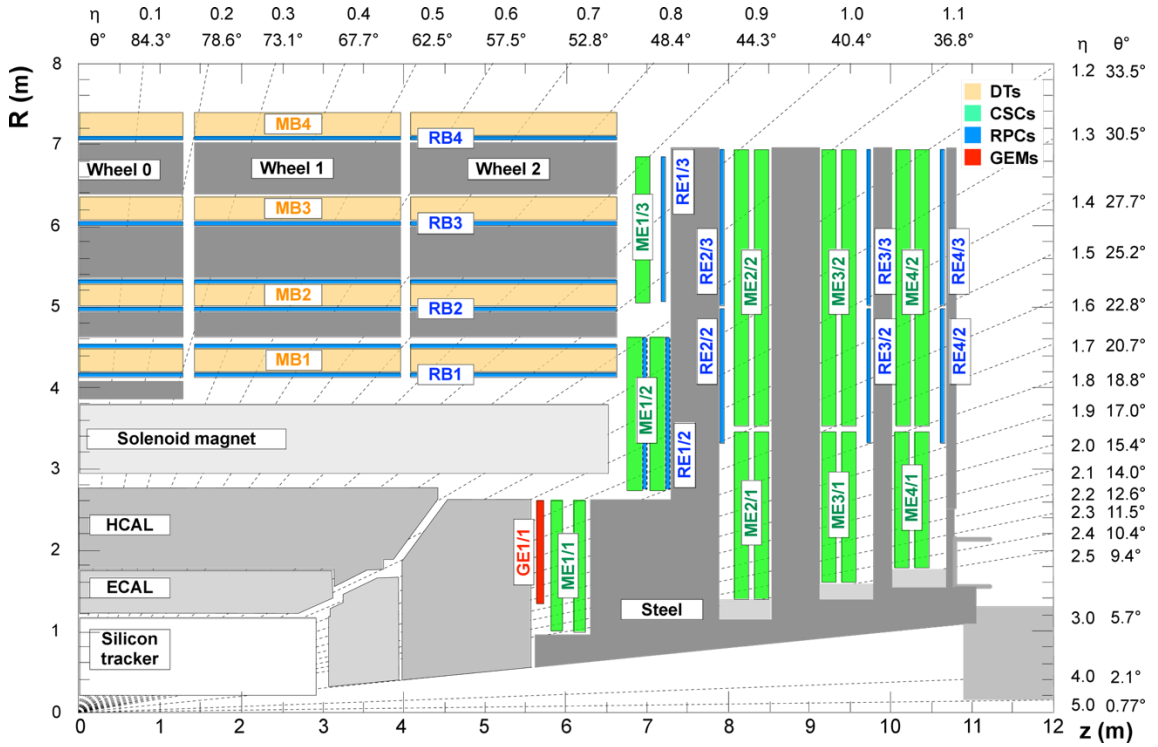

Calorimetry

- The **Electromagnetic Calorimeter (ECAL)**.
- Made of $PbWO_4$ scintillator crystals.

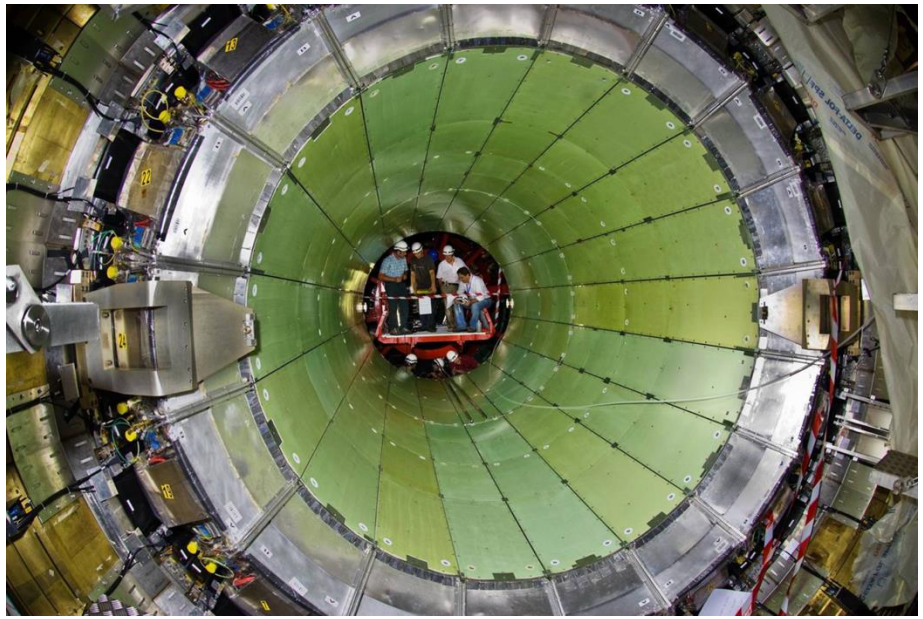

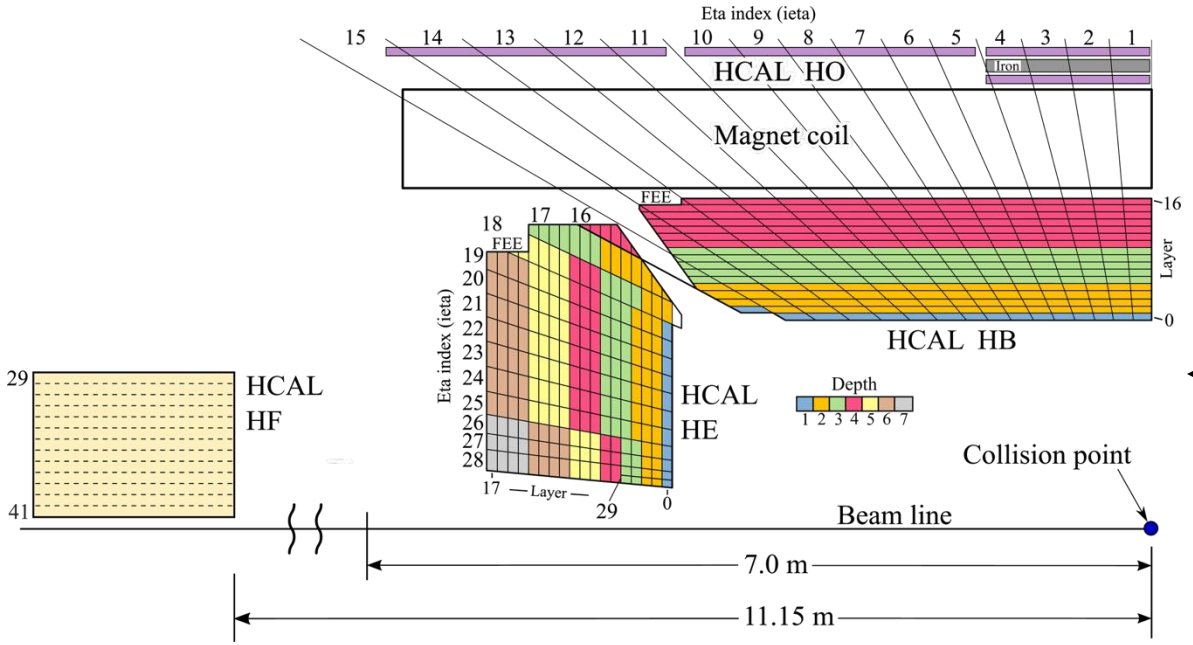

- The **Hadron Calorimeter (HCAL)**.
- Made of brass and plastic scintillators.

How it works

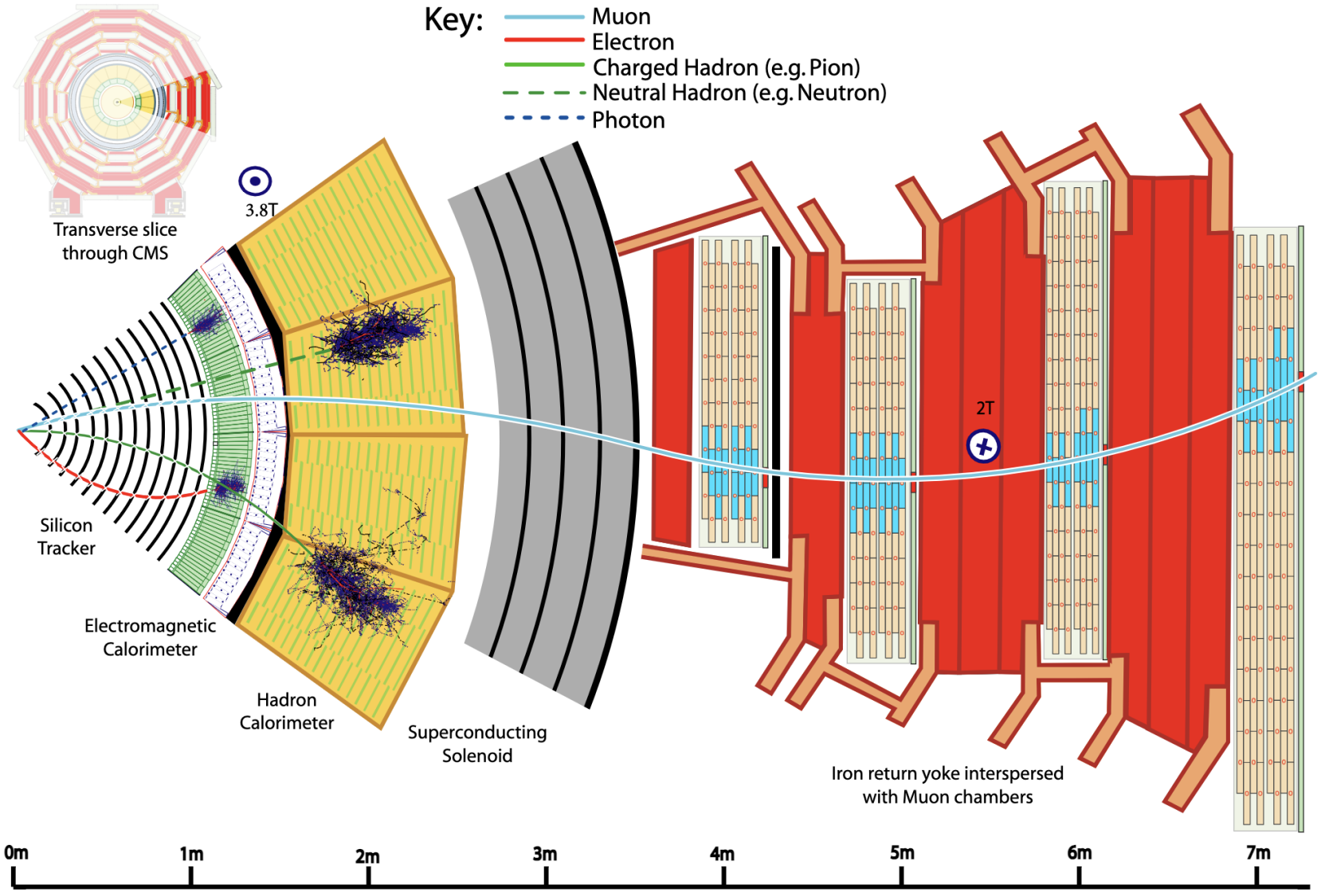
Key:
Muon
Electron
Charged Hadron (e.g. Pion)
Neutral Hadron (e.g. Neutron)
Photon
Transverse slice through CMS
3.8T
2T
Silicon Tracker
Electromagnetic Calorimeter
Hadron Calorimeter
Superconducting Solenoid
Iron return yoke interspersed with Muon chambers
0m
1m
2m
3m
4m
5m
6m
7m

Phase-2 upgrades

- Phase-2 upgrades are set to commence installation next year.
- Calorimetry is getting a lot of attention → **High Granularity Calorimeter (HGCAL)**
- Sampling endcap calorimeter made out silicon and scintillator.
- Will offer 5-D hit information (x, y, z, t, E).
- Other Phase-2 upgrades:
  - ✓new timing layer,
  - ✓improved tracking & vertexing,
  - ✓higher trigger bandwidth,
  - ✓tracking at L1,
  - ✓and more!

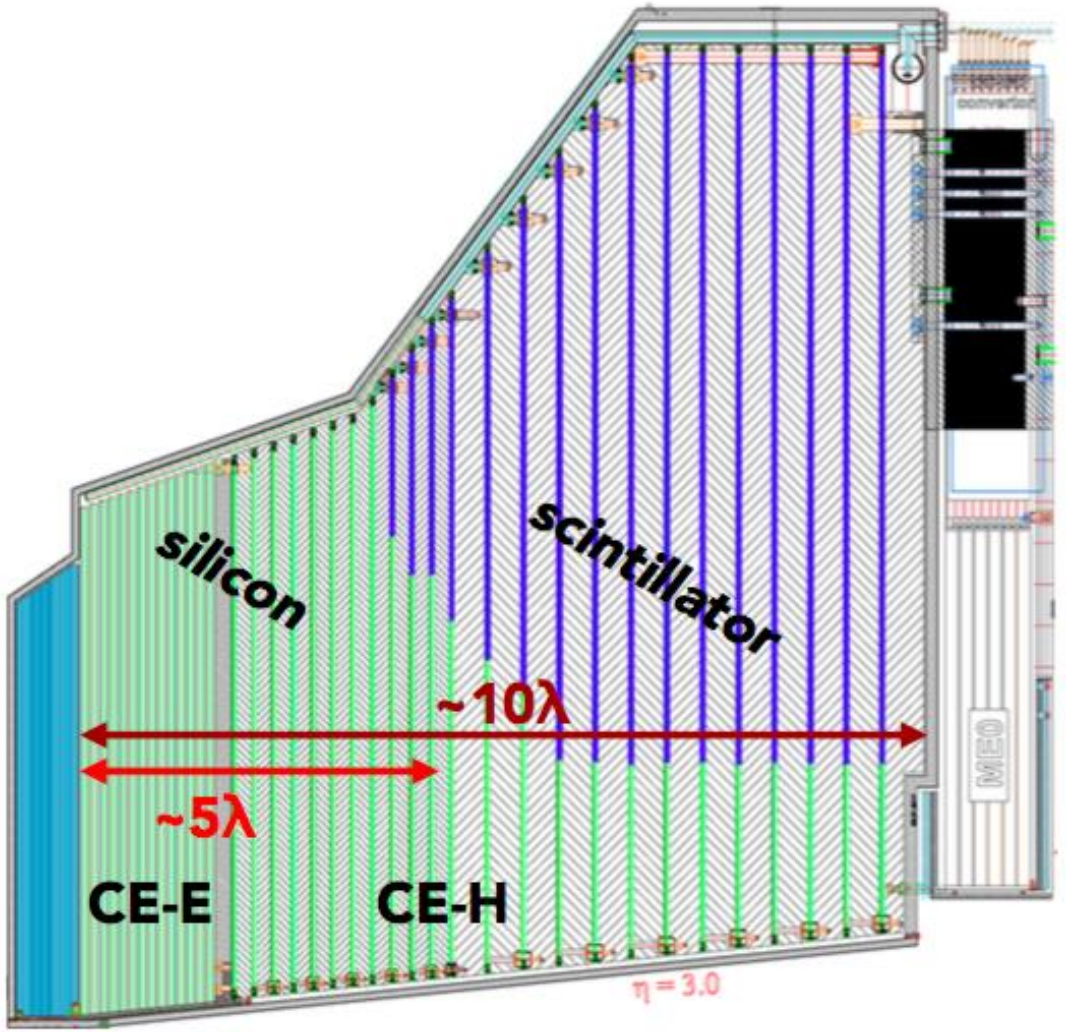

Part I: Detector R&D

Plastic scintillators and radiation hardness

Publications:

1) Papageorgakis, C., Al-Sheikhly, M., Belloni, A., Edberg, T. K., Eno, S. C., Feng, Y., Jeng, G. Y., Kahn, A., Lai, L., McDonnell, T., Mohammed, M., Palmer, C., Perez-Gokhale, R., Ricci-Tam, F., Yang, Z., Yao, Y. (2022). *Dose rate effects in radiation induced changes to phenyl-based polymeric scintillators*, Nucl. Instrum. Methods Phys. Res. A 1042, 167445.
2) Papageorgakis, C., Aamir, M. Y., Belloni, A., Edberg, T. K., Eno, S. C., Kronheim, B., Palmer, C. (2024). *Effects of oxygen on the optical properties of phenyl-based scintillators during irradiation and recovery*. Nucl. Instrum. Methods Phys. Res. A 1059, 168977.

What is a scintillator

Scintillation: process of UV or visible light emission following the absorption of ionizing radiation.

Two main categories:

Inorganic crystals

Most typical examples:
NaI(Tl), CsI(Tl), BGO, $PbWO_4$, LYSO

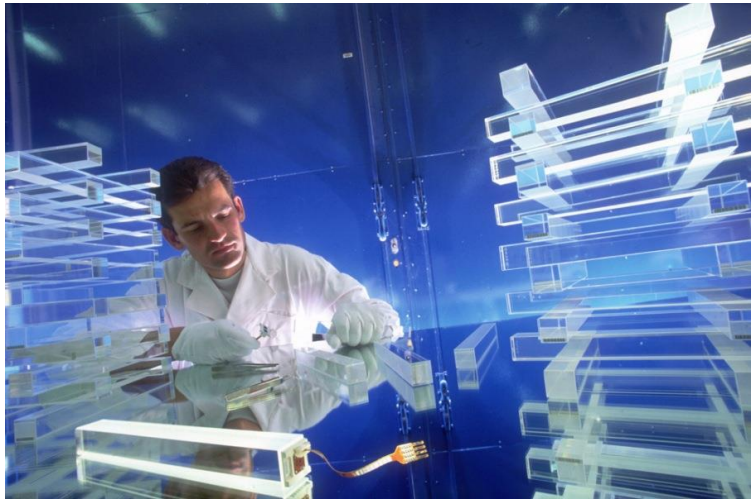

Organic materials

Usually either organic liquids or **plastics**.

Our focus today

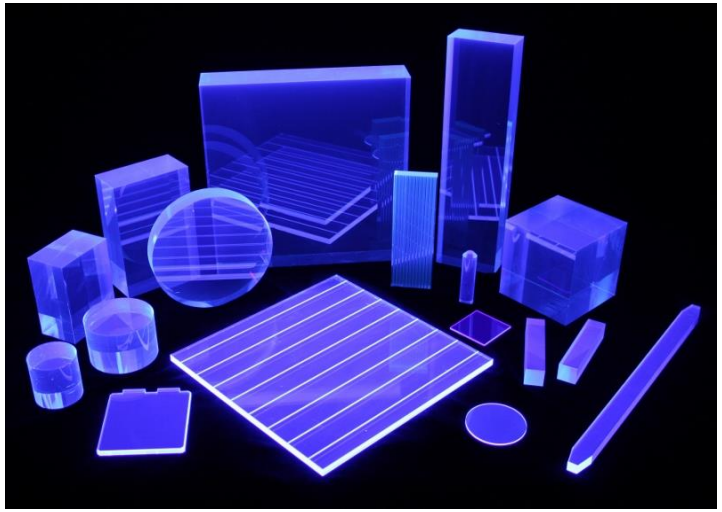

Plastic scintillators in HEP

Many **experiments** are using them or planning to use them:

- **CMS**
  - HCAL
  - HGCAL
- **ATLAS**
  - TileCal

Future experiments considering their use:

E.g., **FCC-ee**: the **IDEA** detector (in the form of scintillating fiber)

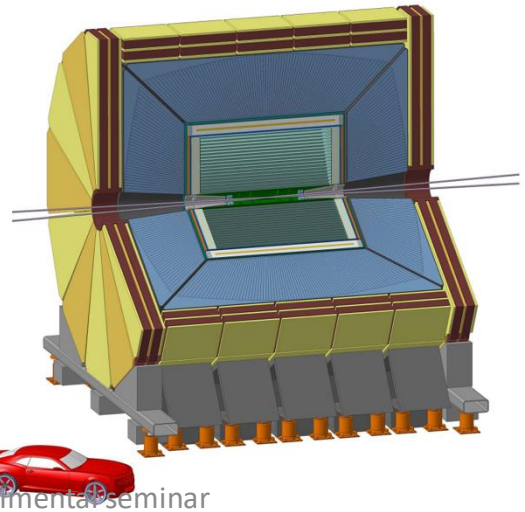

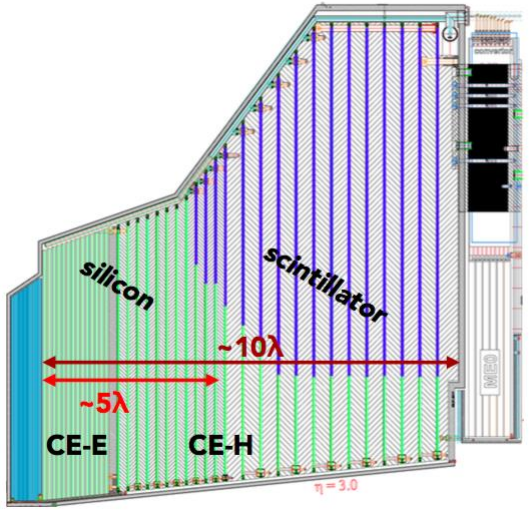

Importance of radiation hardness

- Radiation tolerance has been important for applications with **high particle fluxes**. (doses > 10^3 Gy)
- At CMS, during the 50 fb^{-1} running at 13 TeV in 2017, the HE tiles received **doses up to a few kGy**.

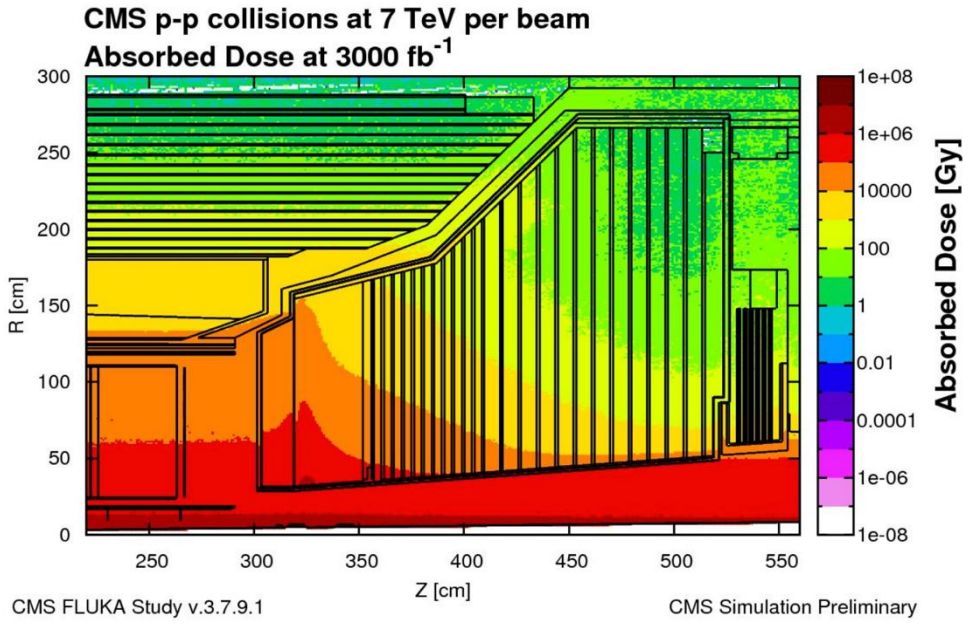

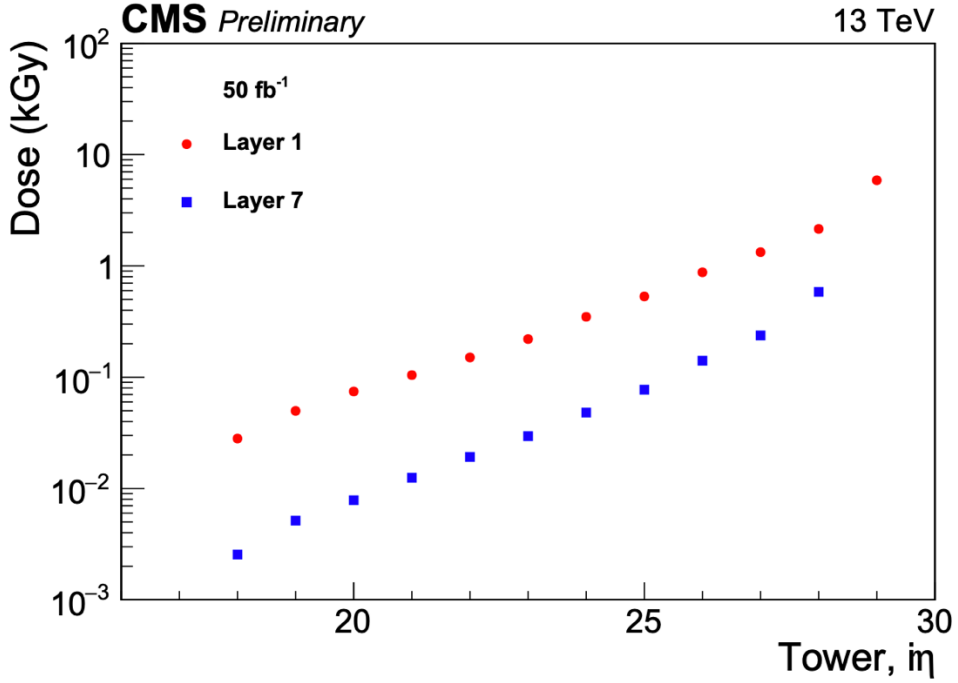

- Typical dose rates from **10^{-3} to 1 Gy/h**.
- During the HL-LHC run, the HGCal detector's scintillator is expected to absorb **doses up to O(100 kGy)**.

Reaching high doses using low dose rates is very interesting!

Plastic scintillators – structure

Plastic scintillators consist of:

- **Substrate material:** Common choices include:

polystyrene (PS)

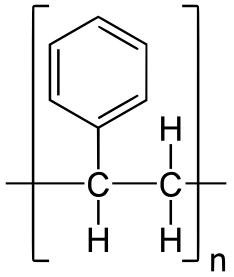

polyvinyl toluene (PVT)

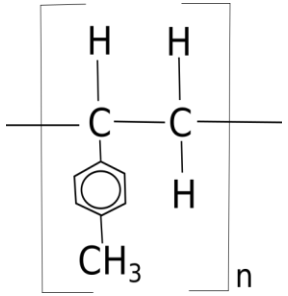

- **Dopants:**

  - **Primary fluors**, like:

p-terphenyl (PTP)

BPBD

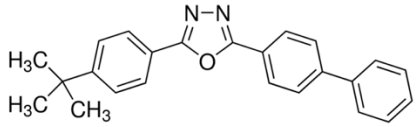

  - **Secondary fluors**, like:

POPOP

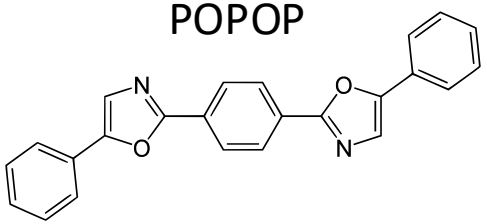

Importance of the phenyl group

- All the materials shown are **aromatic compounds**.
- They contain **benzene rings** 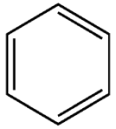
- Bonds are:
  - σ-bonds with sp^2 hybridized electrons and
  - delocalized π-bonds with p_z electrons
- All the interesting properties arise from the **π-electron** orbitals.

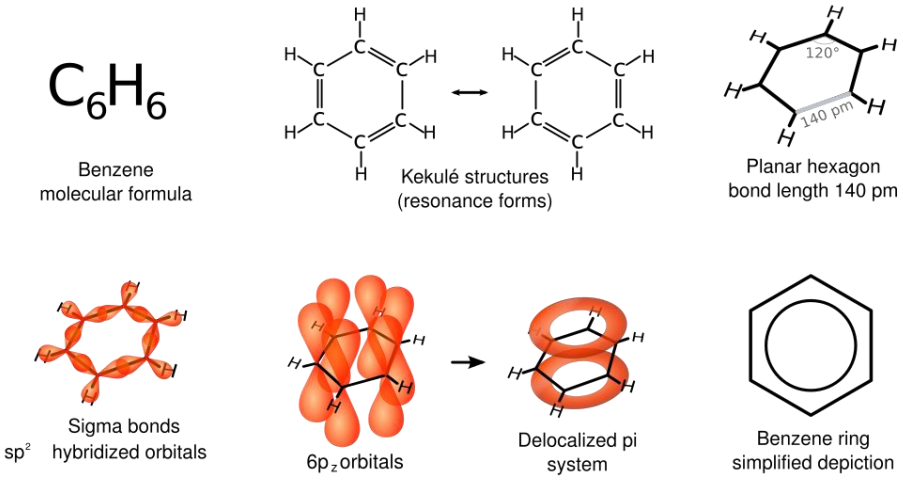

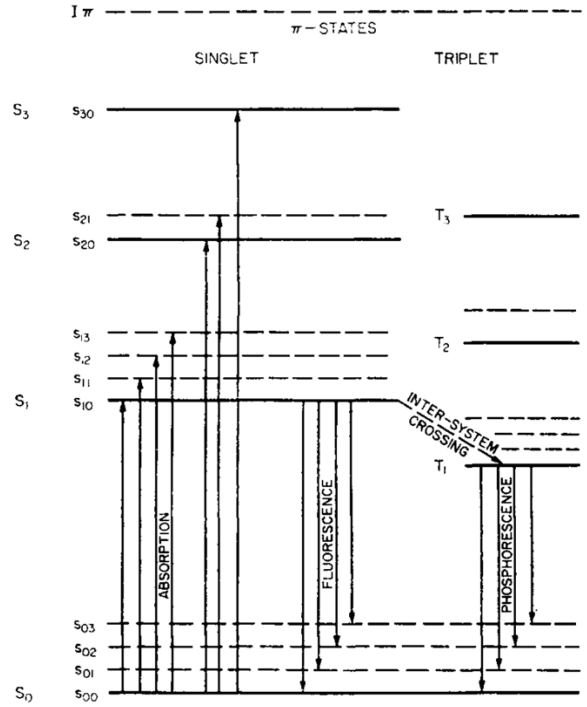

Scintillation:

- excitation/ionization of π electrons
- move between singlet & triplet states
- fluorescence/phosphorescence
- Stoke's shift between absorption/emission spectra

Plastic scintillators – inner workings

The **scintillation process** for a particle that enters the scintillator follows these steps:

1. The particle **excites/ionizes** the the electrons of the substrate.
2. Energy transfer from substrate to primary fluor:
   i. Non-radiative transfer through the **Förster mechanism**.
   ii. Radiative transfer
3. Primary fluor **emits** photon.
4. Secondary fluor **absorbs** photon from primary and **reemits** at different wavelength.
5. Detection of **secondary fluor emission** with photodetector.

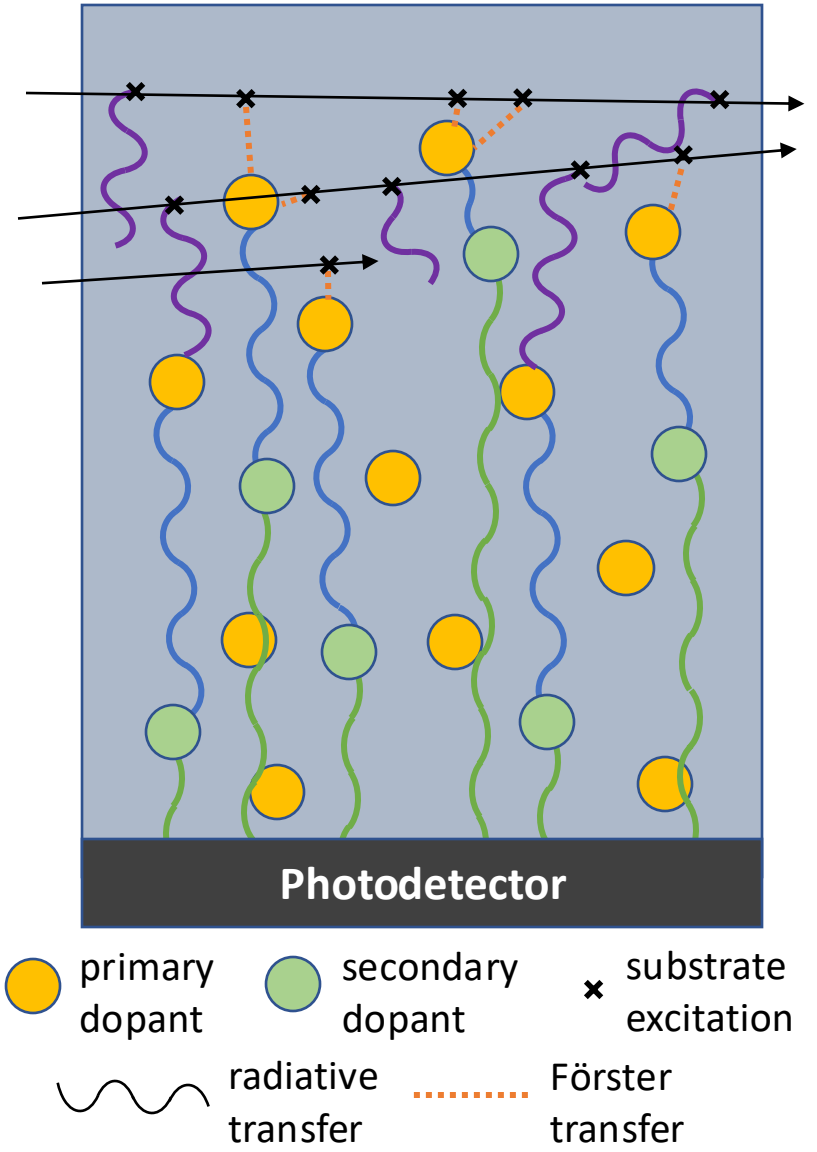

Radiation damage

Mechanisms for **radiation damage** can be categorized as follows:

- Decrease in the **initial light production**
  - ➢Fluor destruction
  - ➢Absorption of light between primary and secondary fluors.
  - ➢Suppression of Förster mechanism.
- Formation of **color centers**
  - ➢Absorption of light emitted from the secondary fluor.

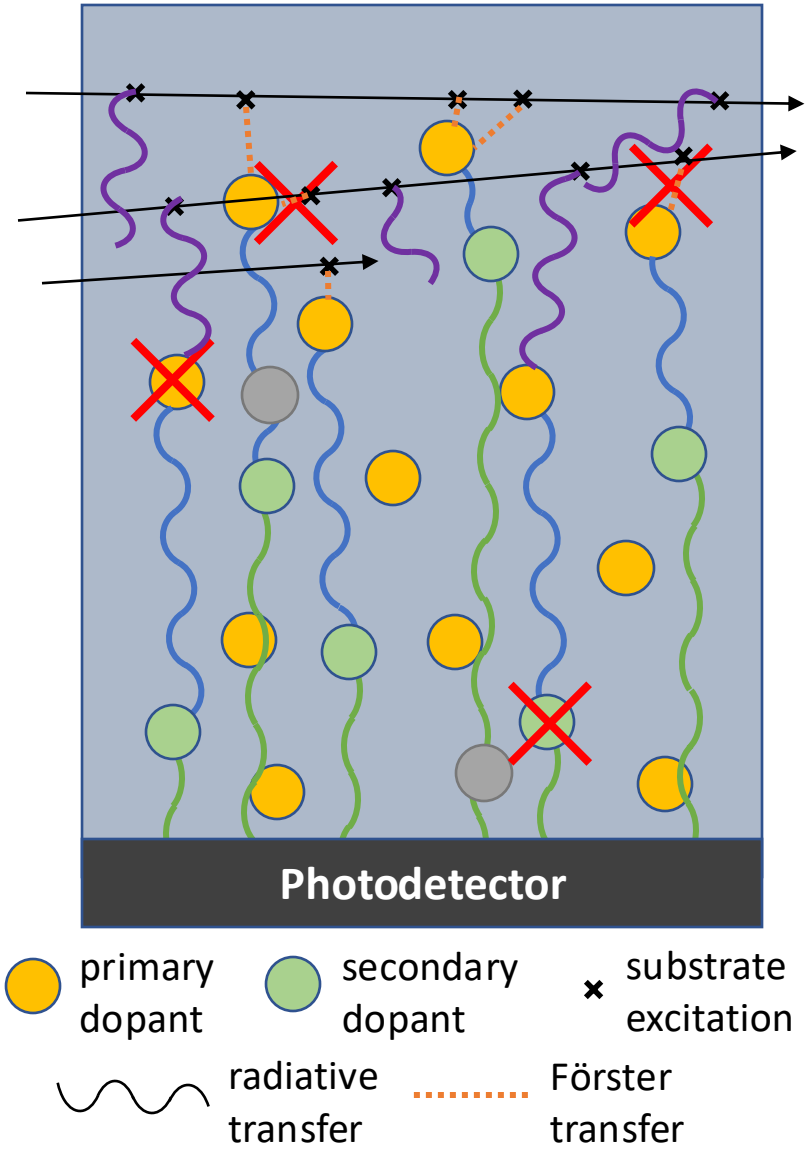

Radiation damage versus thickness

- Decrease in the **initial light production**
  - ➢Fluor destruction
  - ➢Absorption of light between primary and secondary fluors.
  - ➢Suppression of Förster mechanism.
- Formation of **color centers**
  - ➢Absorption of light emitted from the secondary fluor.

Differences:

- ❖**Color centers:** dependence on thickness
- ❖**Initial LY decrease:** independent of thickness

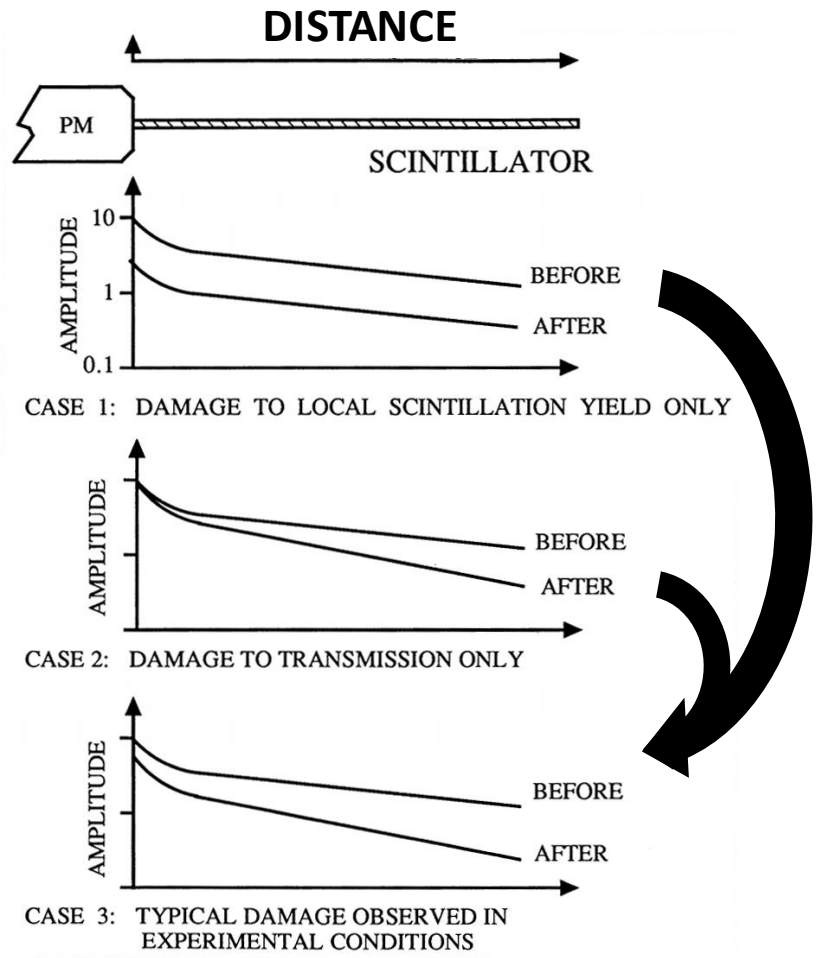

Samples & Irradiations

- Our samples are **scintillating rods** supplied by Eljen Technology (EJ-200 & EJ-260).
- EJ-200 has blue and EJ-260 green-emitting fluors.
- Green expected more rad-hard since color center formation expected much larger at shorter λ.

- Rods vary in **width, matrix material, concentrations of fluors** and **antioxidants**.

- Performed irradiations at **three different facilities**.

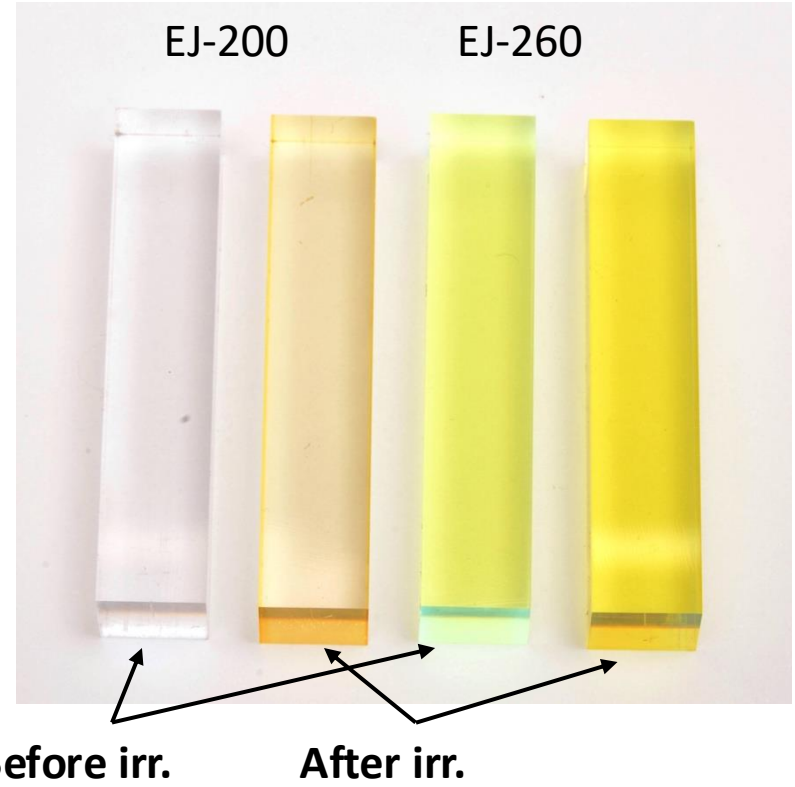

Recovery process

Days after irradiation end:

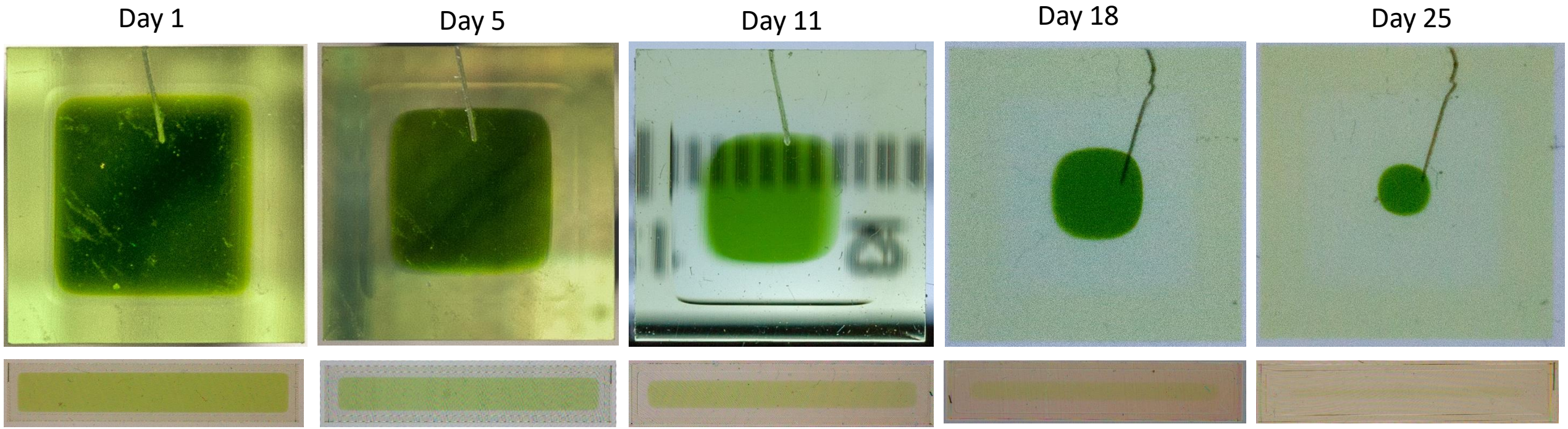

The sample shown above is a EJ200 PS scintillator rod of size $1 \times 1 \times 5$ cm. It was irradiated at NIST in September 2021 and received a total dose of 70 kGy at a dose rate of 460 Gy/h.

Note: Color balance is not universal. The colors on two picture are not directly comparable.

The irradiated scintillator has **two** distinct **visual features**.

Optical features

The features:

- **Green tint** in the center of the rod.
- **Boundary** that looks like a **refractive index change**.
- The boundary depths vary between samples.

Some observations:

- The spatial boundaries of the two features coincide initially.
- The green tint **reduces** and eventually **vanishes** during annealing → matches the predictions for annealing from the models!
- The index change boundary remains stable during annealing.

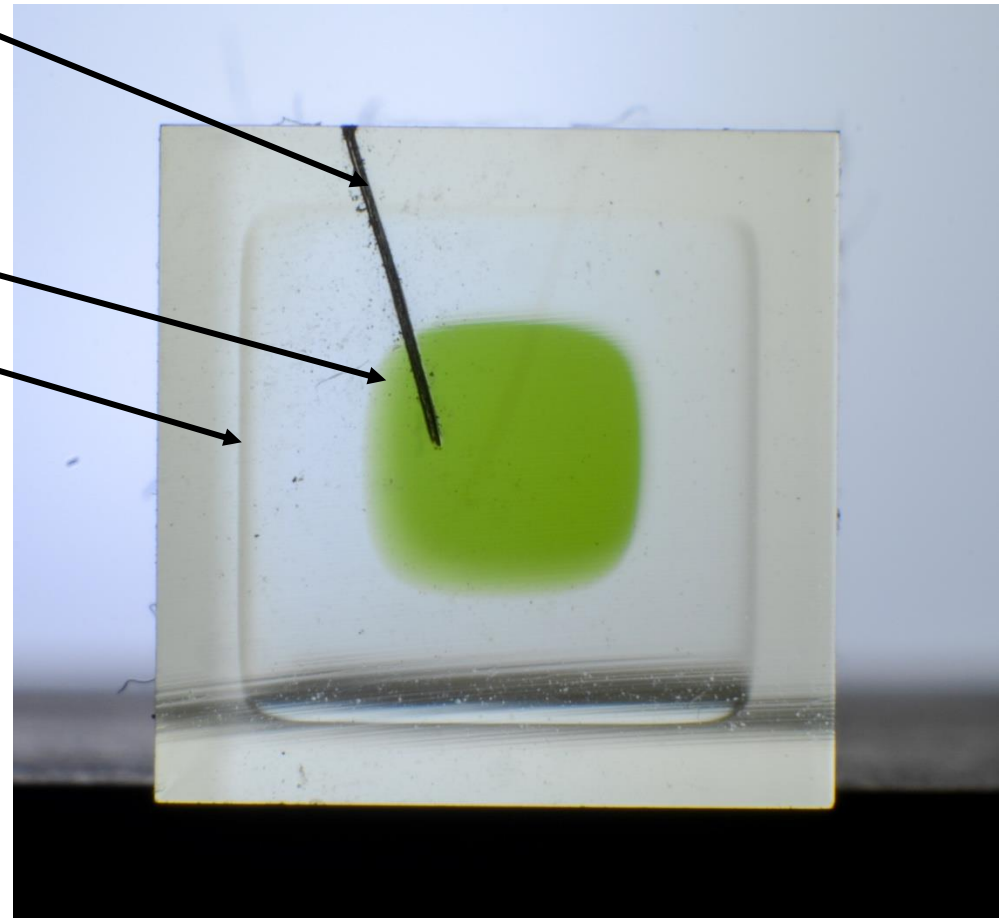

Picture captured by Tim Edberg.

Step 1: Measure the scintillation light

Methodology – Measuring light yield

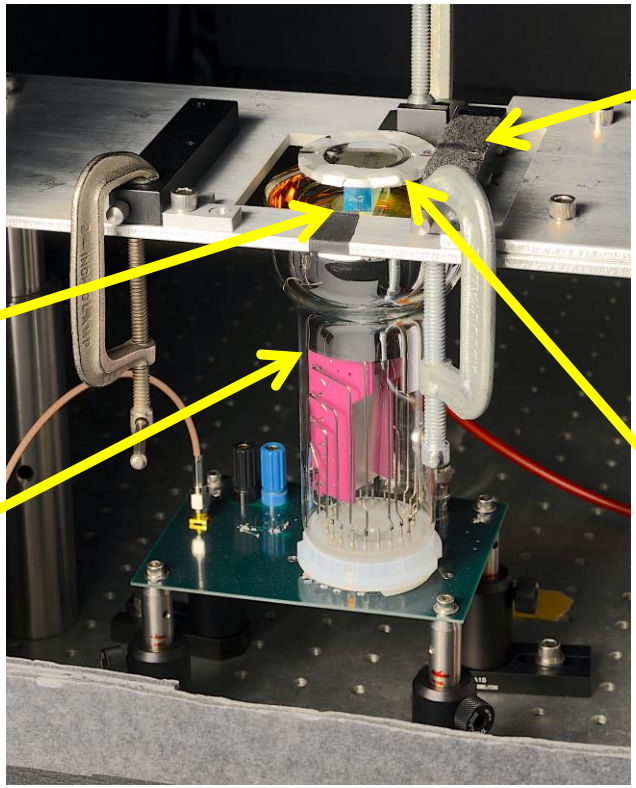

Charge integration over 100 ns

Tektronix TDS7104 oscilloscope

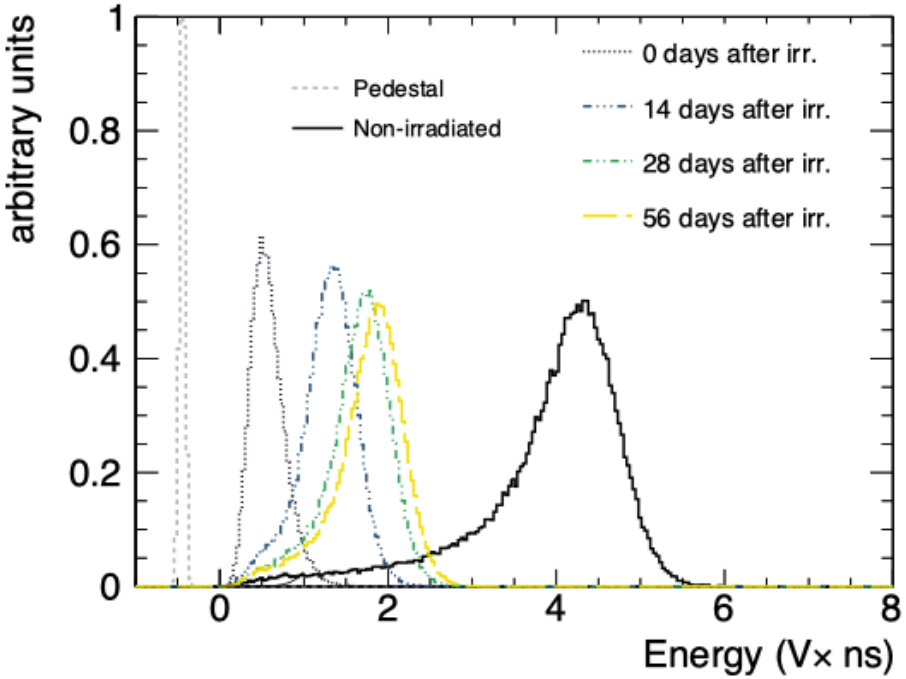

Calibration measurements (dark current, gain) → **+** → **Fit peak of curve**

^{239}Pu → 5.2 MeV α particles penetrate ~28 µm in a straight line

Calibrated light yield values **before** and **after** irradiation.

Dose constant

To quantify radiation hardness, the **dose constant D** is used

$$L_f = L_i e^{-\frac{d}{D}} \quad \Leftrightarrow \quad D = -\frac{d}{\ln\left(\frac{L_f}{L_i}\right)}$$

where L_i, L_f are the light yields before and after irradiation and d is the dose.

- **Larger D** means
  → **more resistant to radiation**.
- If color centers dominate, D expected to depend on sample thickness
  $$D \propto l^{-1}$$
- Interesting to check dose rate dependence!

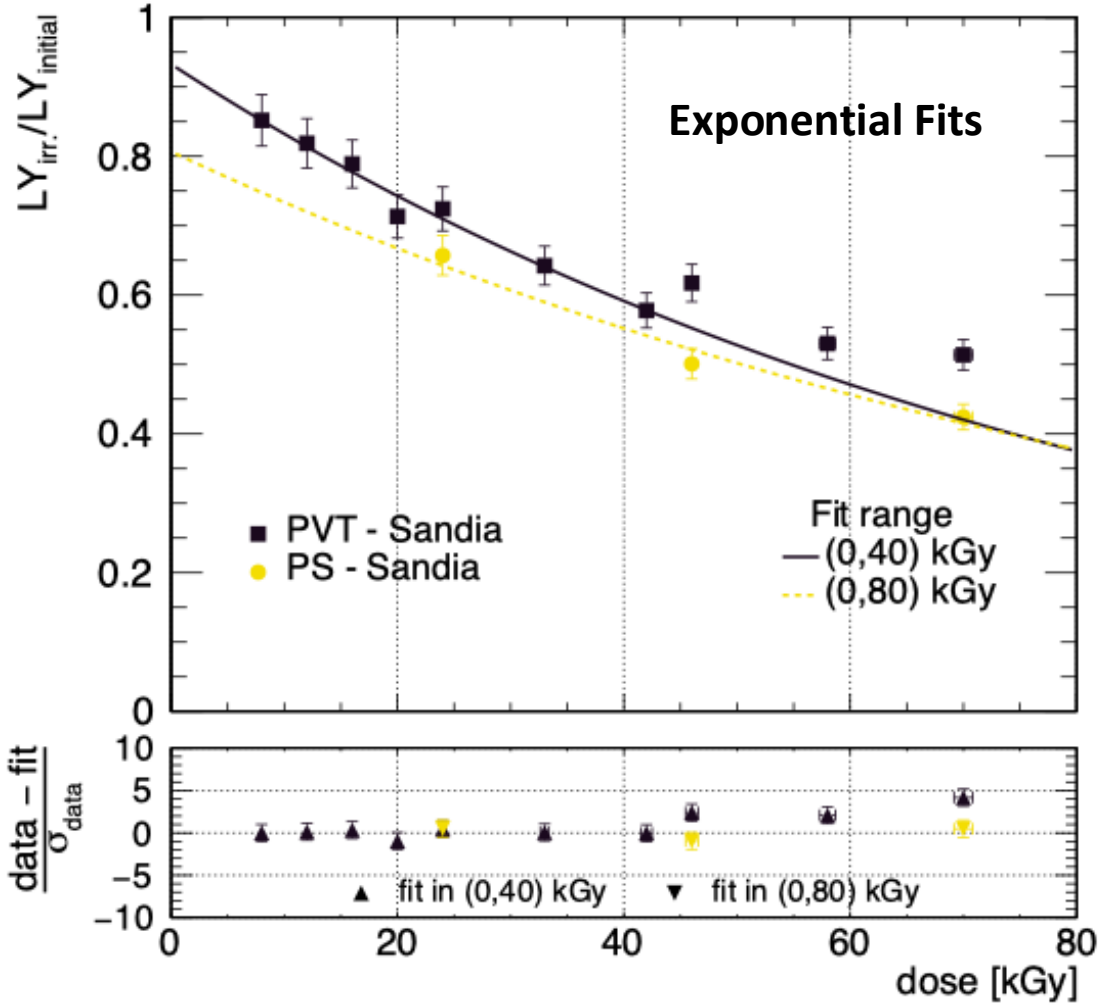

Results – PS vs PVT

About the comparison:

- Comparing rods with **PS and PVT substrates**.
- Both blue (EJ200) and green (EJ260) fluors are considered.
- Fluors and antioxidants concentrations are nominal.

Results:

- **Linear trend** (vs $\log R$) until ~70 Gy/hr.
- PS and PVT show different dose constant behavior above that level:
  - for PVT, remains **constant or continues to rise**.
  - for PS, remains **constant or decreases**.

Depending on the fluor concentrations.

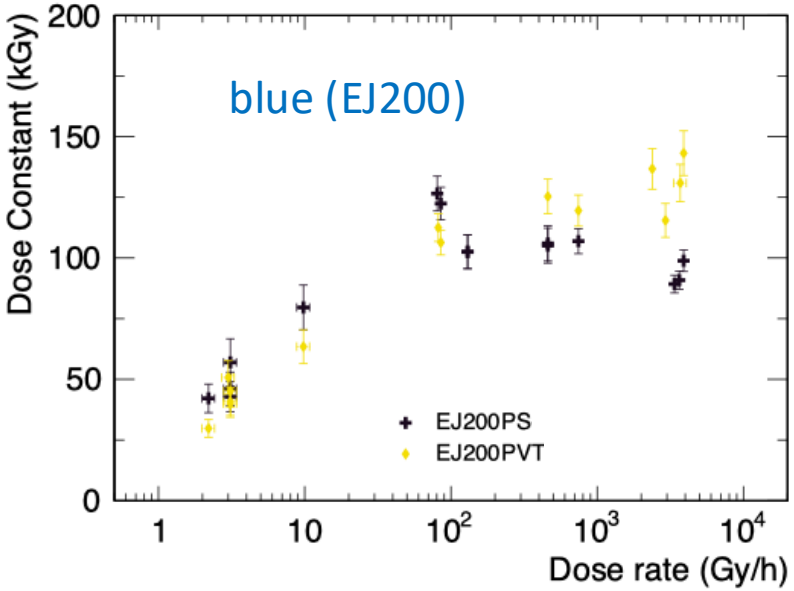

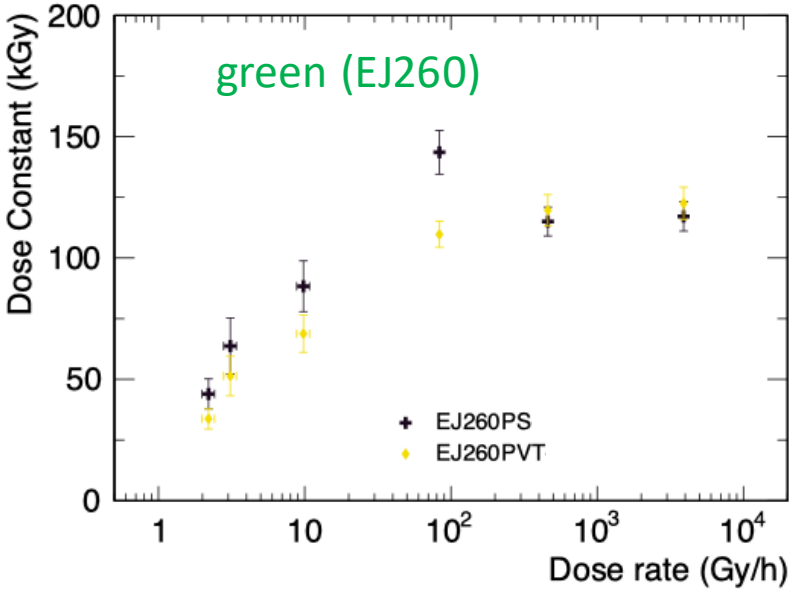

Results – Fluor concentrations

Varying fluor concentrations:

- **1X1P**: nominal primary and secondary
- **1X2P**: double primary and nominal secondary
- **2X1P**: nominal primary and double secondary

Some observations:

- **No significant effect** observed until 70 Gy/hr.
- Behavior above that amount **depends on dopant concentrations**.
- **Increasing the primary dopant** concentration benefits PS samples.
- **No dependence observed** for PVT within uncertainties.

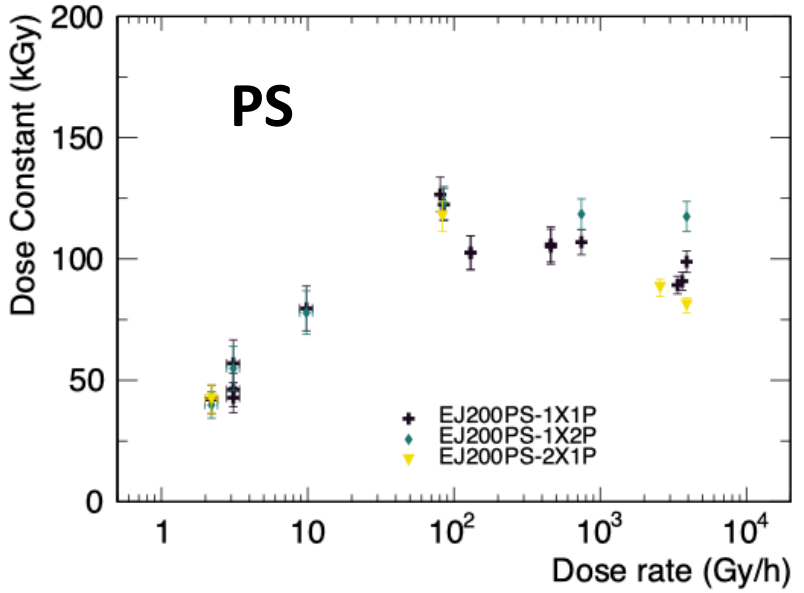

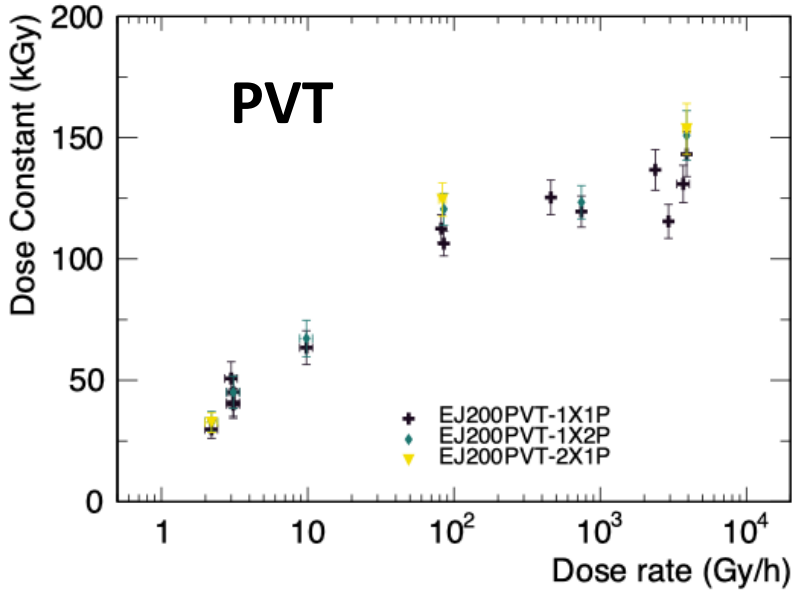

Results – Varying thickness

The two radiation damage mechanisms show **different dependences** of D on **rod thickness**:

- Color center formation gives D that **scale as** $\boldsymbol{l^{-1}}$.
- Damage to initial light production is **independent of** $\boldsymbol{l}$.

Results:

- During the recovery period, the dose constant **depends strongly** on the sample thickness.
- Indication that **color centers (radicals!)** form during irradiation but their number **reduces after annealing**.
- Final dose constants **do not depend strongly** on thickness.
- Dominant radiation damage mechanism is **reduction in initial light production** after annealing.
- The maximum sample thickness (1 cm) is **not large enough** to make color centers dominant.

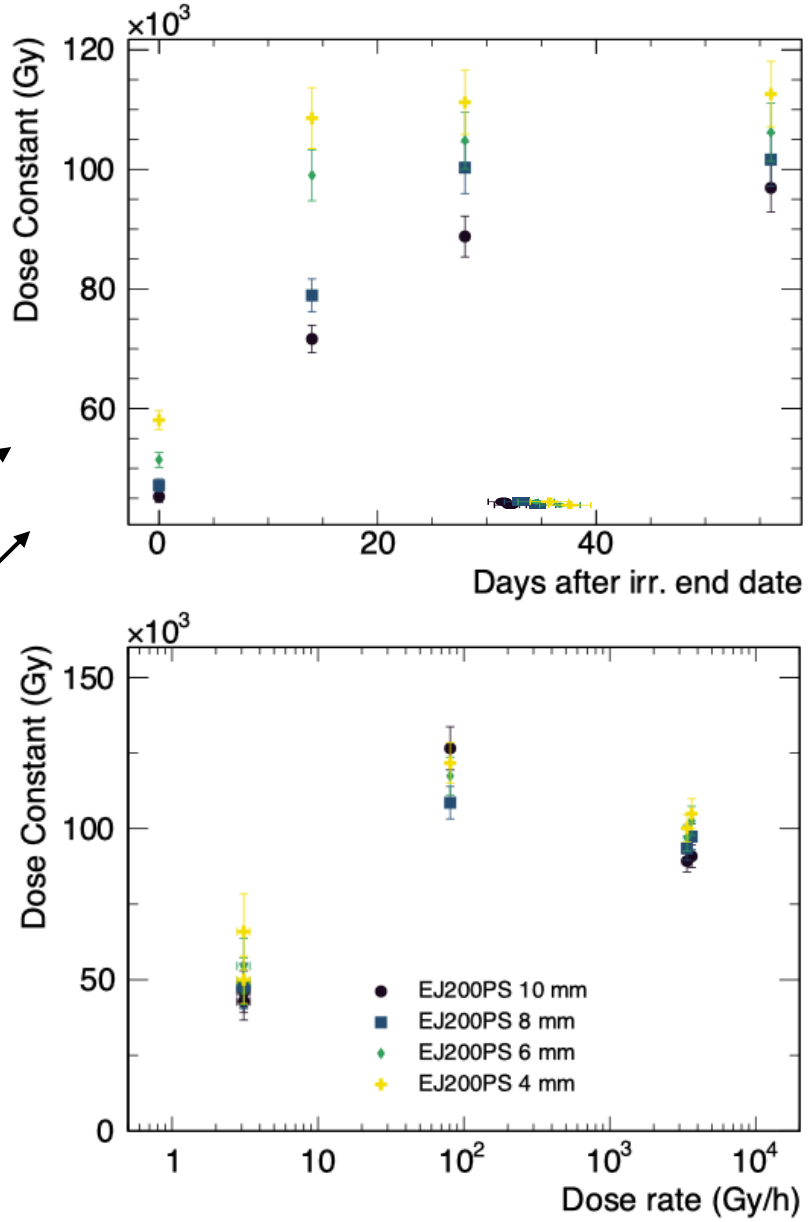

Step 2: Simulate and quantify the boundary depth effects

Radiation damage – JAERI model

- Radiation breaks substrate bonds and creates **free radicals:**

$$\mathrm{P} \xrightarrow{Y\mathcal{R}} \mathrm{P}^{\bullet}$$

- Radicals absorb visible light (stronger at low λ) ➡ **Color centers** (temporary damage)
- The radicals can recombine or crosslink:

$$\mathrm{P}^{\bullet} + \mathrm{P}^{\bullet} \xrightarrow{k_1} \mathrm{P}{-}\mathrm{P}$$

- or oxidize:

$$\mathrm{P}^{\bullet} + \mathrm{O}_2 \xrightarrow{k_2} \mathrm{P}{-}\mathrm{O}_2$$

- These are competing processes described by the equations:

Radical density eq.:
$$\frac{d[\mathrm{P}^{\cdot}]}{dt} = Y\mathcal{R} - k_1[\mathrm{P}^{\cdot}]^2 - k_2[\mathrm{P}^{\cdot}]C(x,t) \quad (1), \text{ and}$$

Oxygen diffusion eq.:
$$\frac{\partial C(x,t)}{\partial t} = D\frac{\partial^2 C(x,t)}{\partial x^2} - k_2[\mathrm{P}^{\cdot}]C(x,t) \quad (2)$$

JAERI model

Note: $C(x,t)$ → oxygen concentration

JAERI model – Simulation

- We solved numerically the model for a set of parameters that match some of our irradiations.
- Begin from a steady steady at the end of irradiation.
- Then simulate annealing until steady state again.
- Oxidation rate experiences **sharp transition** from full rate → 0 at a **depth z_0.**
- Can be shown to be dose rate dependent:

$$z_0 \propto R^{-\frac{1}{2}}$$

- During annealing, **oxidation moves as a front** to the center of the sample**.**

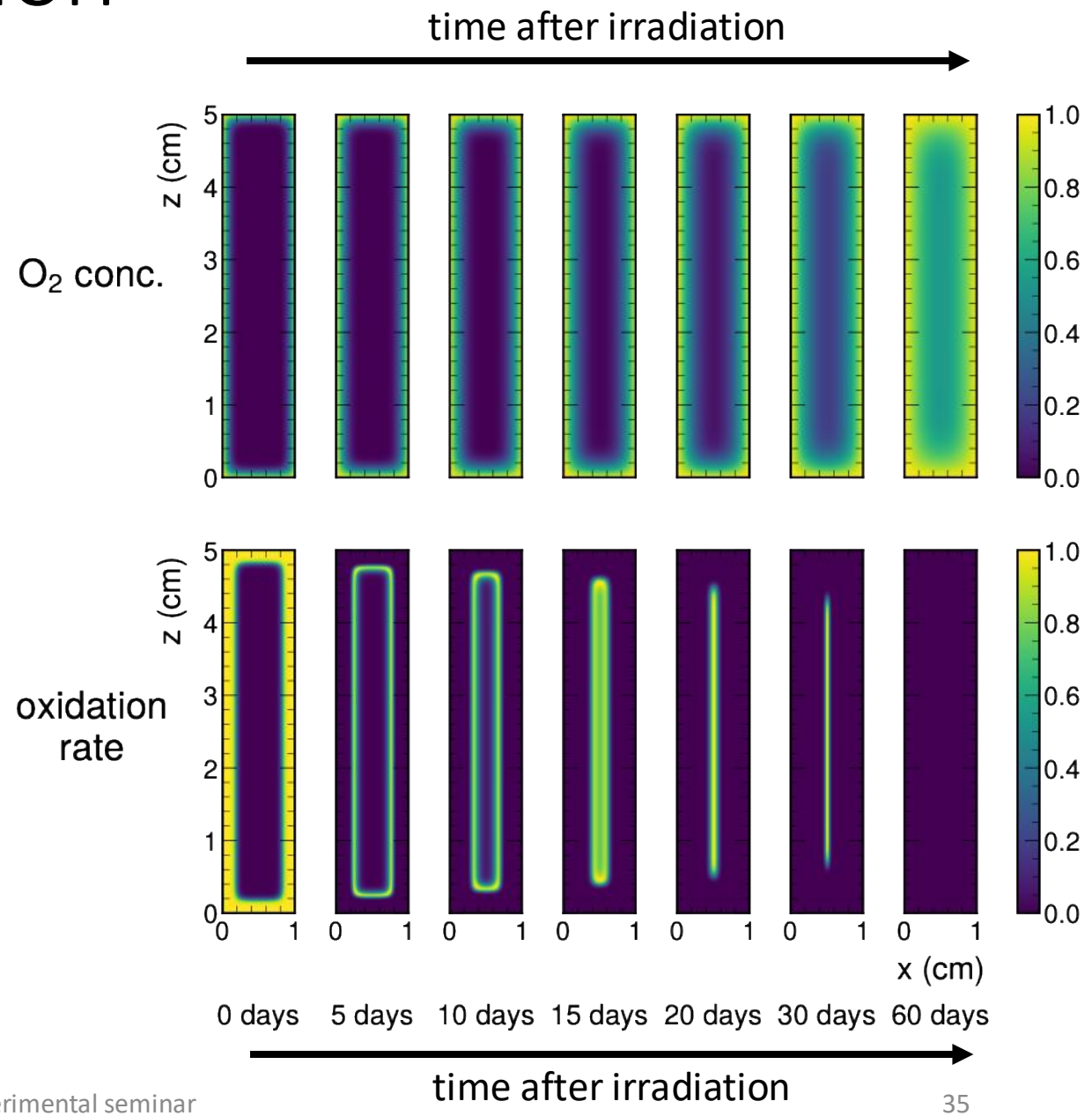

Depth results

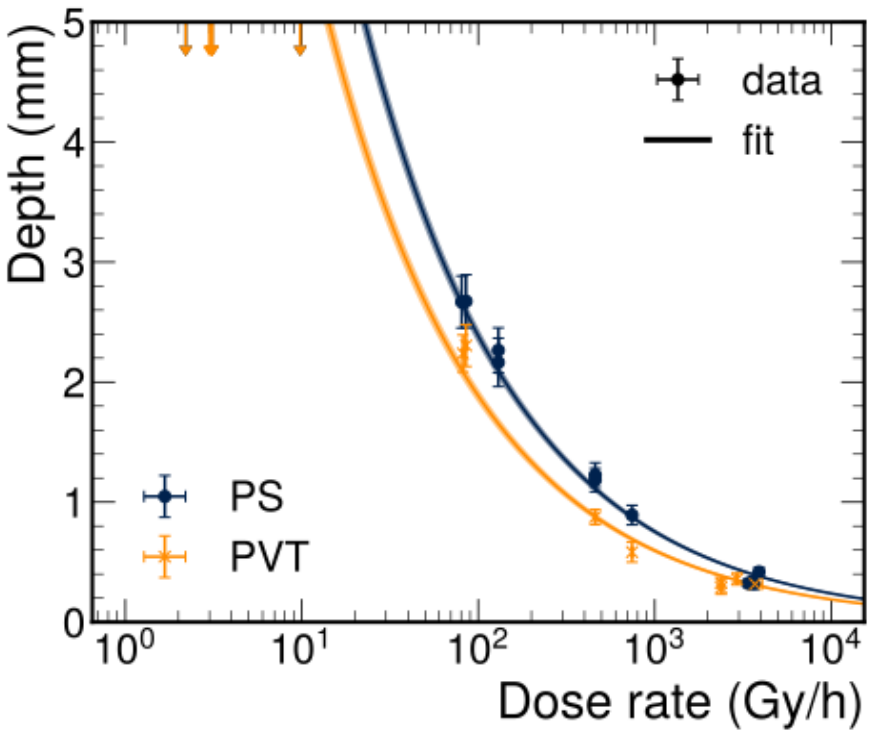

- Boundary depths vs dose rate for PS & PVT.
- Fit with **function** $z = \frac{A}{\sqrt{R}}$.
- Samples with $R < 80$ Gy/h don't have visible boundary (depicted with arrows).
- **Data consistent with this function**.

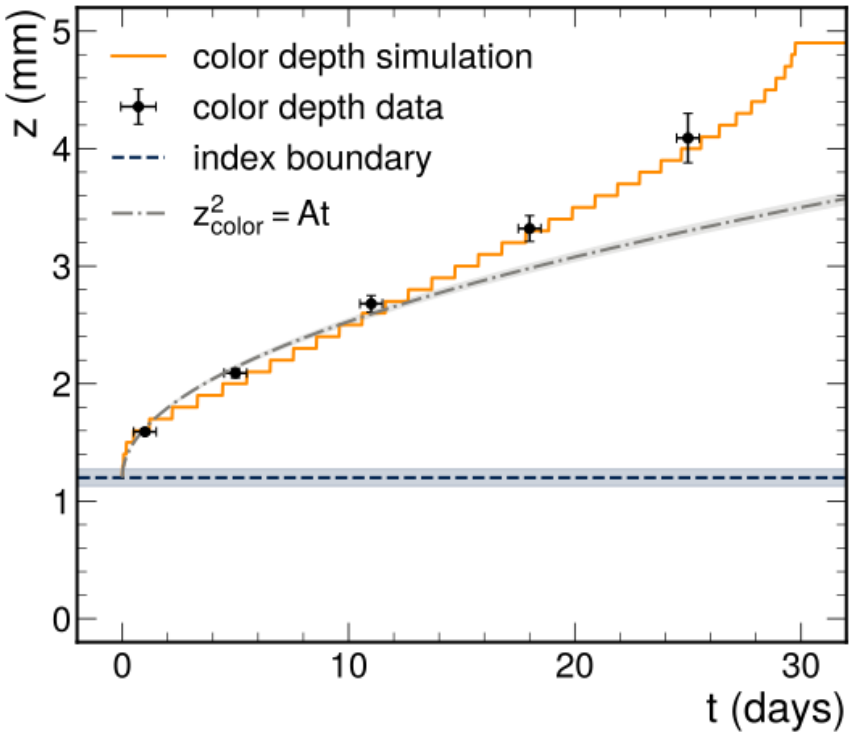

- Depth of the colored boundary over annealing time.
- Including best fit for $z \propto \sqrt{t}$ function.
- Also, the result of a **simulation of the JAERI model**.
- Parameters were fine-tuned to match the data.
- **Full simulation describes the data throughout annealing**.
- Approximating function holds only initially.

Step 3: What about the index of refraction?

Index of refraction

- **Refractive index** for a material:

$$n = \frac{c}{v} = \sqrt{\frac{\varepsilon\mu}{\varepsilon_0\mu_0}} = \sqrt{\varepsilon_r\mu_r} \simeq \sqrt{\varepsilon_r}$$

for non-ferromagnetic materials

tendency to acq. dipole moment $\vec{p}$ when exposed to external elec. field $\vec{E}$

- Microscopically, ε_r related to the **molecular polarizability** of the material $a \equiv \frac{\|\vec{p}\|}{\|\vec{E}\|}$ via the **Clausius-Mossoti equation**.
- **Lorentz-Lorenz equation** connects n with **average molecular polarizability vol.**:

$$\frac{n^2 - 1}{n^2 + 2} = \frac{4\pi}{3} N a_m$$

- Change in the bond structure → potential change in a_m → change in n.
- Materials are characterized using the **Sellmeier equation**:

$$n^2(\lambda) = 1 + \sum_{i=1}^{N} \frac{B_i \lambda^2}{\lambda^2 - C_i}$$

Measuring the index of refraction

- Exploiting the concept of the **apparent depth** to measure n:

$$n = \frac{L_{true}}{L_{apparent}}$$

- The same principle applies to the focus distance of a camera-lens system:
  1. Begin from a position where the camera is in-focus.
  2. Add the sample.
  3. Translate the camera until the new focus position is found.

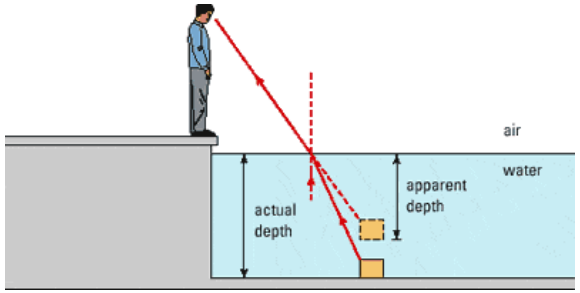

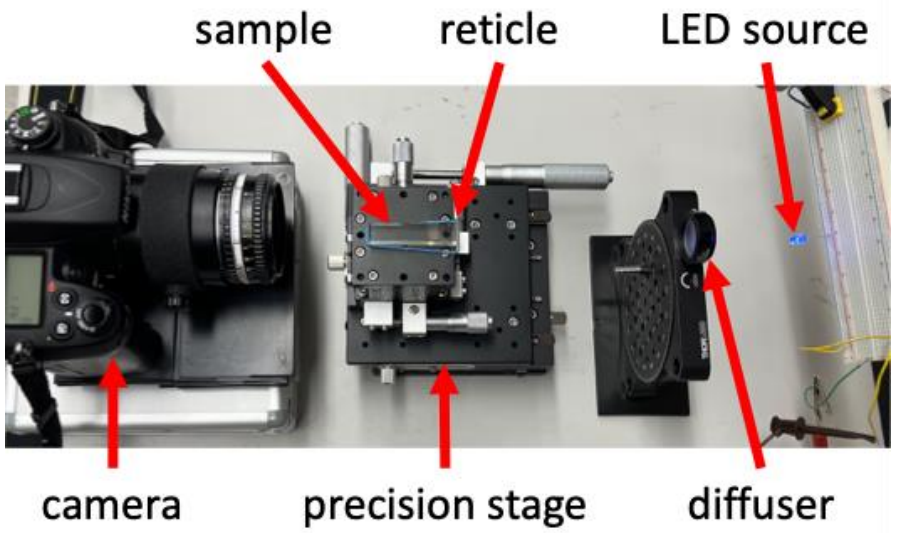

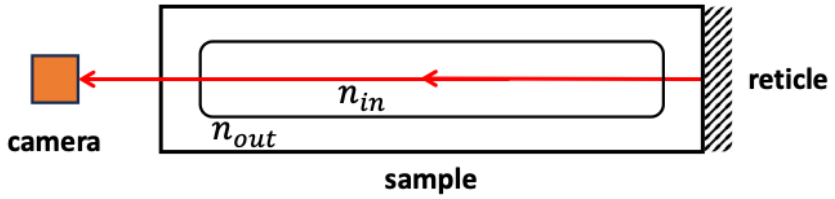

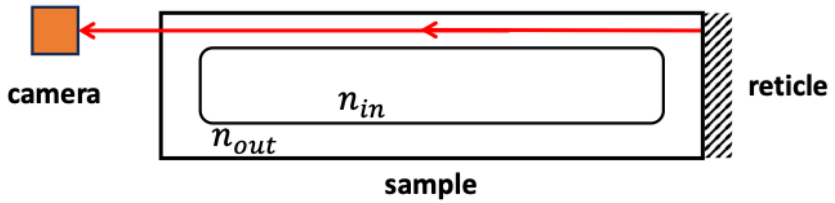

Since our samples have two regions, this must be accounted for as well:

$$n_{in} = n_{out}\frac{L - 2d}{L'n_{out} - 2d}$$

Measuring the index of refraction

- The method is **validated with BGO crystals**.
- The first order Sellmeier equation is shown both as:
  - a fit to the data
  - a reference using coefficients from literature
- **Data consistent with the Sellmeier equation.**
- Fitted parameters reasonably close to reference values.

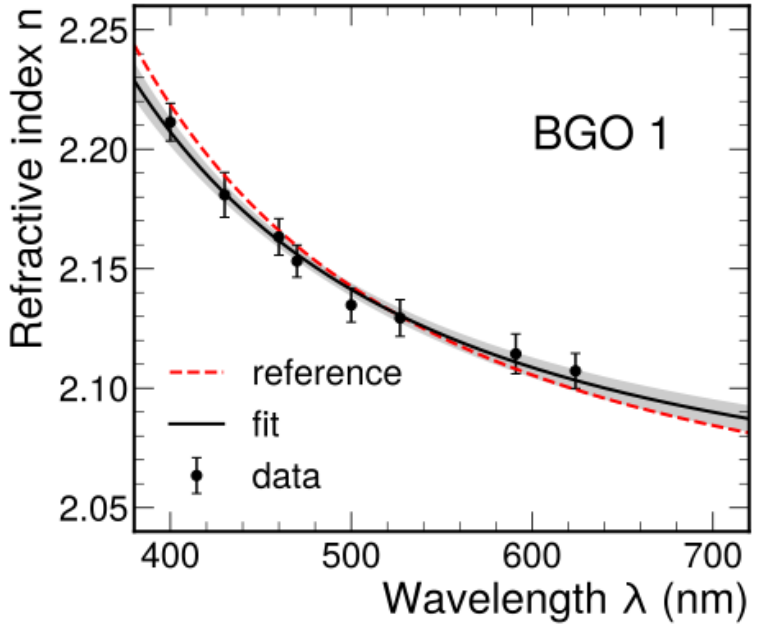

- Measured also **indices for PS & PVT unirradiated EJ-200**.
- Fitted first order Sellmeier equation.
- Values close to the manufacturer's specifications.

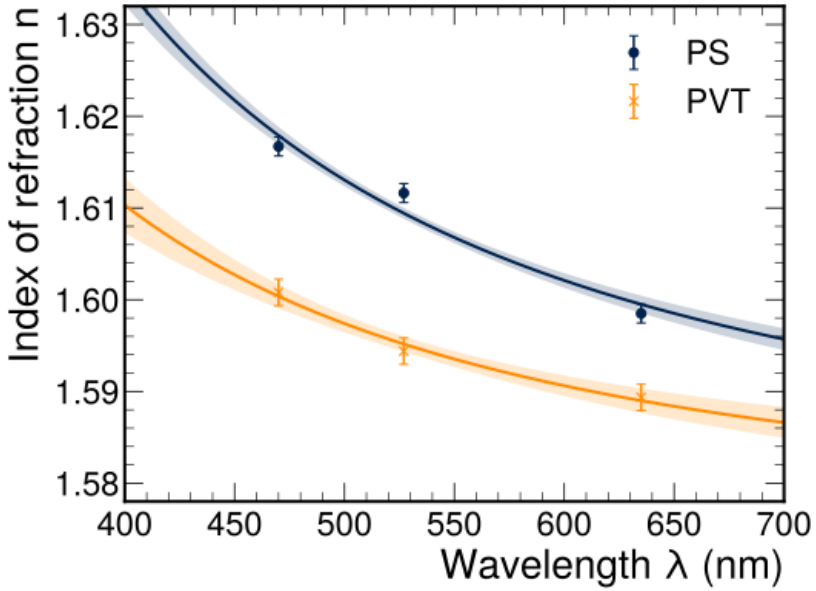

Measuring inner indices

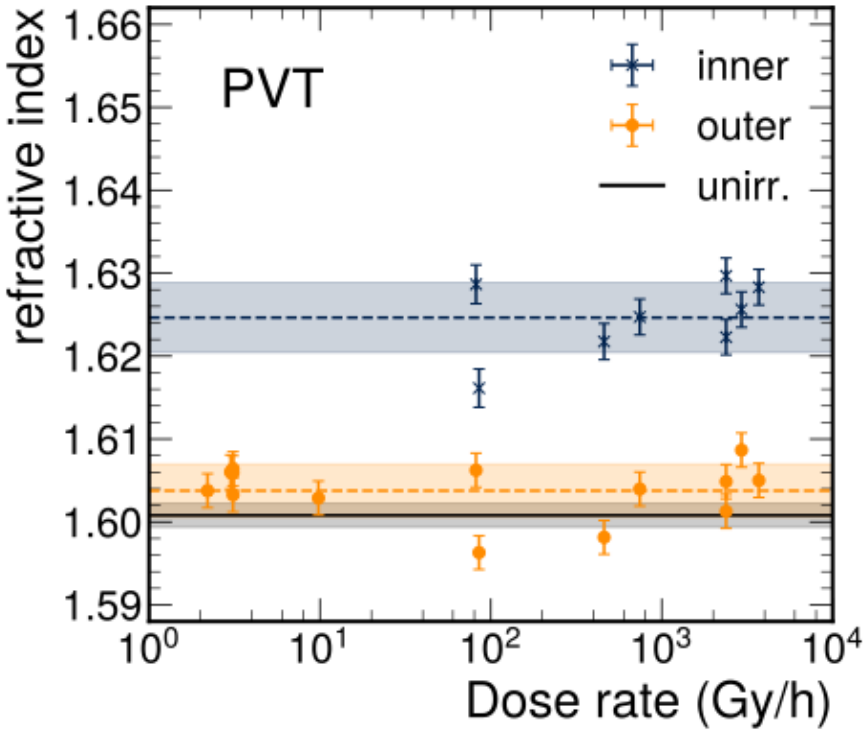

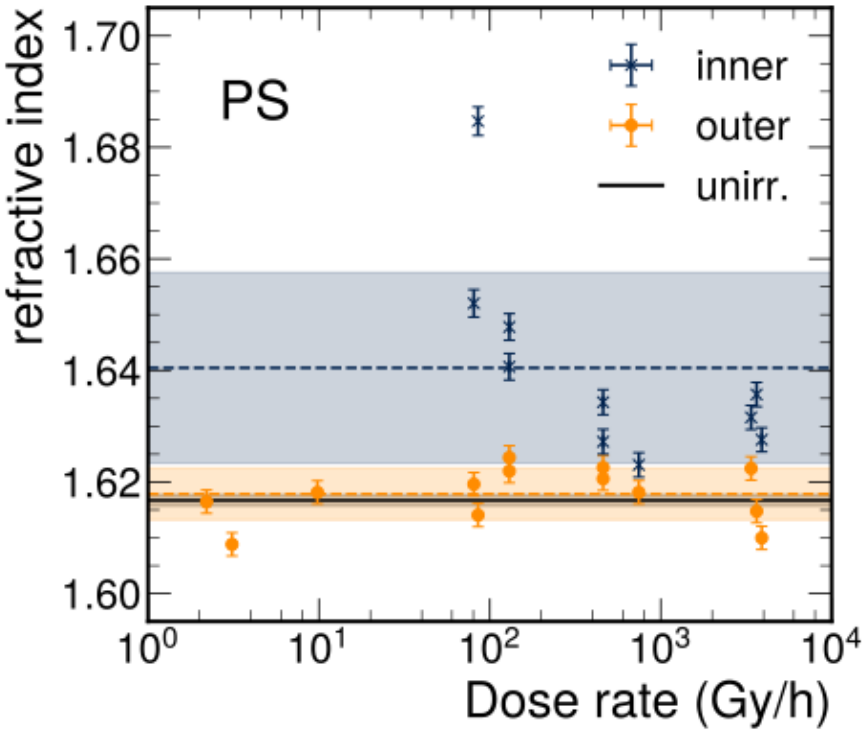

- **Measurements of irradiated rods at 470 nm after full annealing**.
- Indices of outer regions consistent with unirradiated rods.
- **Inner regions** show **increased index** by ~ 0.02.
- No dependence on dose rate.
- Decreasing trend in the inner region for PS (not enough to draw any conclusions, though).

Summary

- **Understanding radiation damage in plastic scintillators is important.**
- **We need the next generation as rad-hard as possible.**
- Presented measurements of a variety of samples irradiated using a range of doses and dose rates.
- **Exponential dependence of D with dose rate verified** below ~ 100 Gy/hr.
- PVT is a little better than PS only at high R.
- Overdoping improves rad-hardness only very mildly and only at high R.
- **Presence (or lack) of oxygen dictates the dominant damage mechanism.**
- Irradiation results simulated and quantified with two chemical models.
- **Refractive index & color internal boundary observed.**
- Matches predictions for oxygen penetration depth.
- **Lack of oxygen during irr. leads to increased refractive index.**

Part II: Searching for BSM physics

Search for Soft Unclustered Energy Patterns with muons at the LHC

Publications:

1) CMS collaboration (2024). *Search for Soft Unclustered Energy Patterns in Proton-Proton Collisions at 13 TeV*, Phys. Rev. Lett. 133, 191902.
2) CMS collaboration (TBD). *Search for Soft Unclustered Energy Patterns in pp collisions with muons*. Under collaboration review.

What lies beyond the SM?

- SM is great but doesn't accommodate dark matter.
- Many new possible directions:
  - WIMPs
  - Axions
  - Sterile neutrinos
  - ***Dark/Hidden sectors*** Today

arxiv:2209.07426

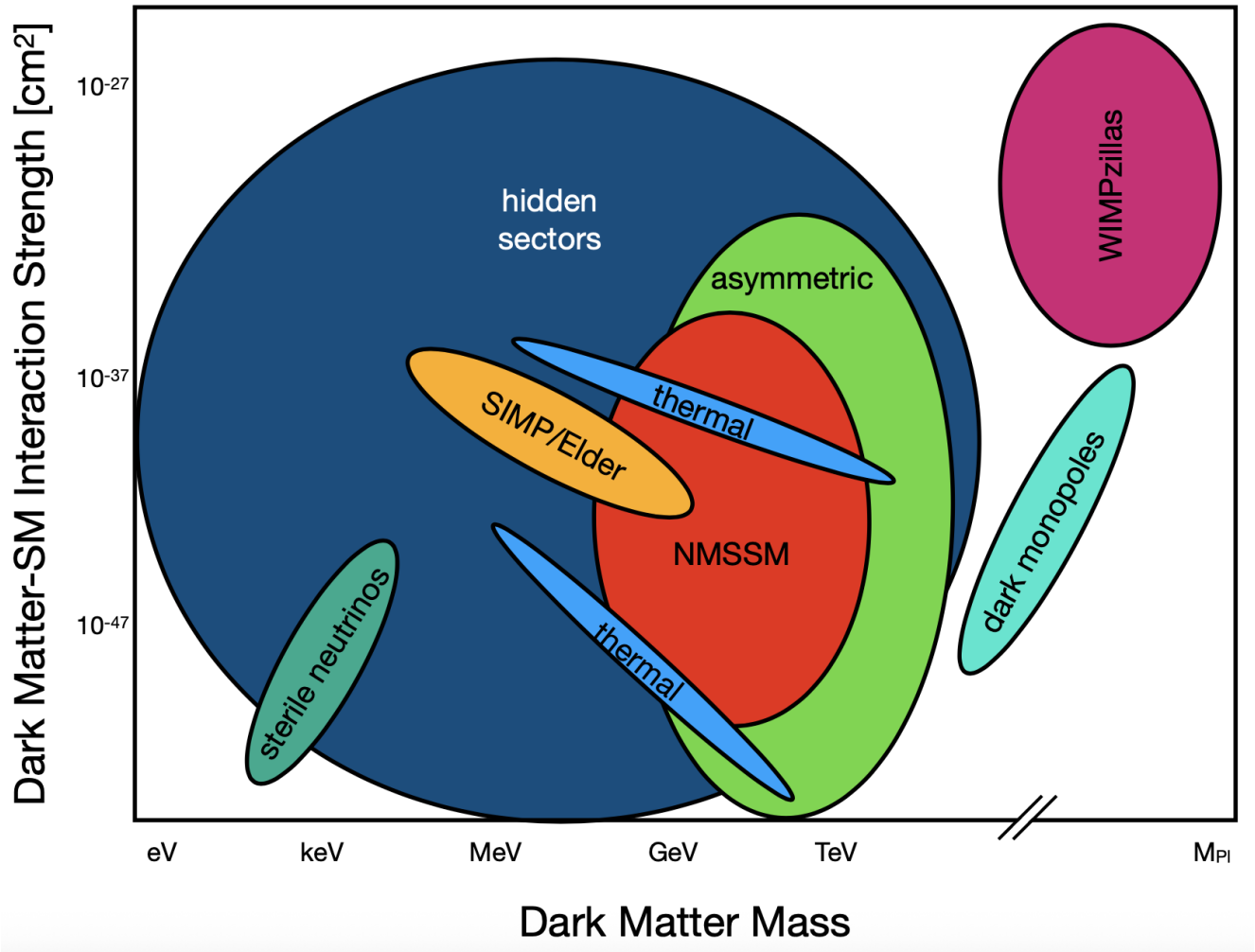

Hidden Sectors

- Extend the SM by a **non-Abelian confining gauge group**:

$$G_{SM} = \mathrm{SU}(3)_c \times \mathrm{SU}(2)_L \times \mathrm{U}(1)_Y \rightarrow \boldsymbol{G_{SM} \times G_v}$$

Strassler, M. J., and K. M. Zurek. Echoes of a hidden valley at hadron colliders. PLB 651.5-6 (2007).

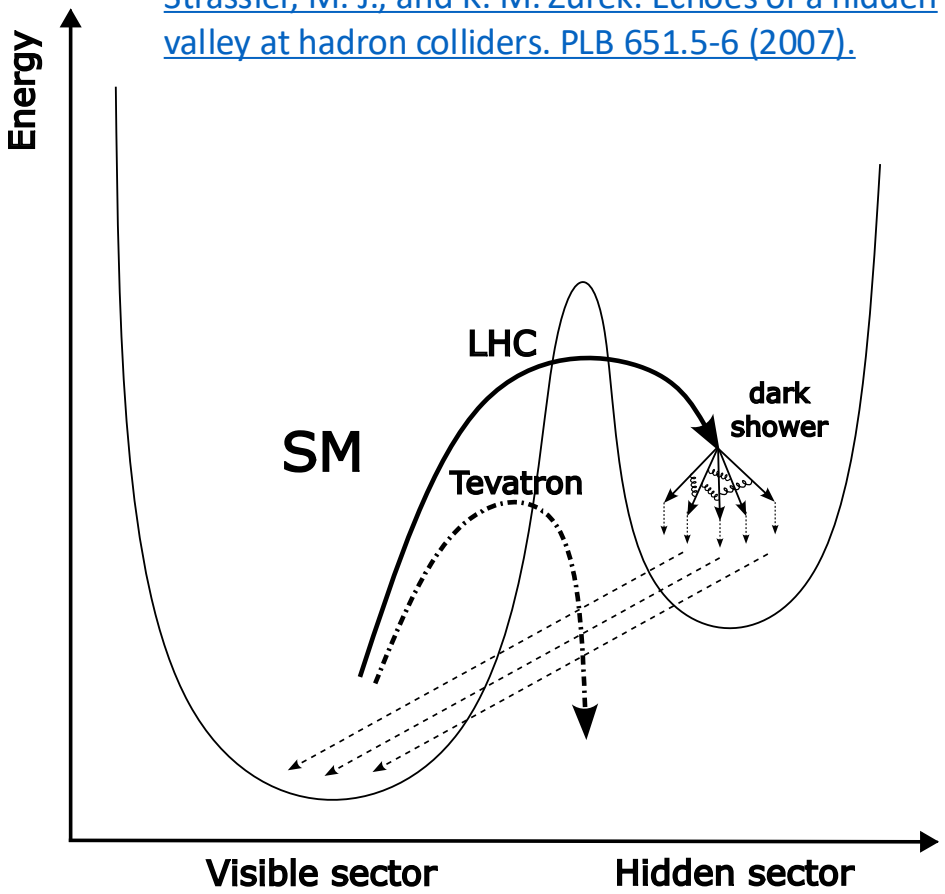

- With enough energy this sector can be accessed through particles acting as *portals*.
- The hidden sector has **QCD-like dynamics**.
- A rich phenomenology is possible!

Can give rise to exotic signatures like:

- Emerging jets
- Semi-visible jets

But it can become even more exotic if tuned very differently than the SM QCD!

Soft Unclustered Energy Patterns

- For this talk we will focus on models with:
  - **Mediator is a heavy scalar, S,**
  - **Large 't Hooft coupling, $\lambda \equiv gN_c$, and**
  - **Low hadronization scale, $\Lambda < 1$ GeV.**

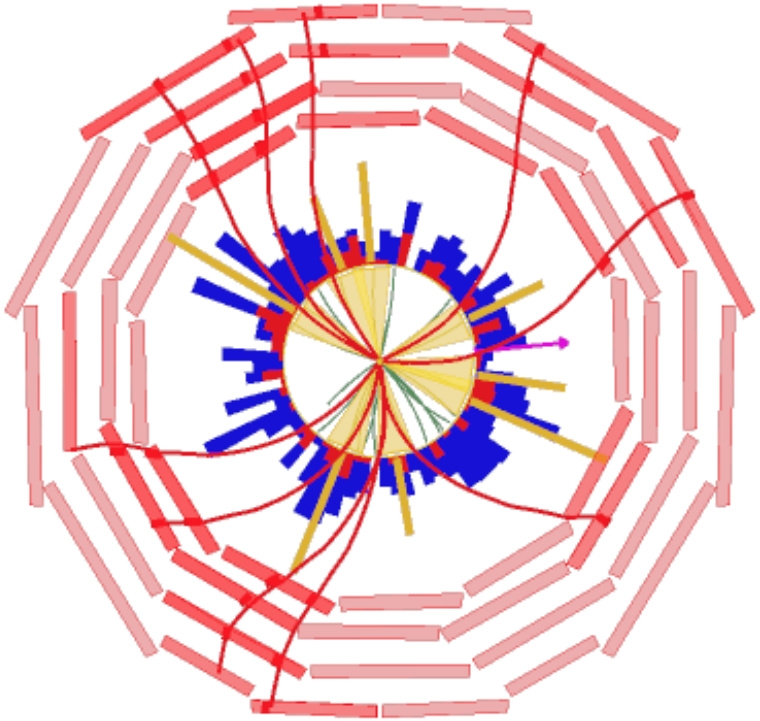

- Large 't Hooft coupling → **large angle emission** of partons.
- Low hadronization scale → **large parton multiplicities.**
- Result is a **soft spray** of particles **distributed uniformly** in the detector.
- They are called **Soft Unclustered Energy Patterns (SUEP).**

A SUEP event

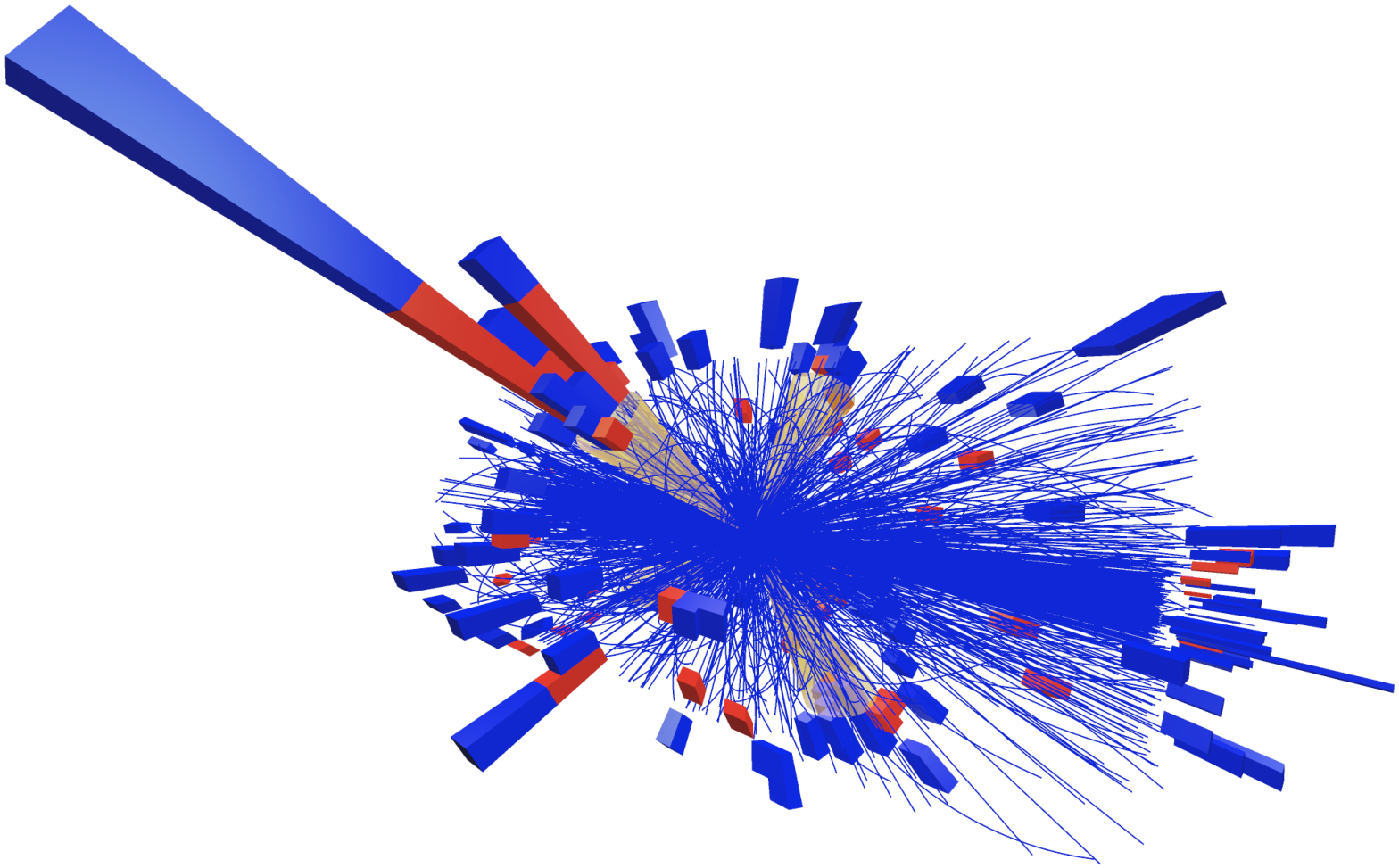

Soft Unclustered Energy Patterns

Our benchmark model:

- **Scalar**, S, produced via ggF or other modes (VH, VBF, etc.).
- S decays to **dark mesons**, ϕ, with Maxwell-Boltzmann kinematics:
  - Their momenta are distributed according to:

$$\frac{dN}{d^3\mathbf{p}} \propto \exp\left(-\frac{\sqrt{\mathbf{p}^2 + m^2}}{T}\right)$$

temperature

- Dark mesons decay to **dark photons**, A', via $\phi \to A'A'$.
- A' decay promptly to **charged SM particles** (e^+e^-, $\mu^+\mu^-$, $\pi^+\pi^-$) → for the studied m_A, values.

Knapen, S., *et al.* Triggering soft bombs at the LHC. *J. High Energ. Phys.* **2017**, 76 (2017).

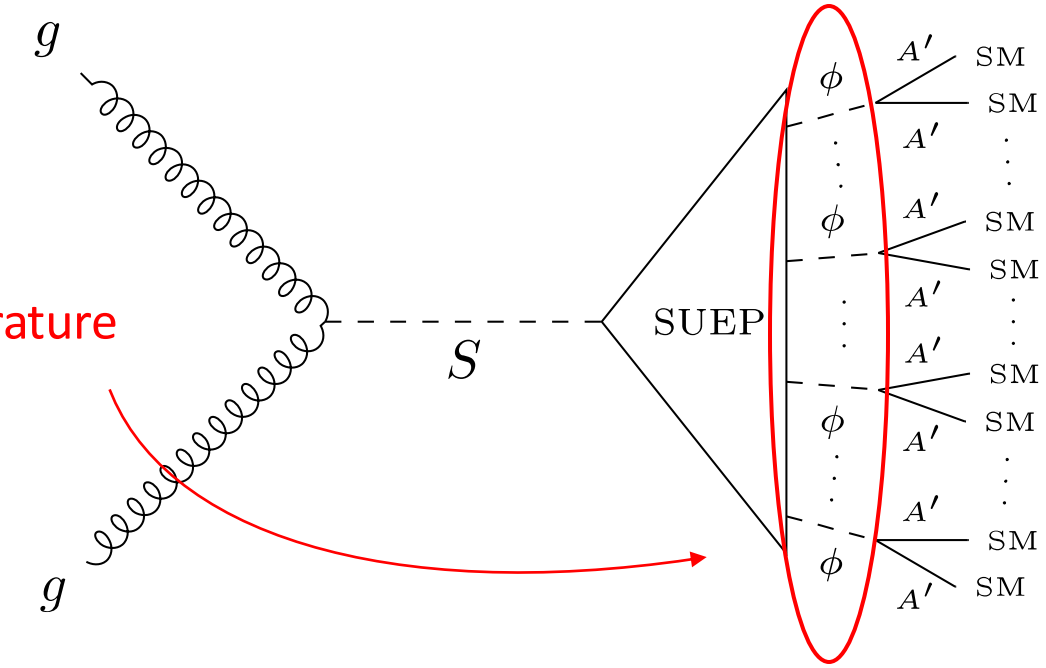

SUEP model parameters

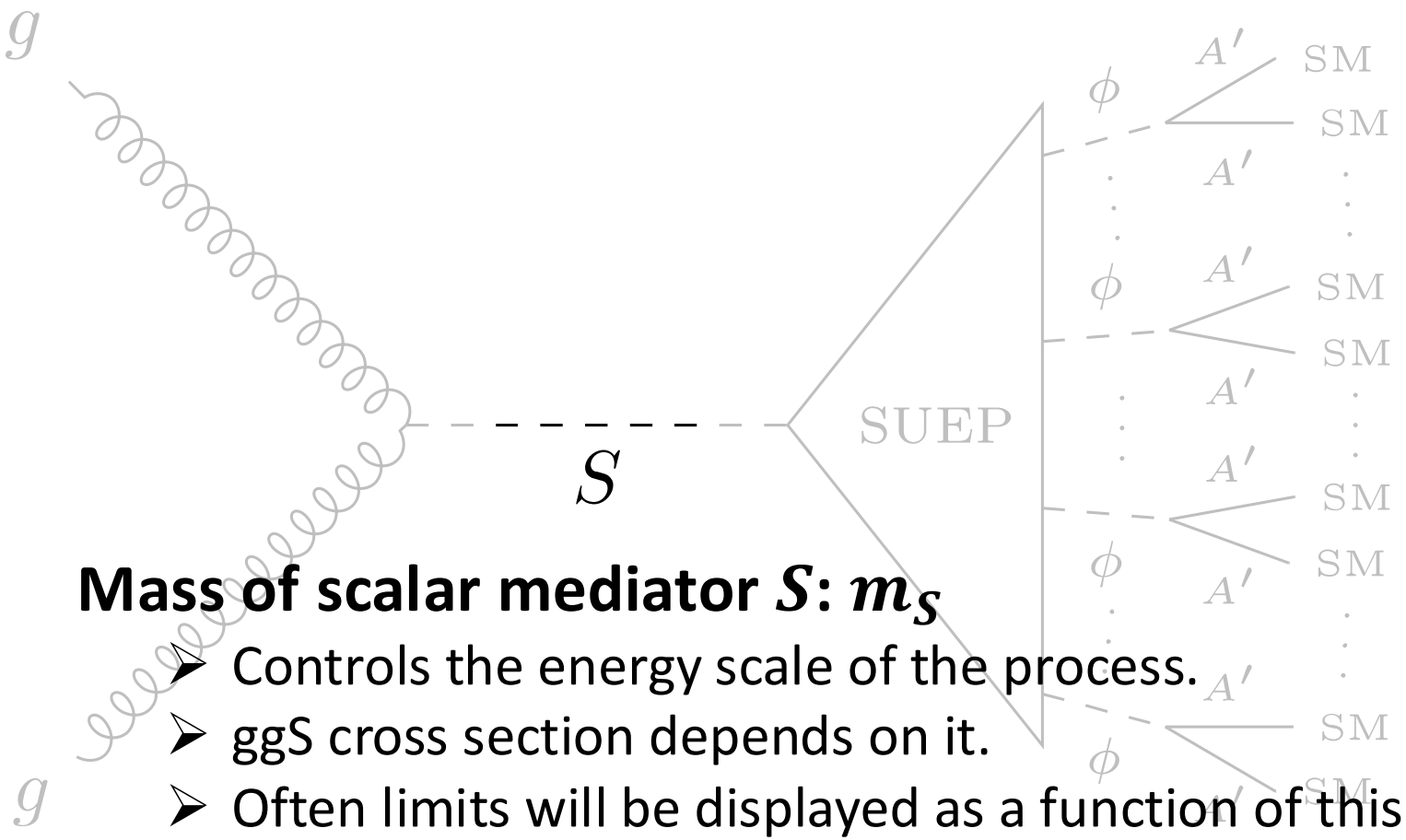

Mass of scalar mediator S: m_S

- Controls the energy scale of the process.
- ggS cross section depends on it.
- Often limits will be displayed as a function of this parameter.

SUEP model parameters

arXiv:1906.10831

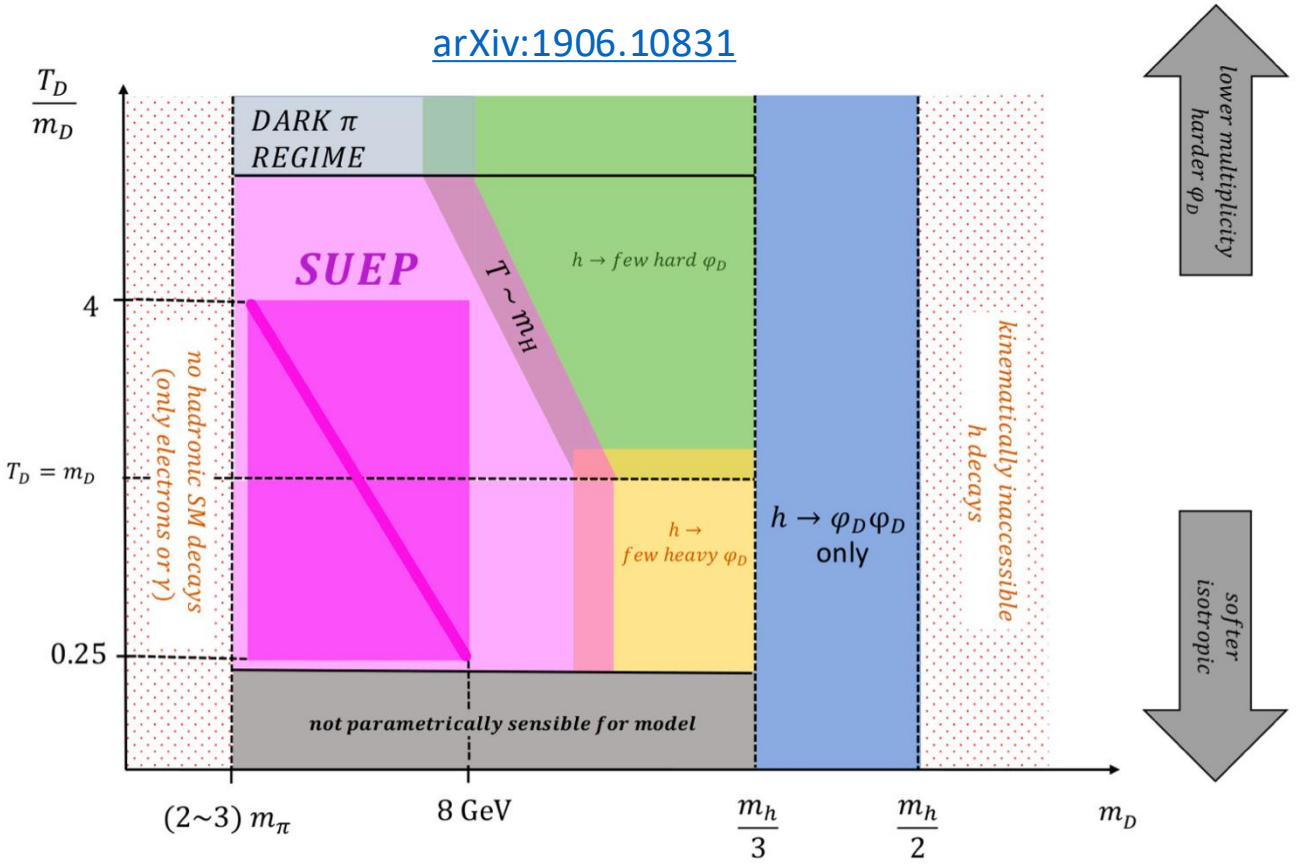

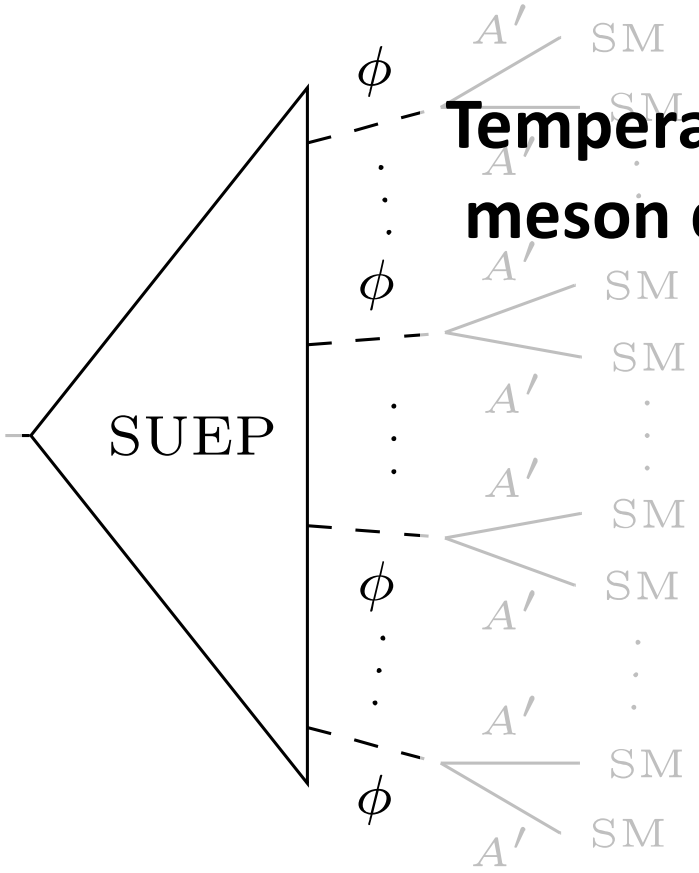

Temperature of ϕ dark meson distribution: T

Mass of dark meson ϕ: m_ϕ

- The ratio of these two parameters, T/m_ϕ, controls the dark shower properties.
- Need to be ~ same order of magnitude for the model to be sensible.

SUEP model parameters

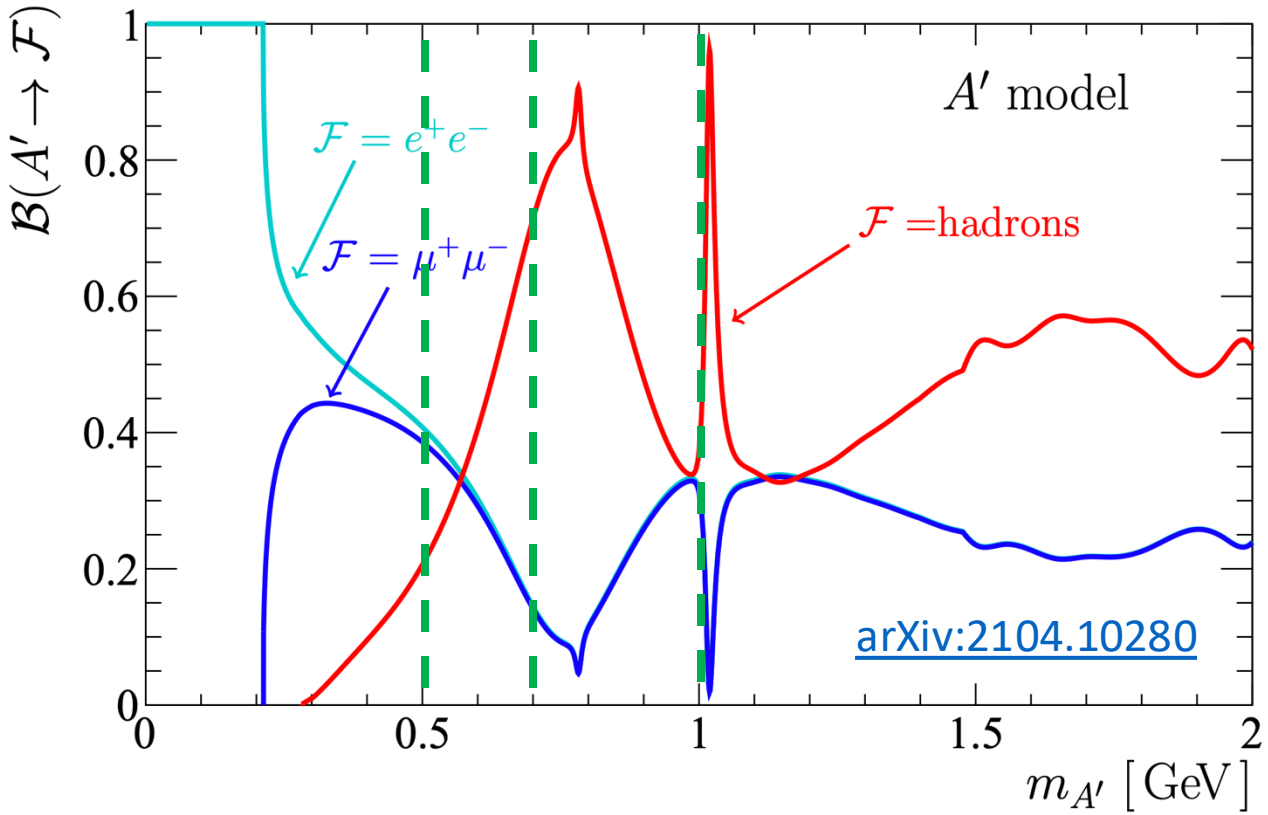

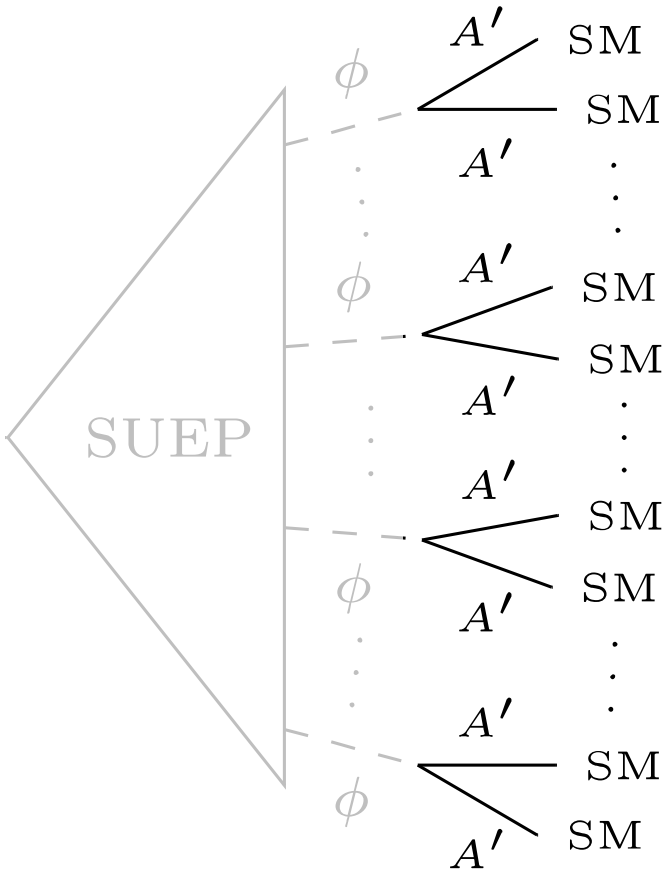

Three decay scenarios:

- **Generic**: $\mathrm{BR}(A' \to \pi^+\pi^-) = 100\%$
- **Semi-hadronic**: $\mathrm{BR}(A' \to \pi^+\pi^-) = 70\%$, $\mathrm{BR}(A' \to l^+l^-) = 15\%$
- **Leptonic**: $\mathrm{BR}(A' \to \pi^+\pi^-) = 20\%$, $\mathrm{BR}(A' \to l^+l^-) = 40\%$

$$l = e, \mu$$

Mass of dark photon A': $m_{A'}$

- Controls the branching ratios back to the SM.

Search for Soft Unclustered Energy Patterns in Proton-Proton Collisions at 13 TeV

AKA the “Offline search”

Offline search – intro/idea

Idea: Look for the recoiling gluon (ISR) from the gluons fusing into a SUEP.

- Will increase the total hadronic energy of the event.
- Should be able to use an existing HT trigger!

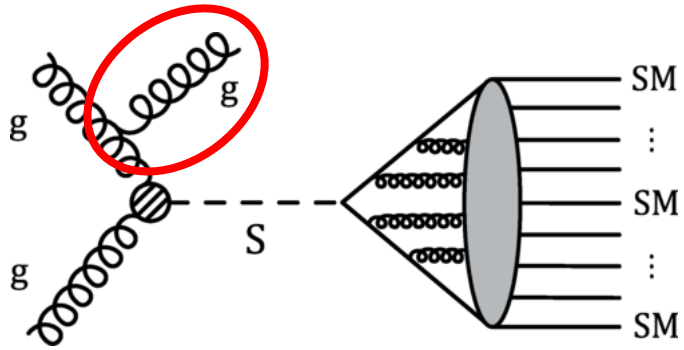

Offline search – SUEP tagging & sphericity

- We have a process to **tag the SUEP cluster**:
  1) Cluster anti-k_T jets with R=1.5.
  2) Jet with most constituents is the SUEP candidate.
- Events expected to look **isotropic in the rest frame of S**.
- Use an **event shape variable → sphericity** is a good candidate:
  1) Boost SUEP jet constituents back to the rest frame of the candidate.
  2) Calculate sphericity tensor using the SUEP jet constituents

$$S_{ab}^{(r)} = \frac{\sum_i |p_i|^{r-2} p_{i_a} p_{i_b}}{\sum_i |p_i|^r}$$

  3) Sphericity variable is $S_1 = \frac{3}{2}(\lambda_2 + \lambda_3)$, where λ_2, λ_2 are the two lowest eigenvalues of $S_{ab}^{(1)}$.

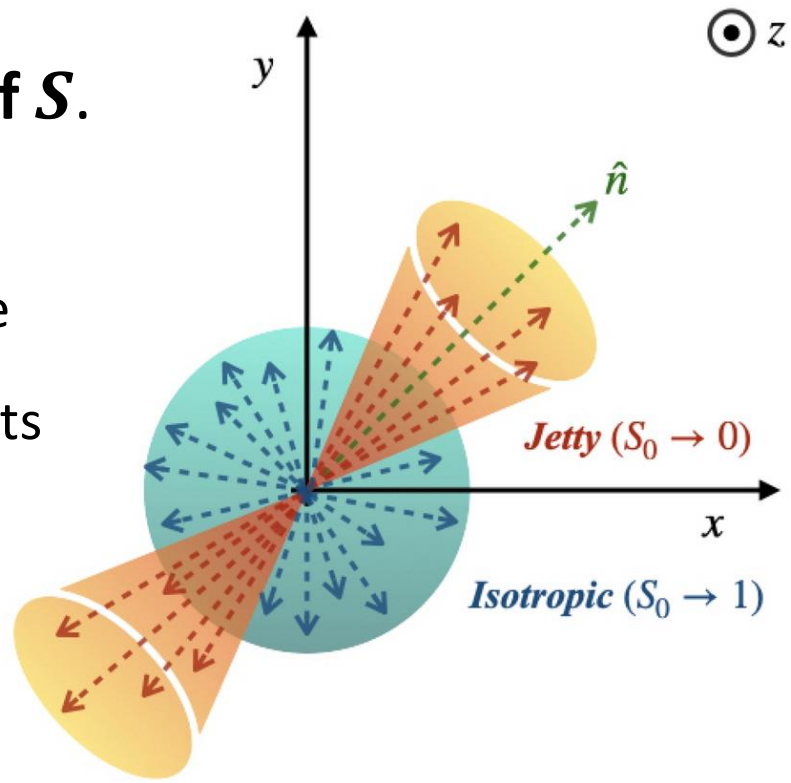

- **S_1 is 1 for perfectly spherical events and 0 for pencil-like events.**

Offline search – background

- Signal region is defined by:
  - $n^{SUEP}_{constituent} > 70$, and
  - $S^{SUEP}_{boosted} > 0.5$.

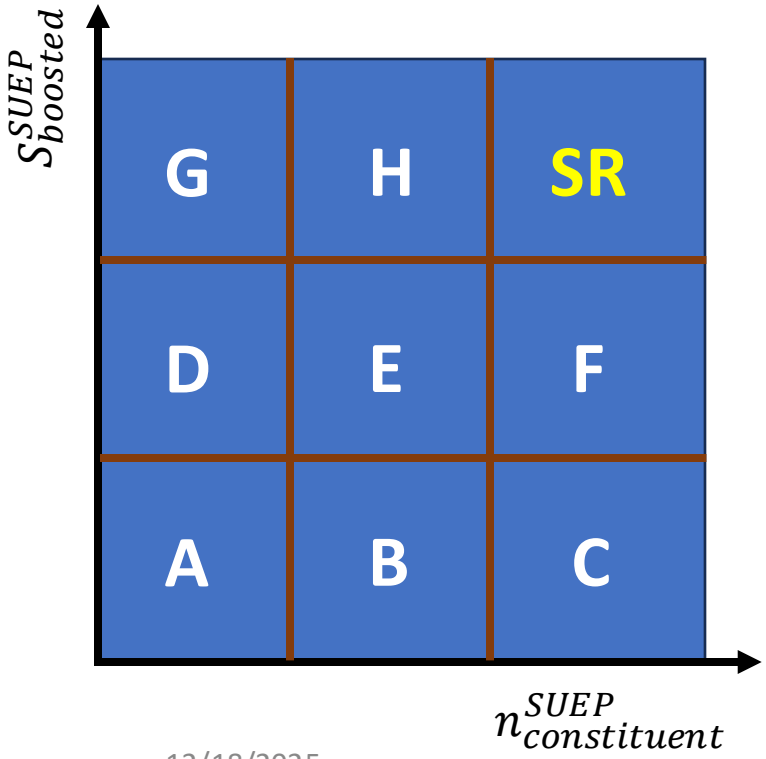

- The background is estimated using an "extended" 9-region ABCD method.
- Data-based method.
- Can account for *some* correlation between the variables.

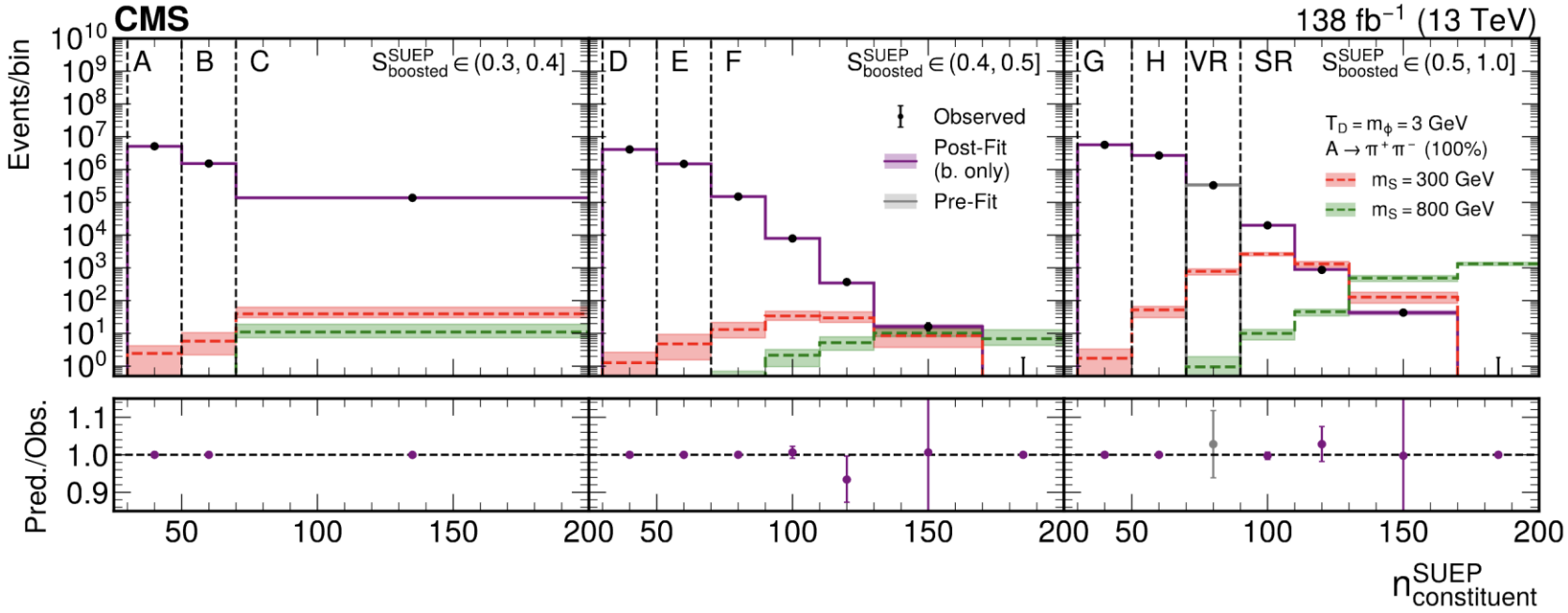

Offline search – limits

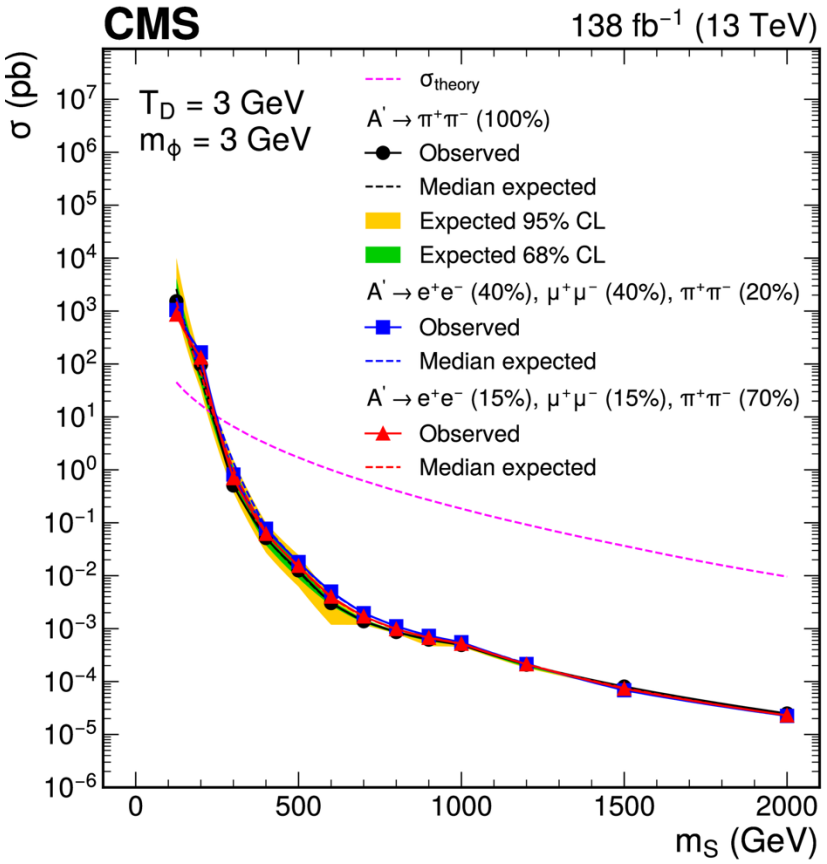

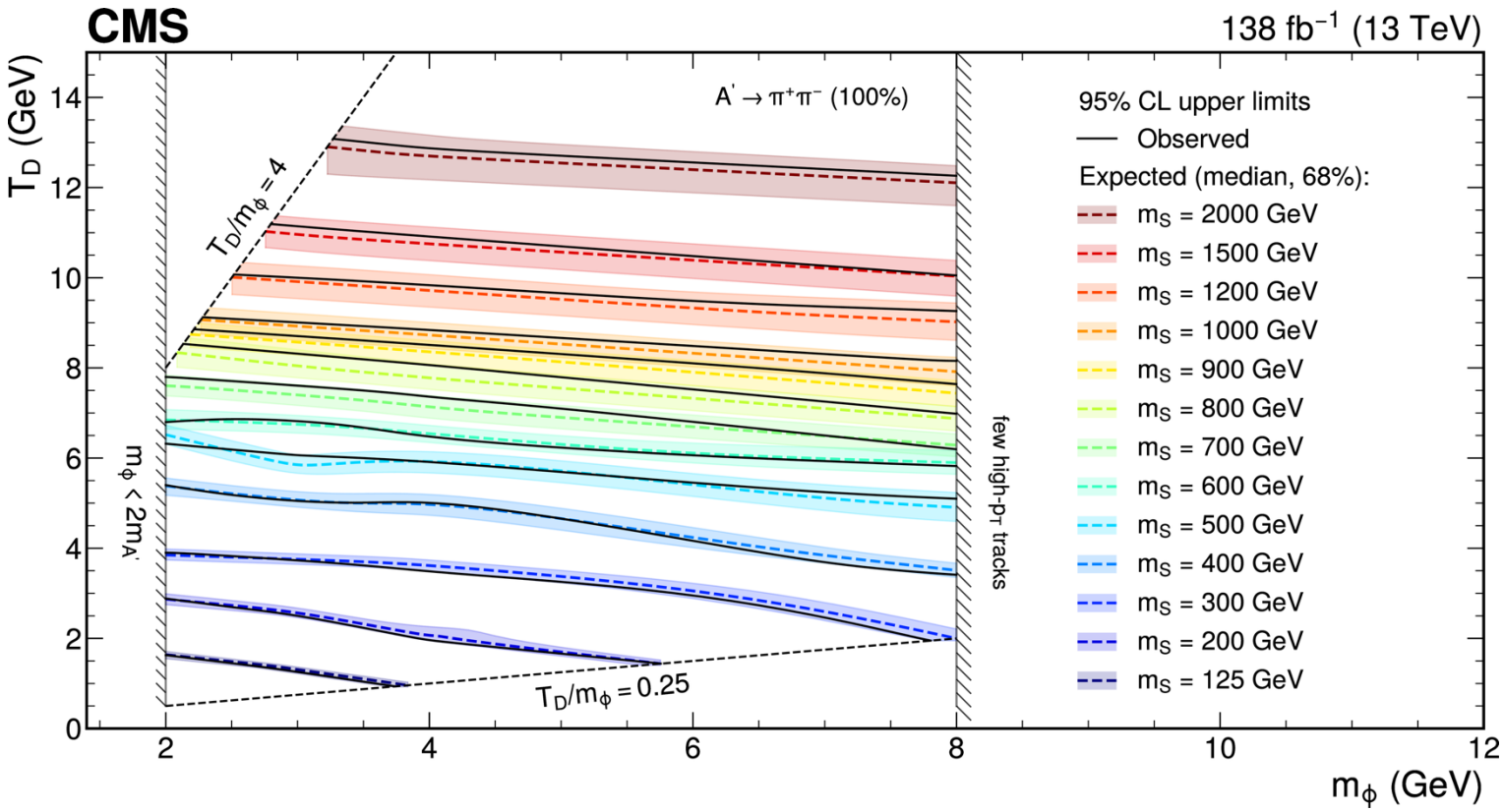

- Very tight limits for larger m_S and more SUEP-y models (lower temperatures).
- Left plot shows the contours of lowest m_S excluded for given parameters.

Search for Soft Unclustered Energy Patterns with muons

Or the “Muon counting search”

Muon counting search

Idea: SUEP events have a lot of muons…
…and CMS is primarily a muon detector.

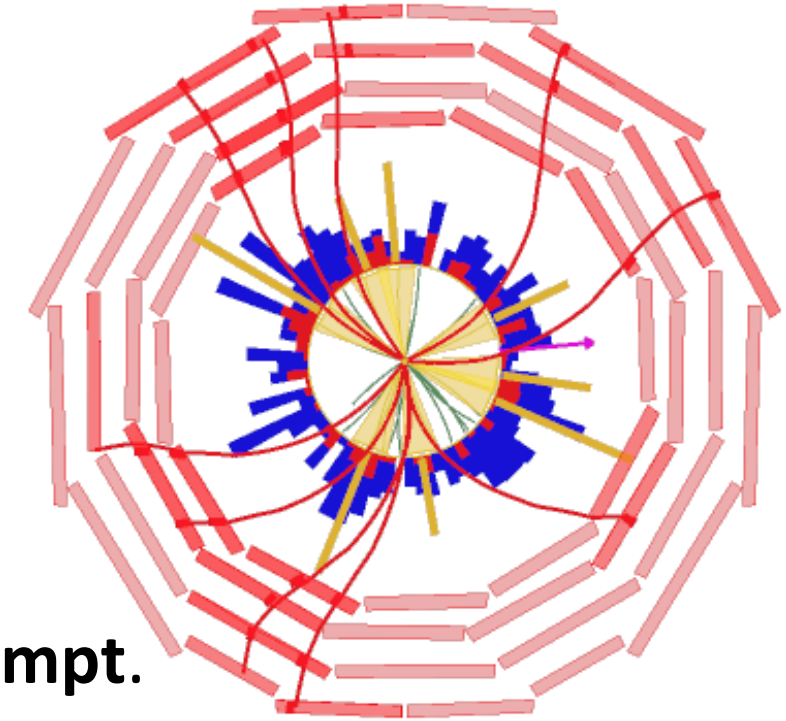

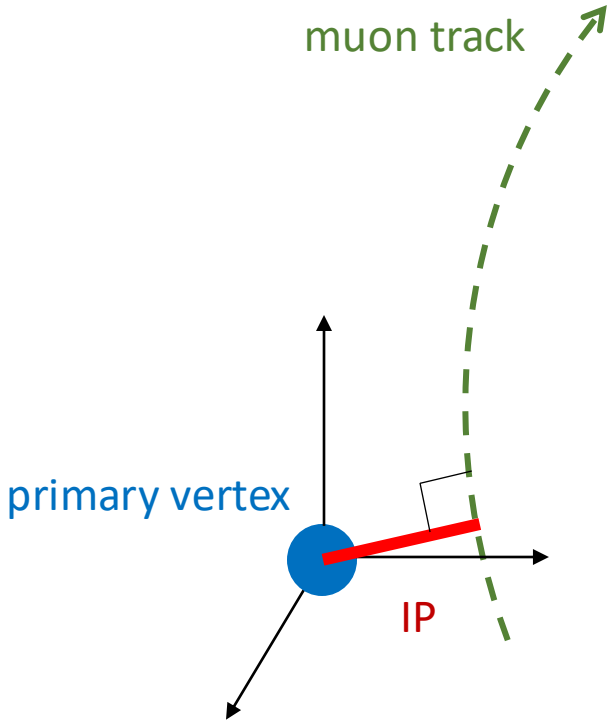

- **Select events with ≥7 muons.**
- A' decays are expected to be **prompt**.
- The signal muons should have **very small impact parameters**.
- Cut on the 3D impact parameter:

$$IP_{3D} < 0.007 \text{ cm}$$

- Also using sphericity and isolation cuts.

Muon backgrounds

- **Background: any process that can give many muons.**
- Generally, there are 4 sources of muons:
  - **prompt muons:** coming directly from the hard scattering process (e.g., $Z \to \mu\mu$)
  - **heavy flavor decays:** b or c quarks created by the hard process or the parton shower that hadronize into B and D mesons that decay leptonically.
  - **light flavor decays:** pion or kaon in-flight decays. Created by either the hard process, the parton shower, or the underlying event.
  - **fake muons:** reconstruction failures that can fake muons.
- Last one negligible since CMS is awesome.
- Jets might contain light/heavy flavor muons → **c & b muons dominant**
- Processes with prompt muons can have jets too.
- Need combinations of these to reach ≥7 muons in an event.

Background estimation

- **Goal:** design an *almost background-less SR*.
- Use MC to predict muon backgrounds in the SR and adjacent regions.
- The dominant processes are QCD and DY.
- They statistically depleted in the SR.
- Use **extrapolation** from adjacent regions to SR to make up for missing statistics.

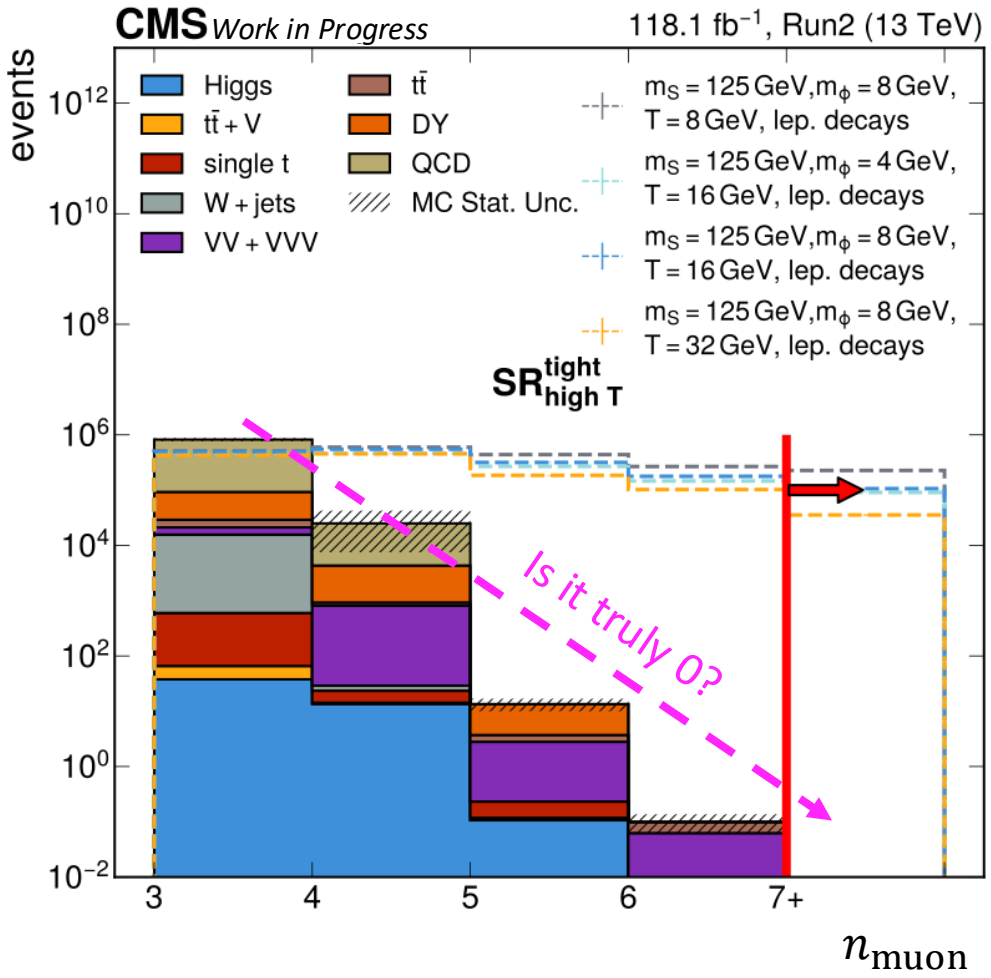

SRs before & after extrapolation

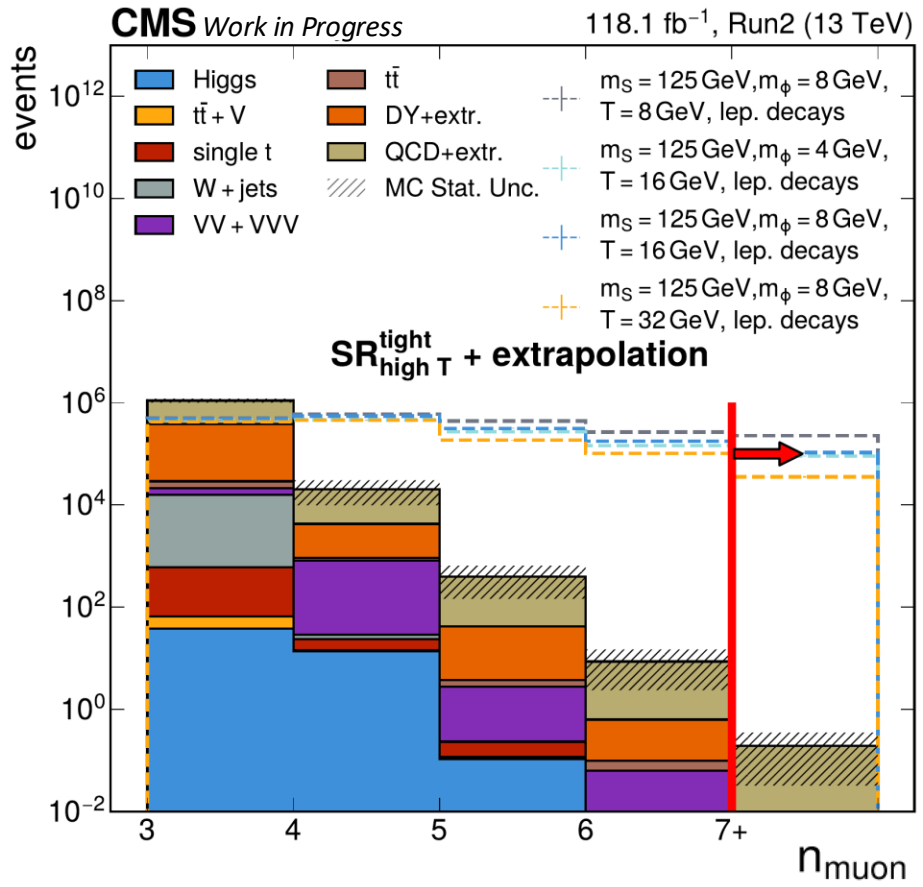

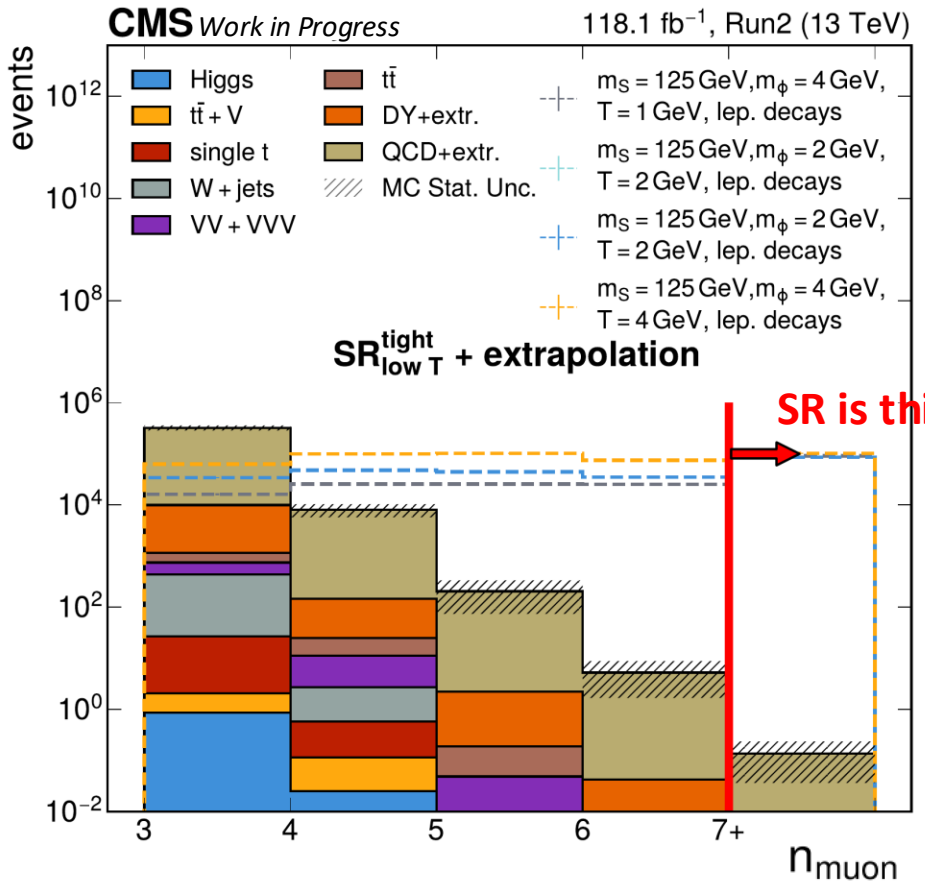

Two SRs optimized for different model parameter ranges.

Process	$SR_{high\ T}$	$SR_{low\ T}$
DY + extr.	0.0082 ± 0.0050	0.0010 ± 0.0021
QCD + extr.	0.18 ± 0.16	0.134 ± 0.099
Total bkg	$\mathbf{0.19 \pm 0.16}$	$\mathbf{0.135 \pm 0.099}$

Muon search upper limits

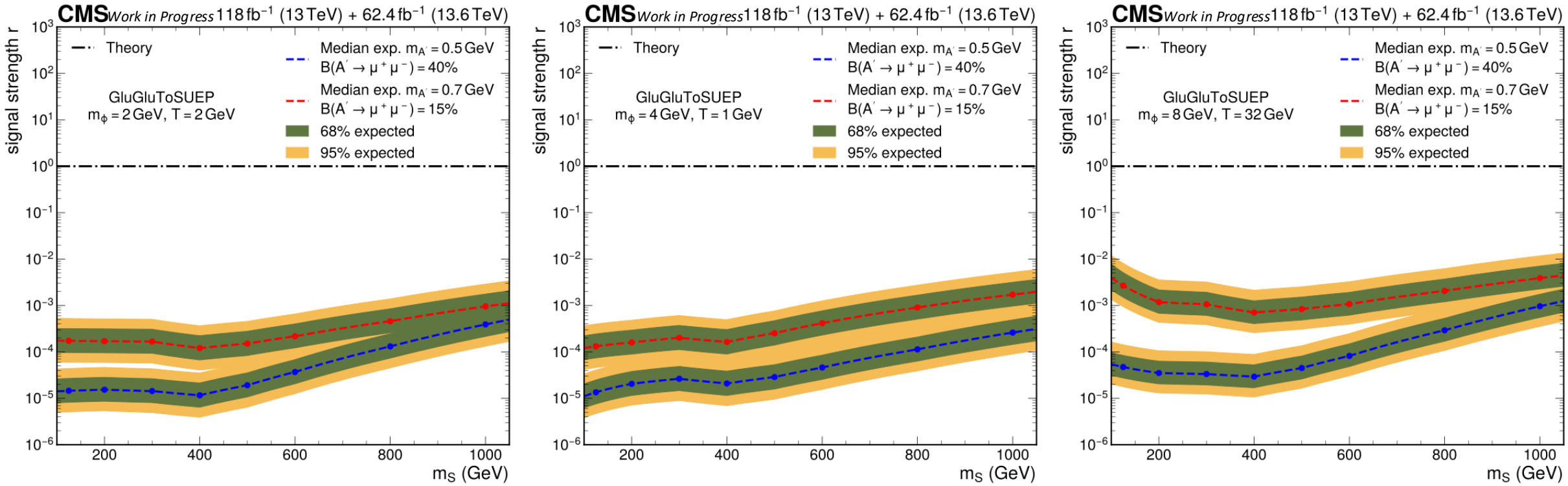

- **Very strong limits for entire m_S range. 3-4 orders of magnitude below theory σ.**
- Great improvement over offline search for the **leptonic decay scenarios**.
- Offline search cannot exclude most models with $T \geq 8$ GeV. Can exclude all these easily!
- Not trigger limited at low m_S.

Summary

- Soft Unclustered Energy Patterns can be the result of a hidden valley extension to the SM.
- Events with isotropic soft spray of charged particles.
- Two **searches for SUEP** with pp collision data were presented.
- First approach uses hadronic activity to target lower T models.
- The other utilizes muon multiplicity to target mid & high T models.
- Both search produce strong limits.
- Great complementarity → significant part of parameter space covered.

Thank you!

Backup slides

Nature is quantum

- Subatomic particles with relativistic energies are described by **Quantum Field Theory (QFT)**.
- Particles are represented as *excitations* of quantum fields.
- QFT allows particles to be **annihilated** and **created**.
- The available energy at the center-of-mass ($\sqrt{s}$) dictates which new states can be created.

Forces

- Particles are not isolated… They interact!
- We observe **four forces** in our world:

  gravity, strong force, weak force, and electromagnetic force

- Electromagnetic force is described by
  → **Quantum Electrodynamics (QED)**.
- There is a unified description of the weak force and QED
  → **the Electroweak Theory (EW)**.
- Strong forces are described by **Quantum Chromodynamics (QCD)**.
- We don’t know how gravity works at the quantum level…

Fields and gauge symmetries

- At a more fundamental level, interactions are introduced via the concept of **local gauge symmetries**.
- Our fields are invariant under local gauge transformations:

$$\psi \rightarrow e^{ia(x)}\psi$$

- Each interaction introduces its own symmetry.
- These symmetries are described by Lie groups.
- The total symmetry is described by the group:

$$\mathrm{SU}(3)_c \times \mathrm{SU}(2)_L \times \mathrm{U}(1)_Y$$

Formulating the model

- We can write down the Lagrangian for this:

$$\mathcal{L} = \underbrace{-\frac{1}{4} F^a_{\mu\nu} F^{a\,\mu\nu}}_{\text{gauge fields}} + \underbrace{\bar{\psi}_f i\gamma^\mu D_\mu \psi_f}_{\text{fermion fields}}$$

- Using the Euler-Lagrange equations, we can recover:
  - the Dirac equation for fermions
  - the wave equation for the photon
  - the Maxwell equations from the photon field
- **One *slight* problem:** most particles (except γ, g, and the neutrinos) are massive.
- However, the equation above doesn't contain any mass terms…

Solving the mass mystery

- Let's introduce a scalar field ϕ with the potential
$$V(\phi) = -\mu^2|\phi|^2 + \lambda|\phi|^4$$
- The minimum energy is the energy of the vacuum and is not at 0.
- The symmetry of the potential *has to* be broken
→ **Spontaneous symmetry breaking**
- Goldstone's theorem predicts a new scalar boson.
- Mixing the scalar field with the EW sector gives mass terms for $W^{\pm}$ and Z.
- Yukawa couplings to the fermions give them mass.
- This is the **Brout-Englert-Higgs mechanism**! → **2013 Nobel Prize in Physics**

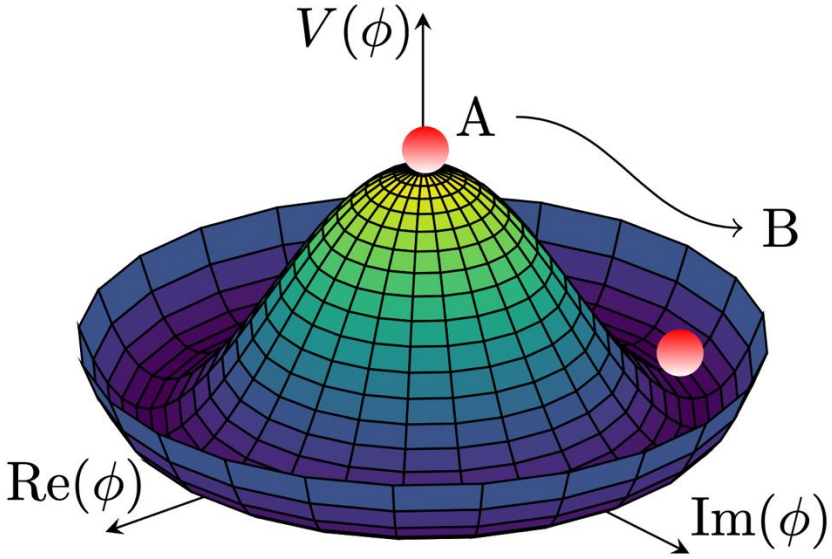

The Standard Model of Particle Physics

- This forms the **Standard Model of Particle Physics**.
- Perhaps, the most successful scientific model in existence.
- Described by the Lagrangian

$$\mathcal{L}_{\mathrm{SM}} = \underbrace{-\frac{1}{4} F^{a}_{\mu\nu} F^{a\,\mu\nu}}_{\text{gauge fields}} + \underbrace{\bar{\psi}_f i\gamma^{\mu} D_{\mu} \psi_f}_{\text{fermion fields}} + \underbrace{\left|D_{\mu}\phi\right|^2 - V(\phi)}_{\text{Higgs field}} + \underbrace{m_f \bar{\psi}_{f,L} \psi_{f,R}}_{\substack{\text{Yukawa couplings} \\ \text{between Higgs} \\ \text{and fermions}}}$$

Accelerating particles

Protons pass multiple stages to reach the LHC:

Stage	Final energy
LINAC 4	150 MeV
BOOSTER	2 GeV
PS	25 GeV
SPS	450 GeV
LHC	13.6 TeV

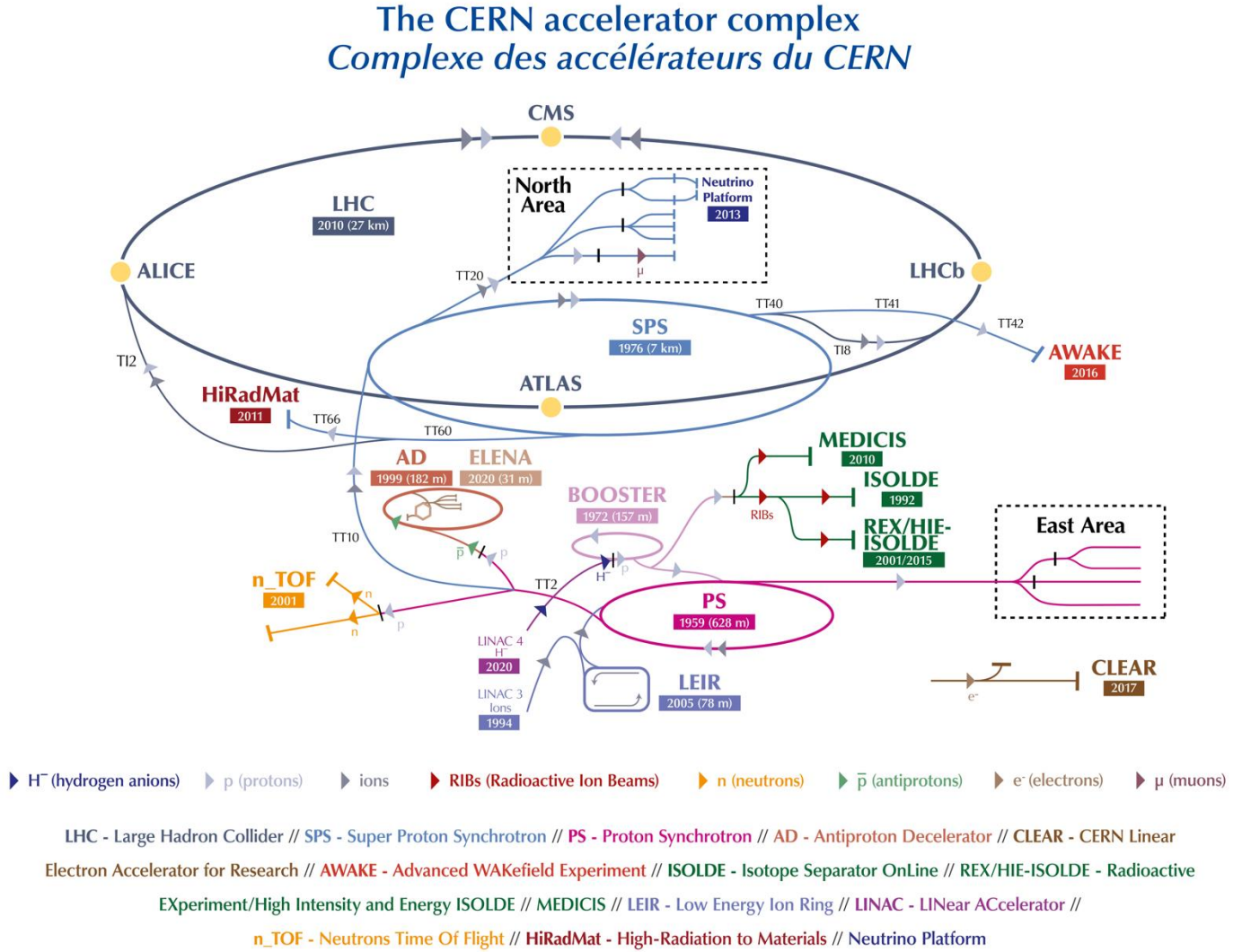

Trigger and data acquisition

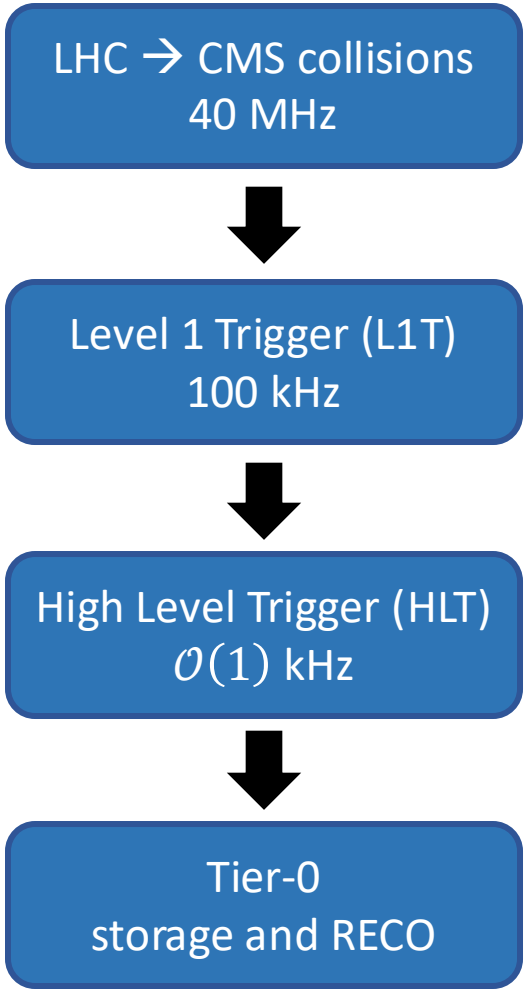

- Collision rate from the LHC is enormous.
- Two-level triggering system used to reduce it:
  - L1T: hardware-level trigger → 100 kHz
  - HLT: software-level trigger → $\mathcal{O}(1)$ kHz

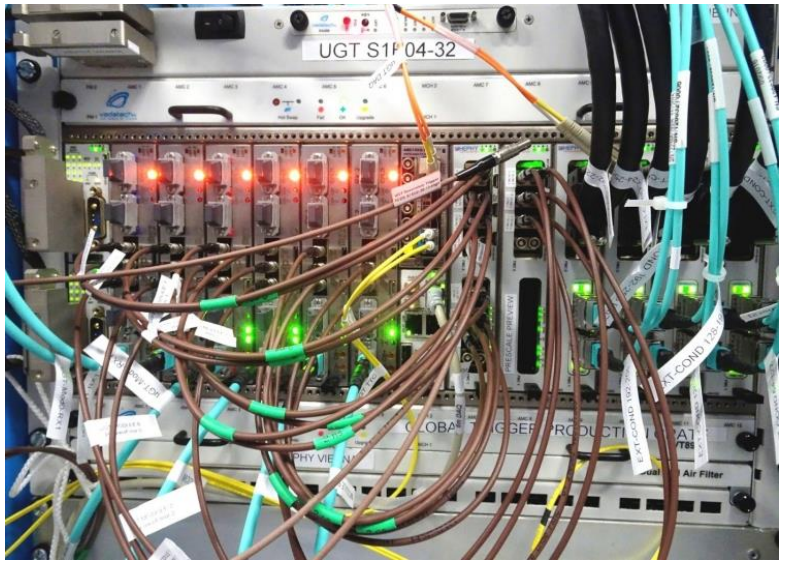

- At the same time, the DAQ system:
  - buffers the data as long as needed by the trigger to decide
  - collects and combines the data
  - sends the data to Tier-0 for storage

Detector operations

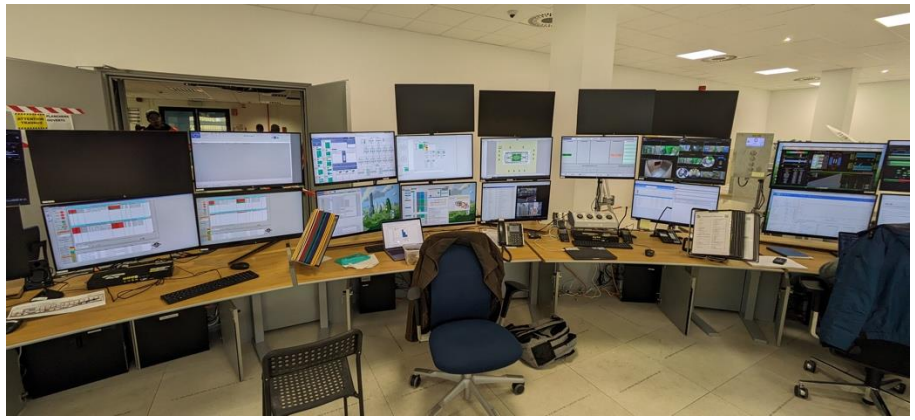

Technical shifter station in the new control room.
Taken on 02/28/2024.

The Underground Service Cavern during a safety tour.
Taken on 07/10/2022.

- 24/7 operations when any systems are on. (always except for Xmas break)
- 2 shifters minimum. 5 during data-taking periods.
- Dedicated shifts for:
  - Shift leader
  - Technical shifter
  - DAQ
  - Trigger
  - DQM

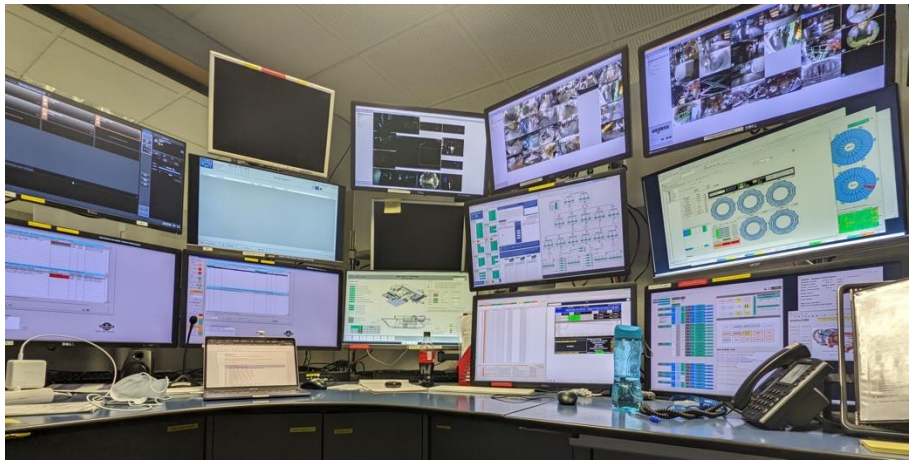

Technical shifter station in the old control room.
Taken on 07/10/2022.

Luminosity

- CMS has been collecting vast amounts of pp collision data.
- Run 2 was from 2016 → 2018.
- Run 3 began in 2022.
- Using the measured total inelastic pp cross section 69.2 mb
  - ➢ 25 quadrillion (10^{15}) pp collisions in Run 2 + Run 3

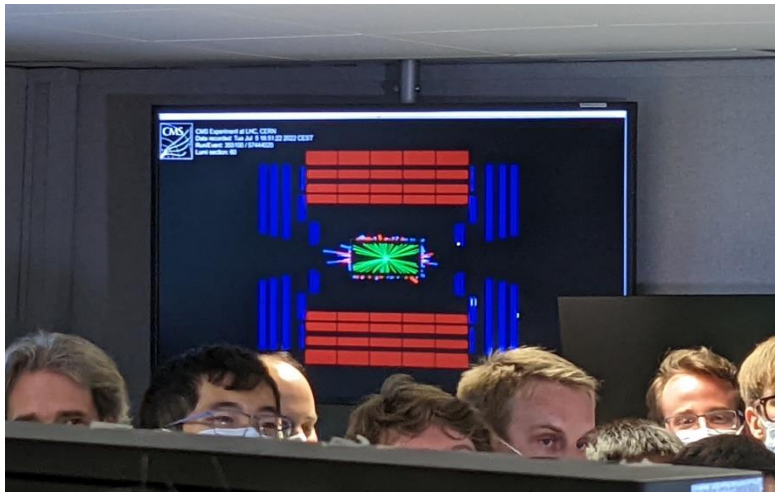

Some of the very first events of Run 3.
Taken on 07/5/2022.

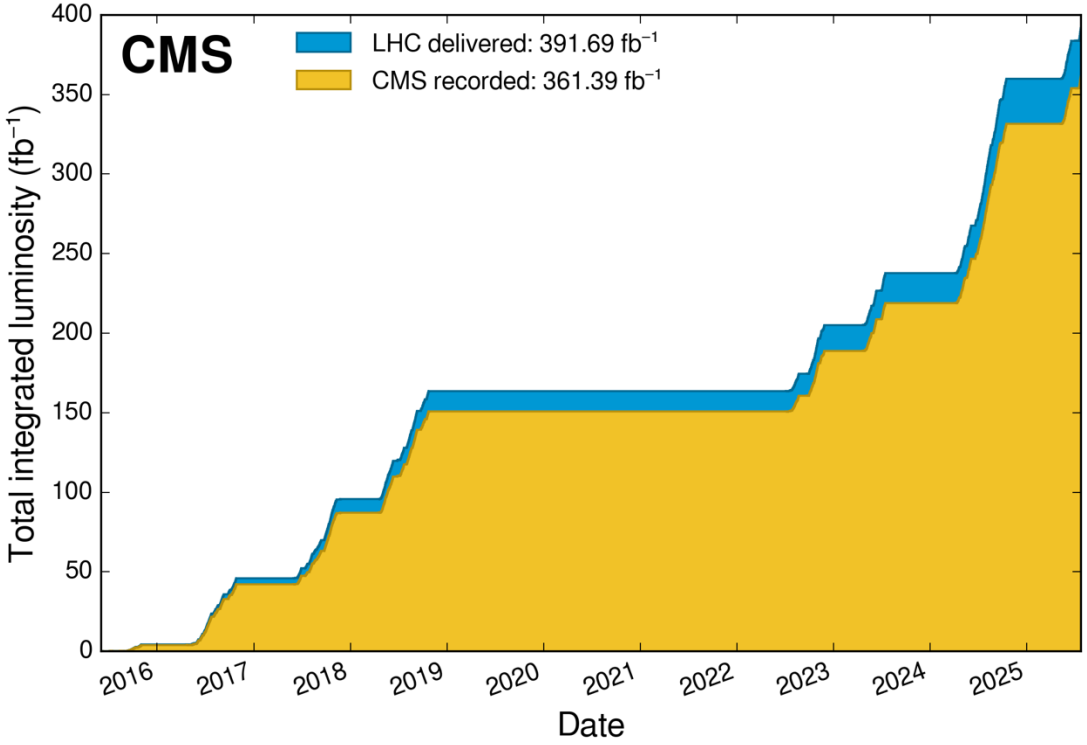

Plastic scintillators in HEP – past

Many experiments have used them in the past:

- **CDF**
  - Hadronic Calorimeter
- **DØ**
  - outer tracker (scintillating fiber)
  - Preshower detector

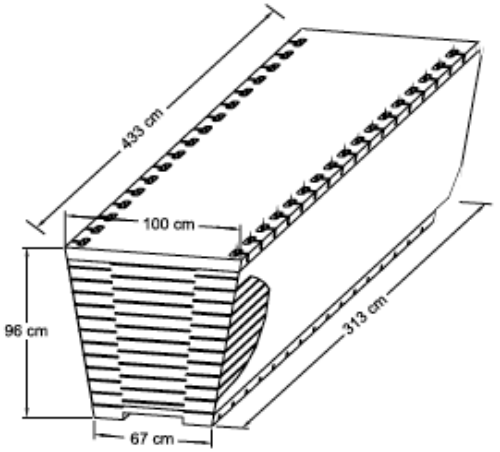

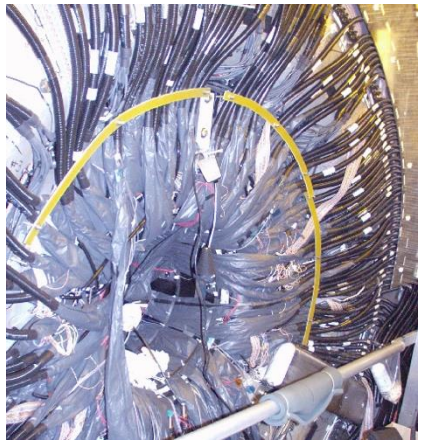

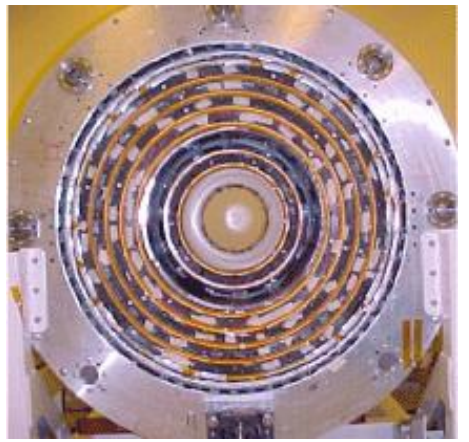

Related work

Many studies of the **dose rate dependence** exist:

- Previous measurements without wavelength-shifting fiber were **limited to high dose rates**.
- **Power-law dependence between D and R** was published by CMS in 2020.
- These low-R measurements are for tiles with wavelength-shifting fibers and 20% of the observed damage was in the fibers.

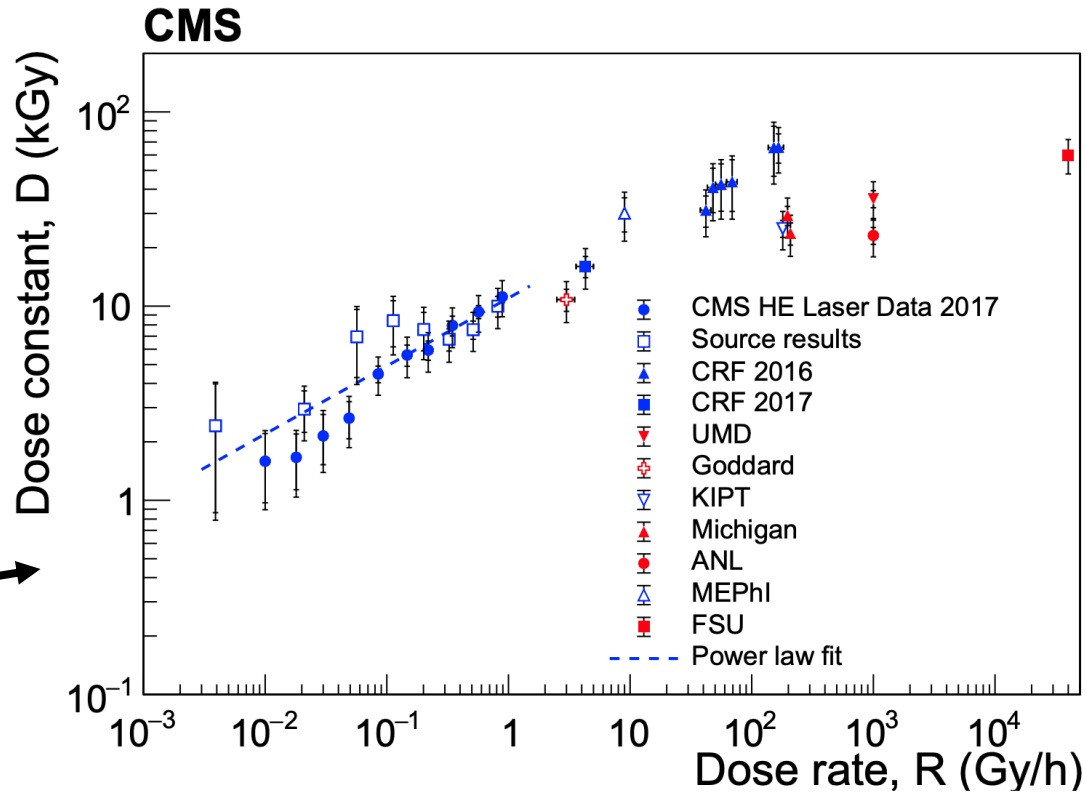

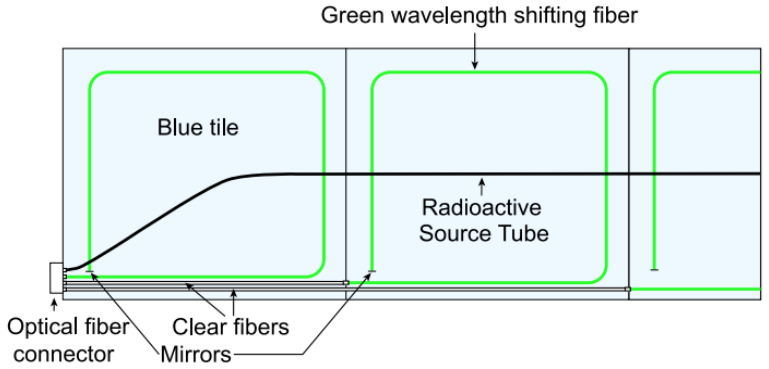

Samples & Irradiations

- Our samples are **scintillating rods** supplied by Eljen Technology (EJ-200 & EJ-260).
- EJ-200 has blue and EJ-260 green-emitting fluors.
- Green expected to be more rad-hard since color center formation expected much larger at shorter λ.
- Rods vary in **width** and concentrations of **fluors** and **antioxidants**. (Tables 1 and 2)
- Performed irradiations at **three different facilities**. (Table 3)

Table 1: 1x1x5 cm samples (units of nominal concentration)

Scintillator type	Substrate	Primary fluor	Secondary fluor	Antioxidants
EJ200, EJ260	PS	1	1	0, 1, 2
			2	1
		2	1	1
	PVT	1	1	0, 1, 2
			2	1
		2	1	1

Table 3: Irradiations

Irradiation facility	Source	Dose (kGy)	Dose rate (Gy/hr)
GSFC REF	Gamma	12.6	3.1
		42	9.8
NIST	Co-60	47	470
		70	83.4, 85.3
			744
			2570, 3900
GIF++	Cs-137	13.2	2.2

Table 2: Variable width samples

Substrate	Width (cm)	Fluors/ Antioxidants
PS	0.2, 0.4, 0.6, 0.8, 1.0	Nominal concentrations
PVT	0.2, 0.4, 0.6, 0.8, 1.0	

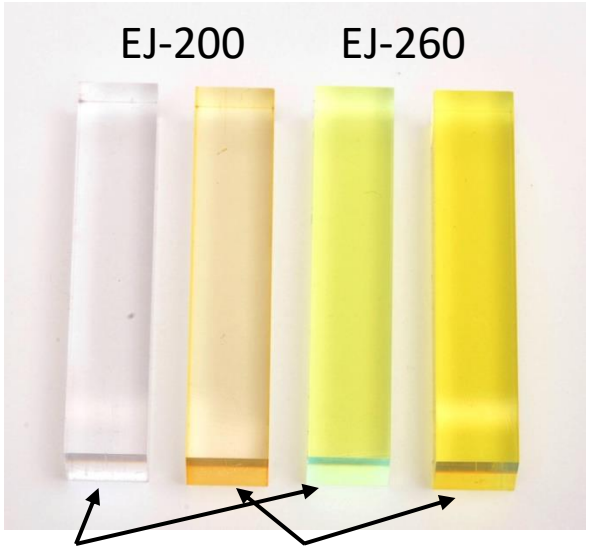

Methodology – Measuring T

- Used a Varian Cary 300 spectrophotometer to measure **transmission**.
- The **pseudo inverse of D** is defined as:

$$\mathcal{D}^{-1} = \frac{\ln(T_o) - \ln(T_f)}{d}$$

where T_o and T_f are the transmissions before and after irradiation, and d is the total dose.

- The **values of $\mathcal{D}^{-1}$** indicate:
  - increase in T when negative
  - decrease in T when positive
- A typical **unirradiated** sample:
  - very low transmission at the absorption spectrum of the fluors
  - high transmission at the emission spectrum of the fluors

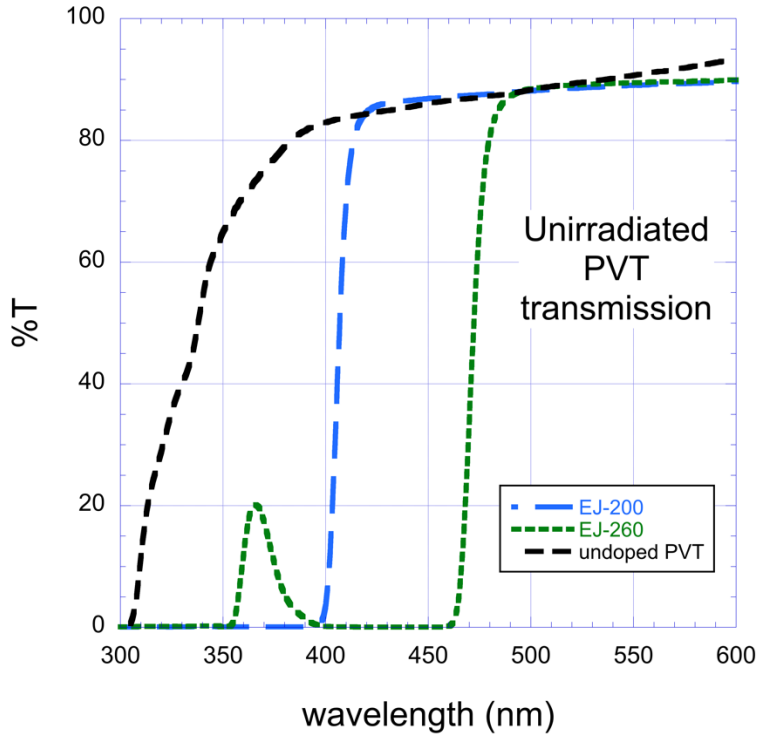

Results – Transmission

Some general remarks:

- Large positive values of $\mathcal{D}^{-1}$ indicate **color center formation**.
- Negative values probe **fluor destruction**.

Both are indicators of radiation damage.

Our observations show:

- Radiation damage for both scintillator types.
- **Fluor destruction** for the blue scintillator (EJ200).

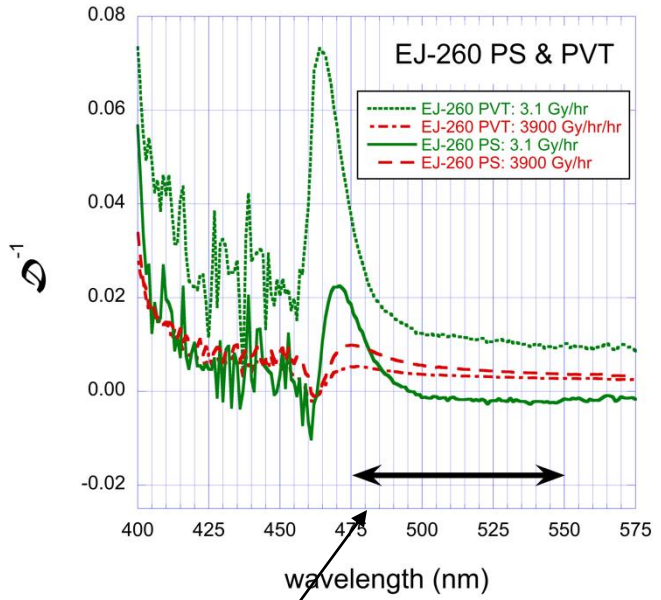

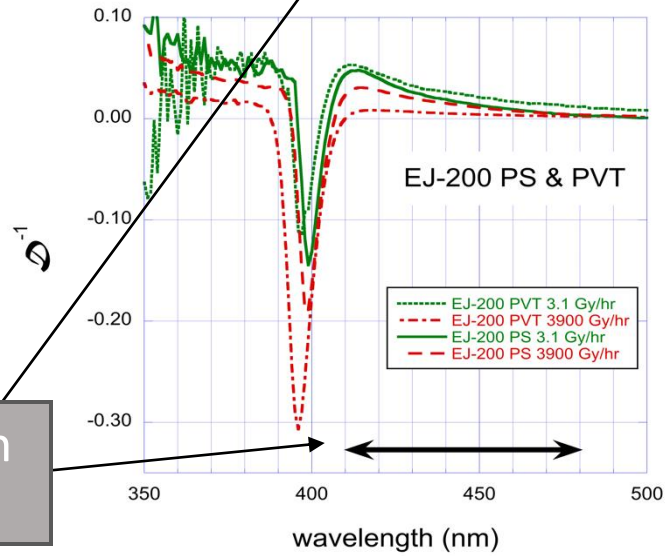

Black arrows indicate the emission spectrum of the secondary.

Radiation damage – Sandia model

- A similar model for radiation damage can be motivated from polymer photo-oxidation.
- Free radial reaction chain with initiation, propagation, and termination steps

Oxygen diffusion:

$$\frac{\partial C(x,t)}{\partial t} = D\frac{\partial^2 C(x,t)}{\partial x^2} - R(C(x,t)) \qquad (1), \text{ and}$$

Reaction rate:

$$R(C(x,t)) = \frac{c_1 C(x,t)}{c_2 C(x,t) + 1} \qquad (2)$$

- Solved numerically until the irradiation steady state is reached.
- Very similar effects observed

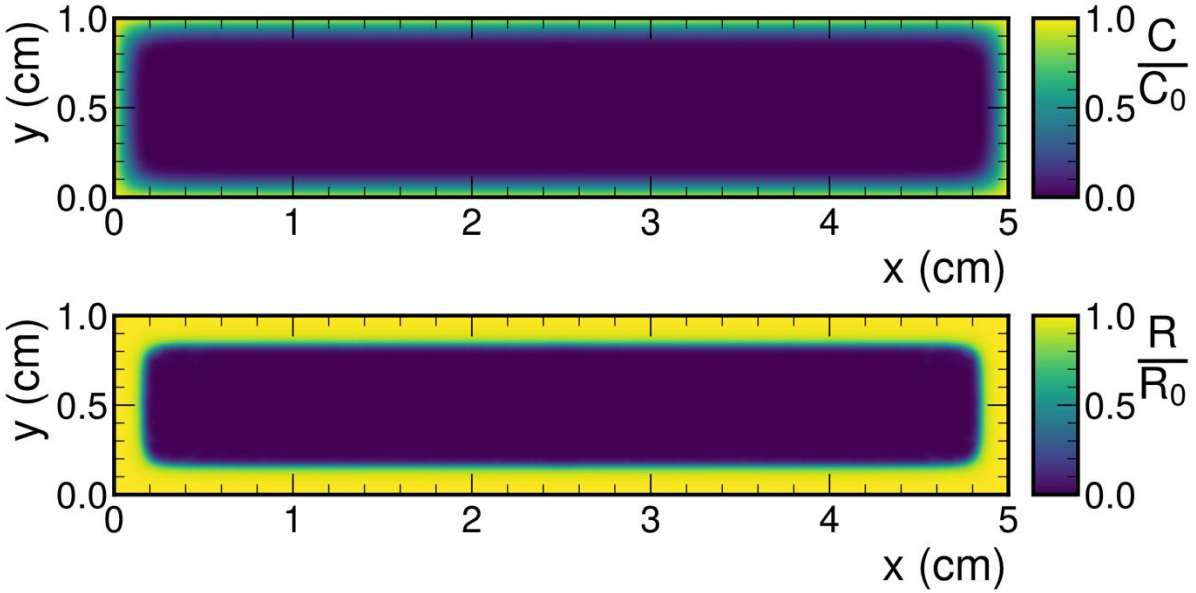

Measuring the index boundary depth

Procedure to **measure the index change depths**:

1. Photograph the 1×1 cm faces of the rods.
2. Denoise and improve contrast.
3. Extract lightness and profile it.
4. Calculate lightness gradient.
5. Smoothen with Savitzky-Golay filter.
6. Find peaks and their widths.
7. Calculate image scale (mm/px) using total rod width.
8. Obtain boundary depths.
9. Repeat over more pictures to estimate uncertainty.

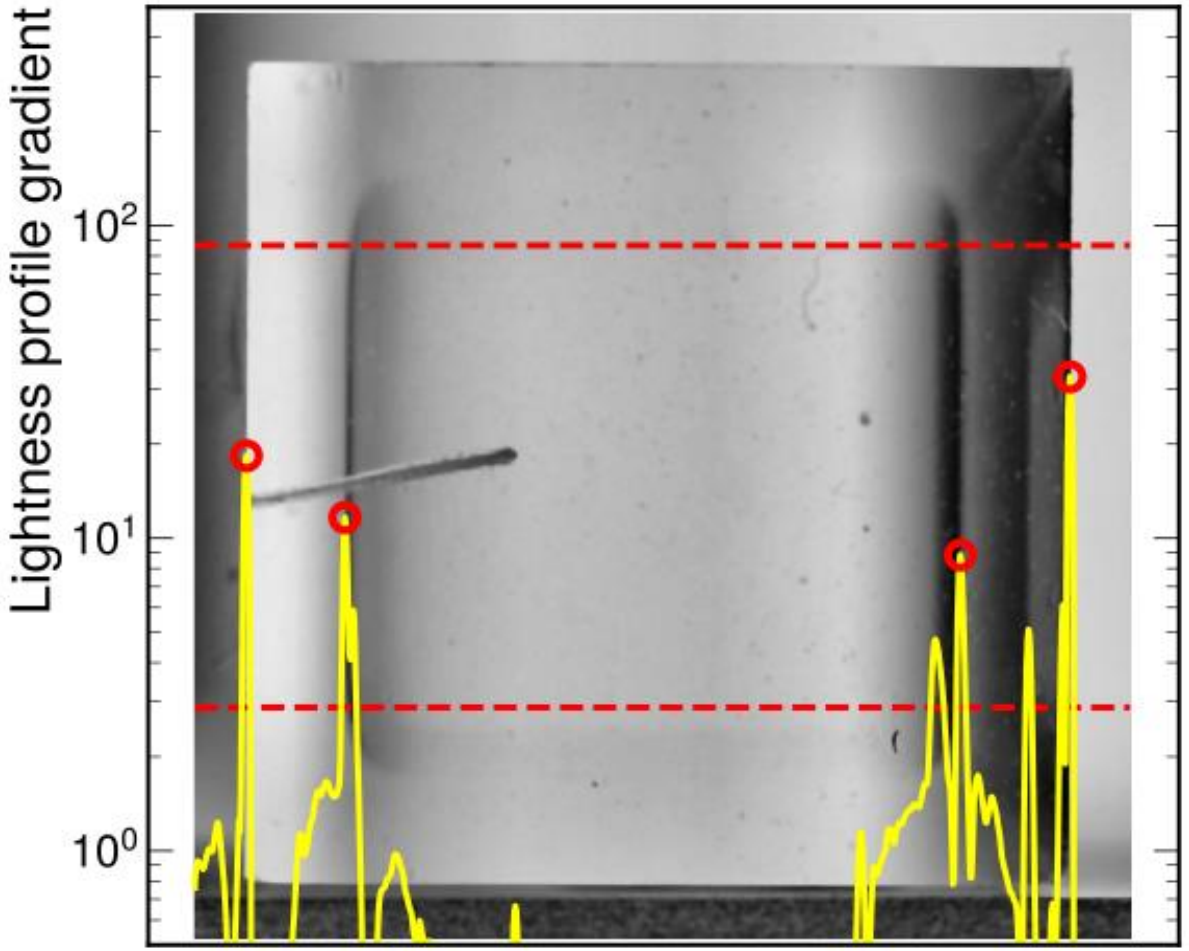

SUEP parameter space

arXiv:1906.10831

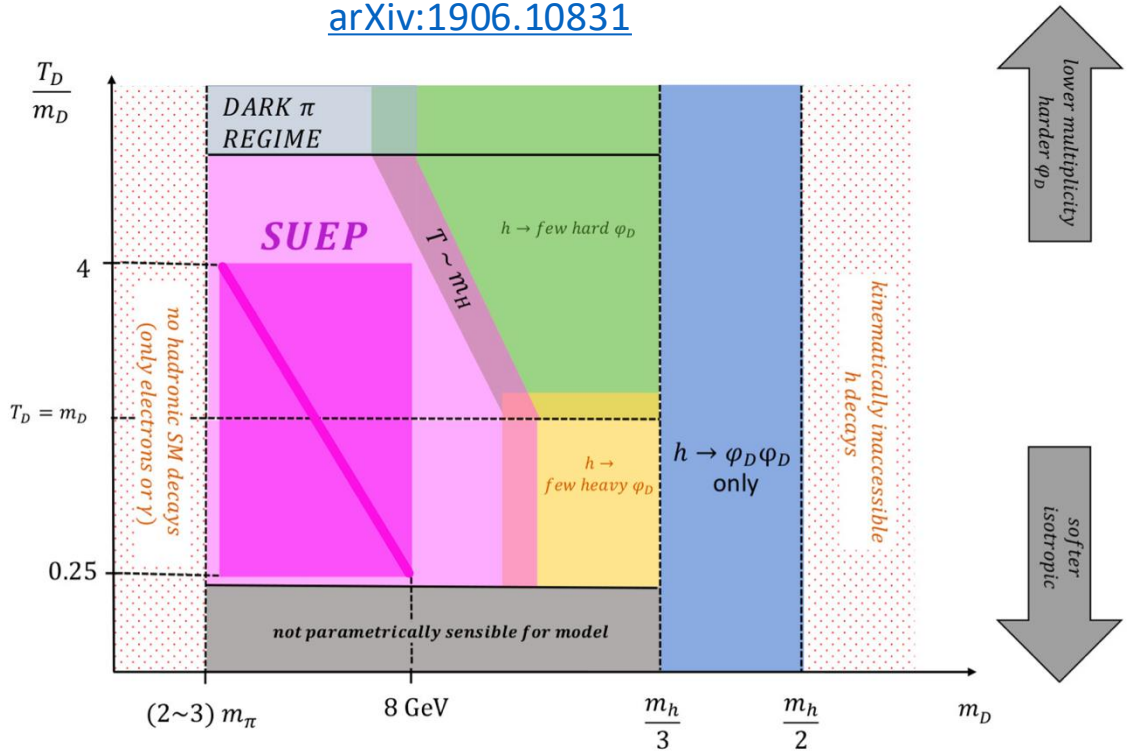

- The **SUEP parameter space** is large → **4-D**
- Parameters:
  - m_S
  - m_D (or m_φ)
  - $m_{A'}$
  - T
- The model has *"validity" limits*:
  - T and m_D should be of *similar order*.
  - m_D needs to be *sufficiently smaller* than m_S.

- $m_{A'}$ affects directly the **branching fractions** of A' to SM particles.
- This is scanned with 3 values that correspond to 3 **decay modes**:
  - **Semi-hadronic**: $\mathrm{BR}(A' \to \pi^+\pi^-) = 70\%$, $\mathrm{BR}(A' \to l^+l^-) = 15\%$
  - **Leptonic**: $\mathrm{BR}(A' \to \pi^+\pi^-) = 20\%$, $\mathrm{BR}(A' \to l^+l^-) = 40\%$

$$l = e, \mu$$

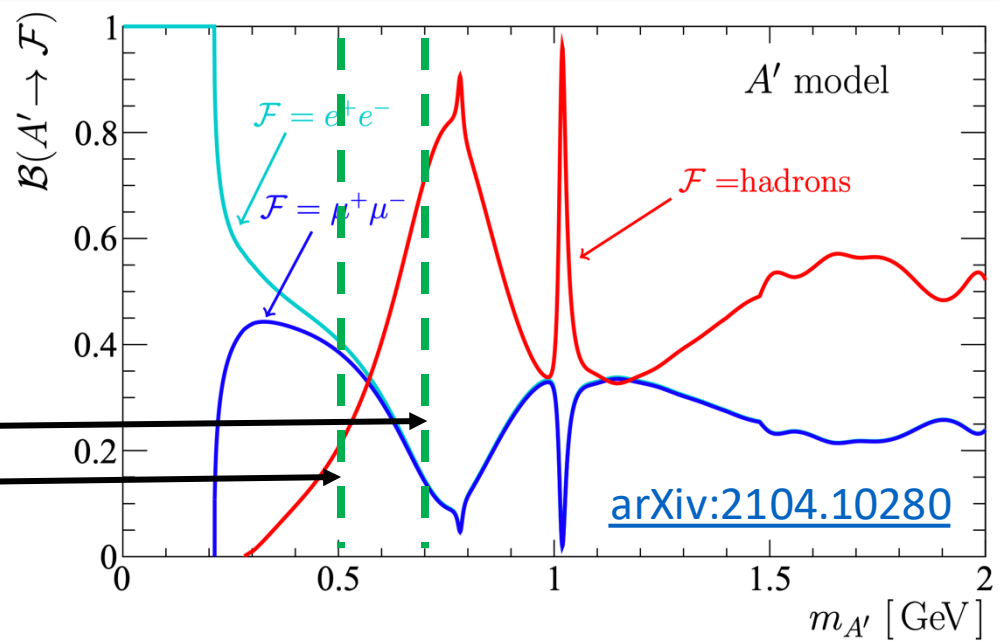

SUEP landscape in CMS

The SUEP program in CMS includes analyses that target different production modes or regions of the SUEP parameter space:

1) gg-fusion

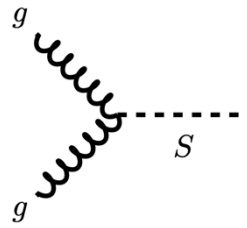

a) EXO-23-002: Search for Soft Unclustered Energy Patters (Offline)
PUB in PRL
b) EXO-23-001: Search for SUEPs using scouting dataset
GOING TO APP

Today

c) Leptonic decays search:
Targeting mostly leptonic BRs
EXO-25-011

2) Z associated production (ZH)

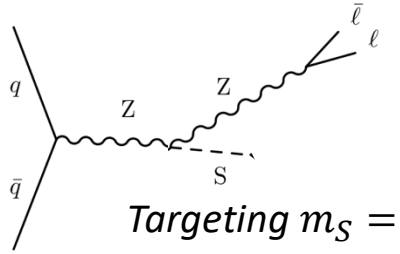

EXO-23-003: Search for SUEPs in association with a vector boson
PAS + **VH comb. (EXO-25-007)**
Targeting $m_S = m_H(125\ GeV)$

3) W associated production (WH)

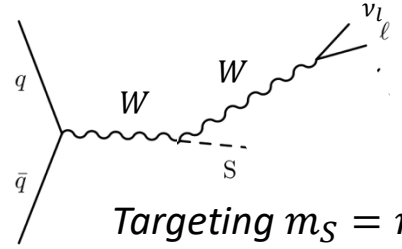

EXO-24-030: Complements **EXO-23-003 (ZH)**!
PAS + **VH comb. (EXO-25-007)**
Targeting $m_S = m_H(125\ GeV)$

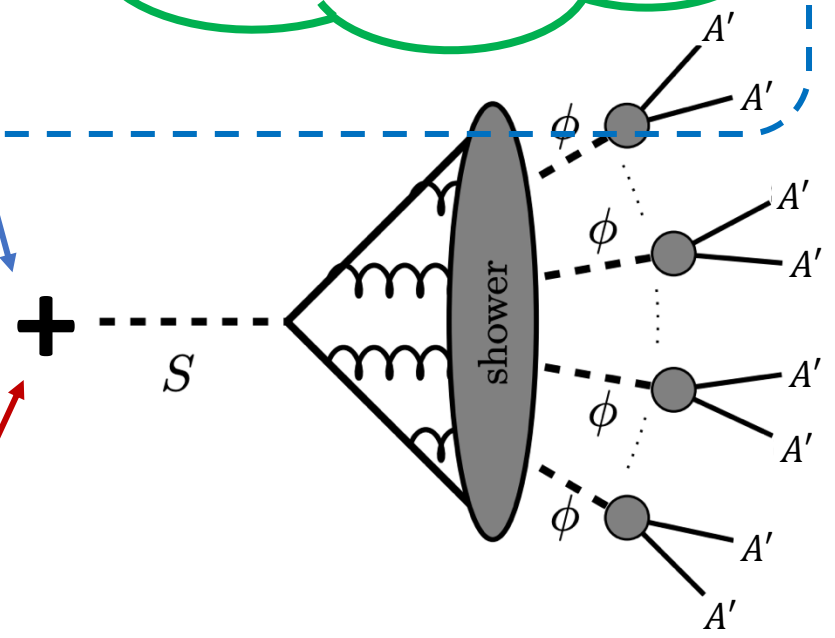

Other Higgs production modes can be used but expected event yields are too low

Data & MC

- **Data:**
  - **Run 2** (2016, 2017, and 2018) used.
  - Using `DoubleMuon` primary dataset.
  - In total: **118.1 fb^{-1} at 13 TeV**.
- **Signal:**
  - MC simulation with Pythia BSM Higgs module.
  - Scans over the 4D parameter space.
  - 320 scan points in total.
  - Theory cross sections given → LHC Higgs XS WG for BSM Higgs production.

- **BKG:**
  - ➢ MC simulations are used:

QCD (μ-enriched)
DY + jets $\rightarrow ll$ + jets ($m_{ll} > 50$ GeV, NLO)
DY + jets $\rightarrow ll$ + jets (10 GeV $< m_{ll} <$ 50 GeV, LO)
$t\bar{t}$ (POWHEG)
Single t (t-channel & tW)
VV (WW & WZ & ZZ)
VVV (WWZ & ZZZ)
W + jets
$t\bar{t}V$ ($t\bar{t}Z$ & $t\bar{t}W$)
Higgs ($H \rightarrow ZZ^* \rightarrow 4l$)

1) hard process
(Pythia, MadGraph, POWHEG)

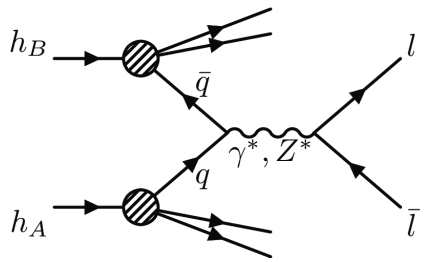

2) PS, hadronization (Pythia)

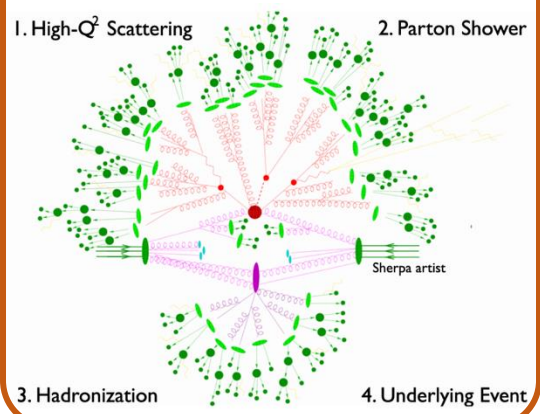

3) Full detector simulation
(Geant4)

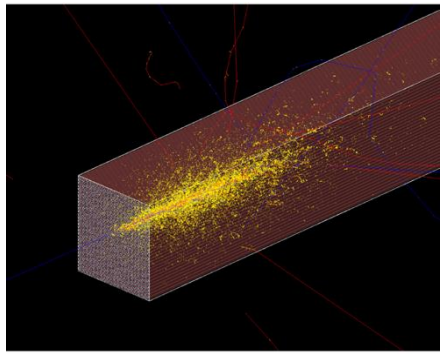

SUEP tagging

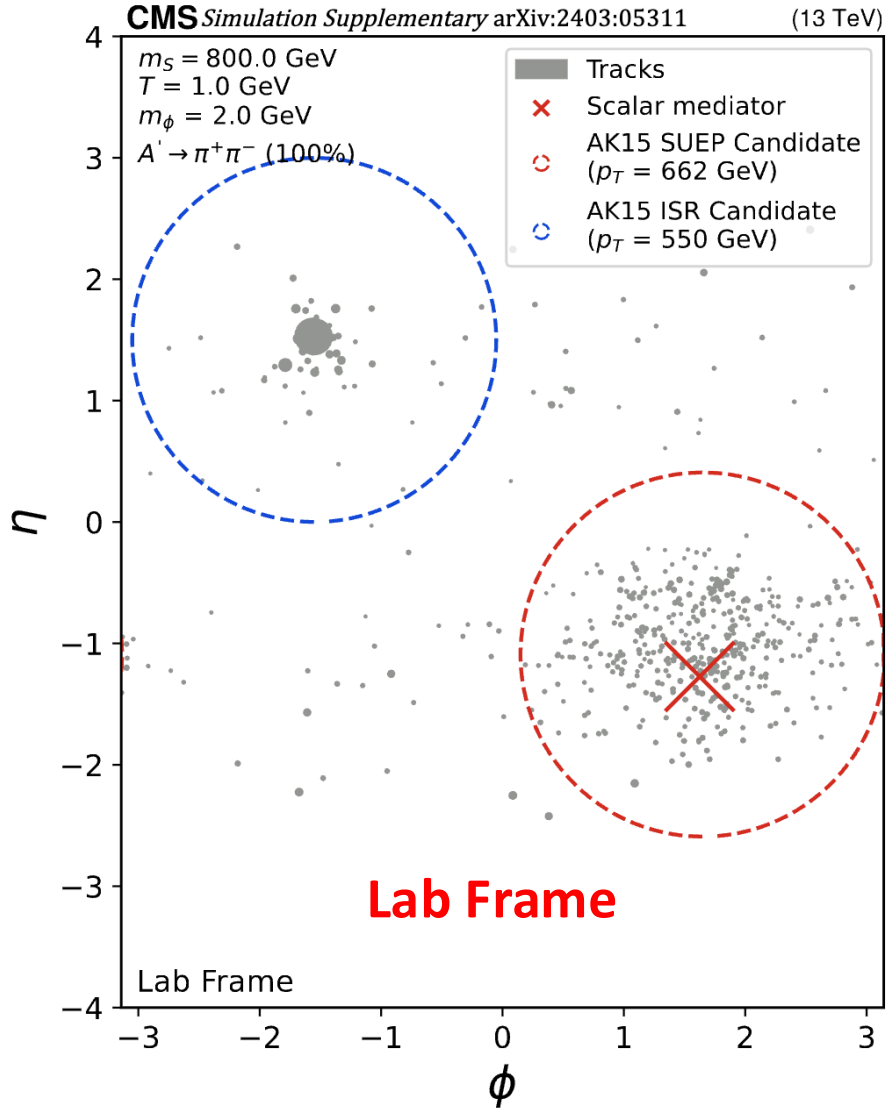

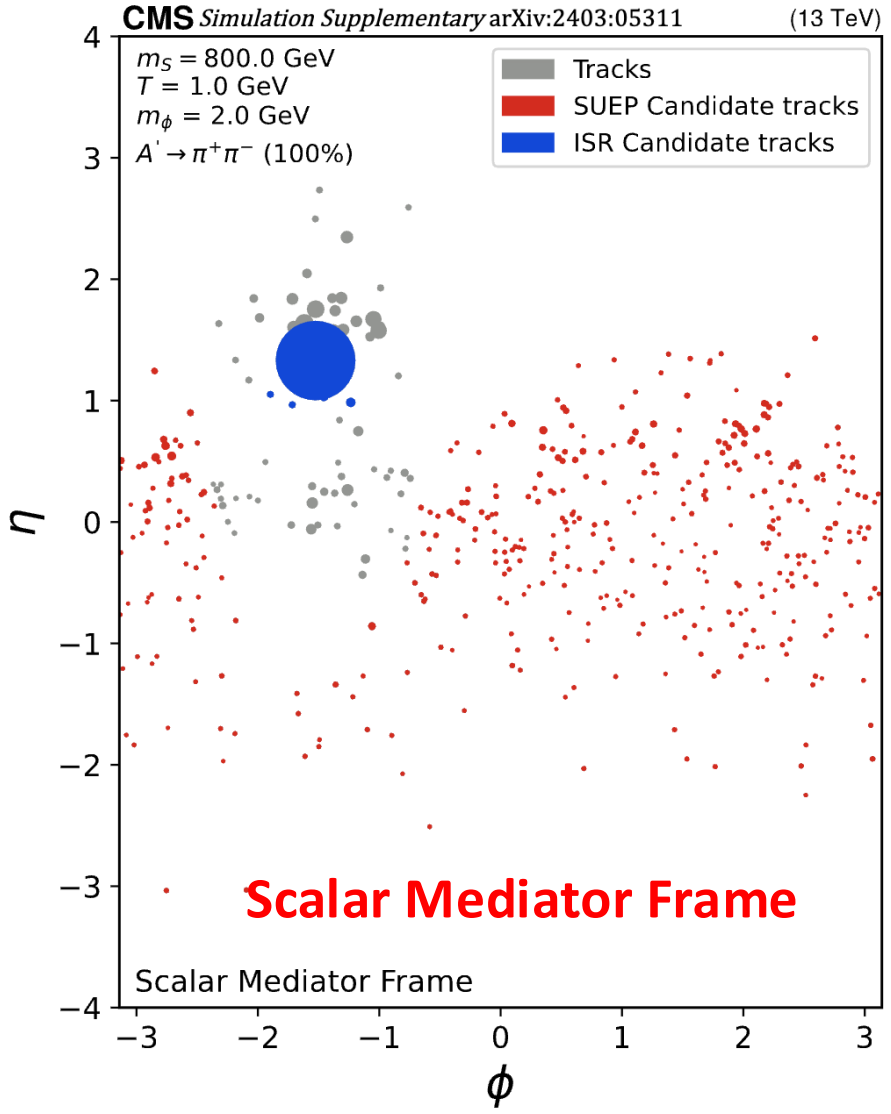

Search strategy

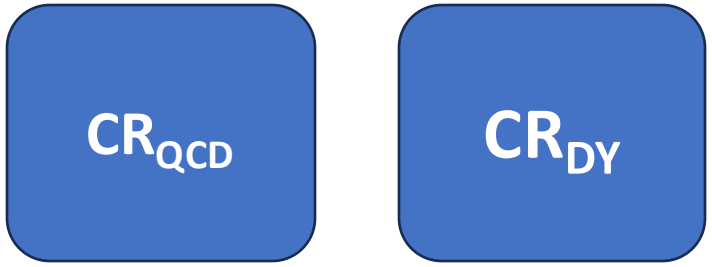

- Two **control regions** to get the QCD and DY normalization and constrain the systematics.

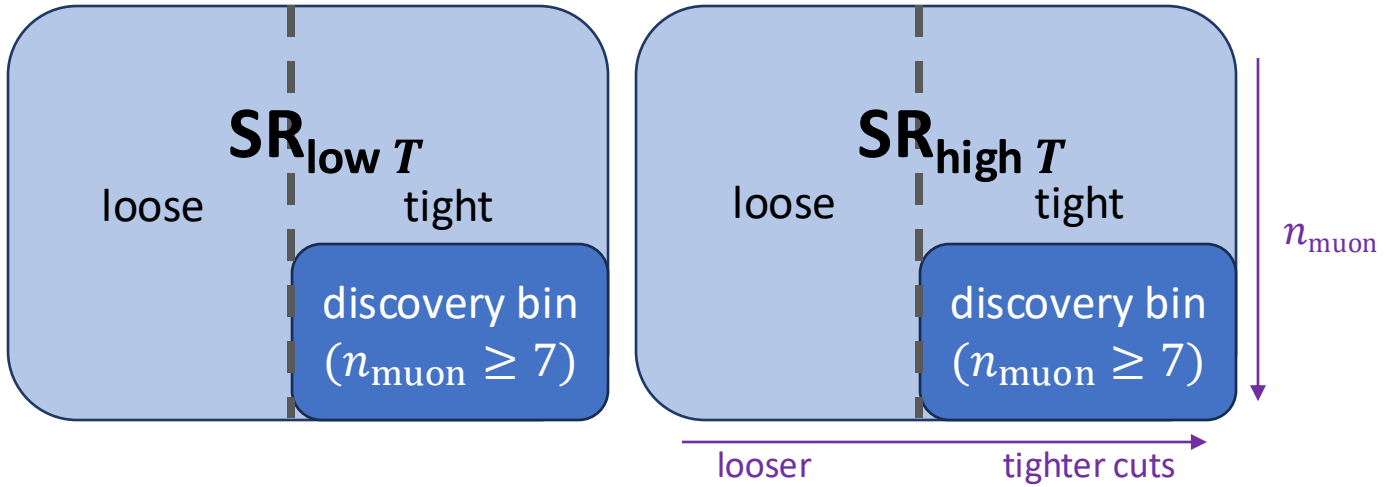

- Two **signal regions** with $n_{\mathrm{muon}} \geq 7$, targeting low and high temperature events.
- SR extended with **side bands** that go to lower n_{muon} and loosen the selections.
- Define these side bands as **tight and loose SR regions**.
- Side bands are used by the **extrapolation method** for the bkg prediction.
- *Eventually*, **only the regions** depicted by **dark blue** boxes are included in data fit.
- **Only the dark blue regions will be unblinded in data!**
- Not unblinding the side bands due to signal contamination
  → **Sizeable** bkg ($\gg 1$ event) *and* **large uncertainty**.
- SRs not orthogonal → not fitted simultaneously.
- *Instead*, picking most suitable SR for each scan point of the signal model.

Non-QCD bkgs

- List of processes:
  - DY (M-10to50 & M-50)
  - TT (powheg)
  - TTW & TTZ (NLO)
  - ST (NLO)
  - WJetsToLNu
  - VV & VVV (NLO)
  - HToZZTo4L (ggH, VBF, ZH, WH, ttH)
  - and many more I checked and found to be negligible.

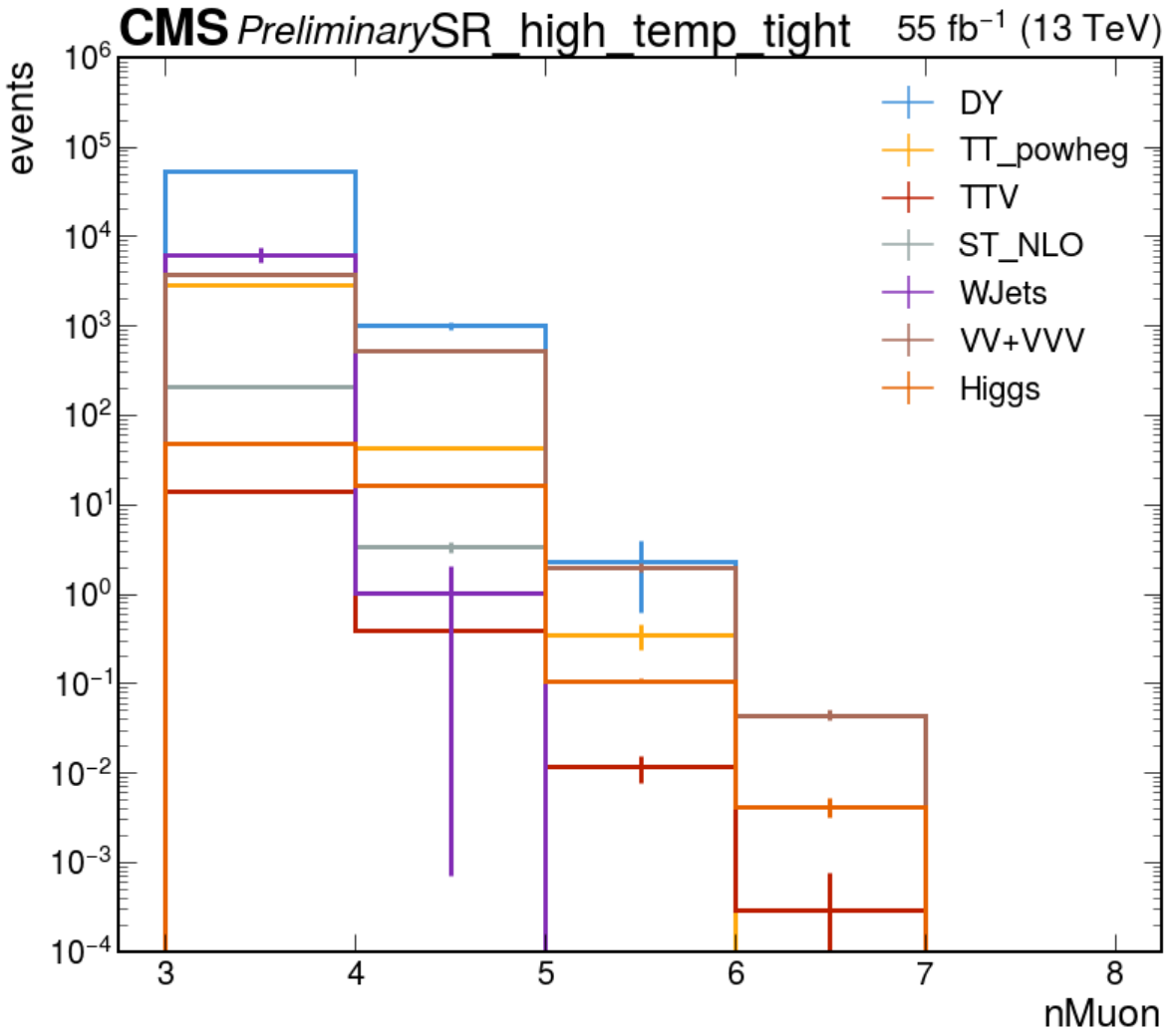

$SR_{\text{high } T}$ – Isolation cuts

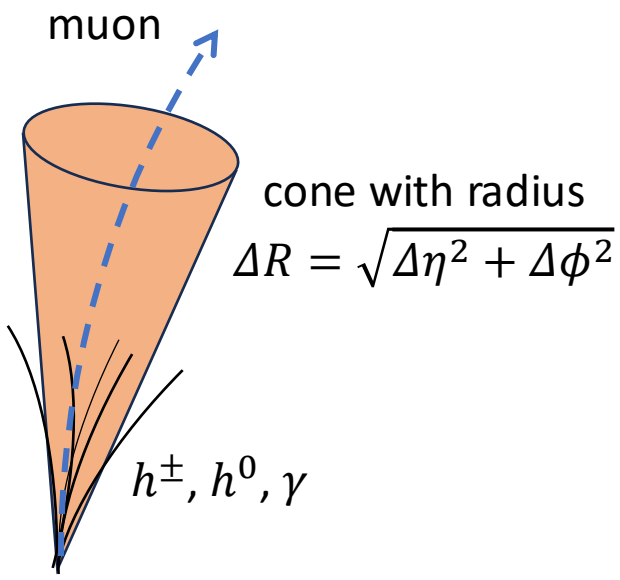

Reminder: $\eta \equiv -\ln\left(\tan\left(\frac{\theta}{2}\right)\right)$

θ: azimuthal angle

- High temperature signals → less particles with higher momenta.
- Muons will not be surrounded by a lot of other particles.
- Define **muon relative isolation**:

$$Iso_{\text{all}} = \sum_{i \in \{\text{all } h^{\pm}, h^0, \gamma\}}^{\Delta R_{\mu,i} < R_0} \frac{p_T^i}{p_T^{\mu}}$$

- Similarly, define a Iso_{neutral} only for h^0, γ.
- Require both **isolations** to be **below some threshold** for $SR_{\text{high } T}$.

Selections

- **Preselection:**
  - `HLT_TripleMu_*`
  - Muon MediumId
  - Muon $|d_z| < 0.2$ cm
  - ≥ 3 muons
- **CR_{QCD}:**
  - ✓slightly higher dxy
    $(0.01 \text{ cm} < |d_{xy}| < 0.2 \text{ cm})$
- **$SR_{high\ T}$:**
  - ✓Muon $IP_{3D} < 0.007$ cm
  - ✓Very loose muon isolation (< 0.65)
  - ✓Muon neutral isolation (< 0.5)
  - ✓Limit on OS dimuon mass (< 70 GeV)
- **CR_{DY}:**
  - ❖Prompt muons:
    - ✓$p_T > 25$ GeV
    - ✓$Iso < 0.1$
    - ✓Very tight impact parameter selections
      ($|d_{xy}| < 0.008$ cm, $|d_z| < 0.01$ cm, $IP_{3D} < 0.01$ cm)
    - ✓OS pair within Z peak mass window
  - ❖Non-prompt muons:
    - ✓$Iso > 0.1$
    - ✓Non-prompt
      ($|d_{xy}| > 0.01$ cm, $|d_z| > 0.01$ cm, $IP_{3D} > 0.015$ cm)
- **$SR_{low\ T}$:**
  - ✓Event sphericity $S_1 > 0.7$
  - ✓Muon $IP_{3D} < 0.007$ cm
  - ✓Upper limit on muon p_T (< 35 GeV)
  - ✓Limit on OS dimuon mass (< 35 GeV)

For both $SR_{high\ T}$ and $SR_{low\ T}$, the discovery bin is for nMuon≥7.

Sources of muons in the SR

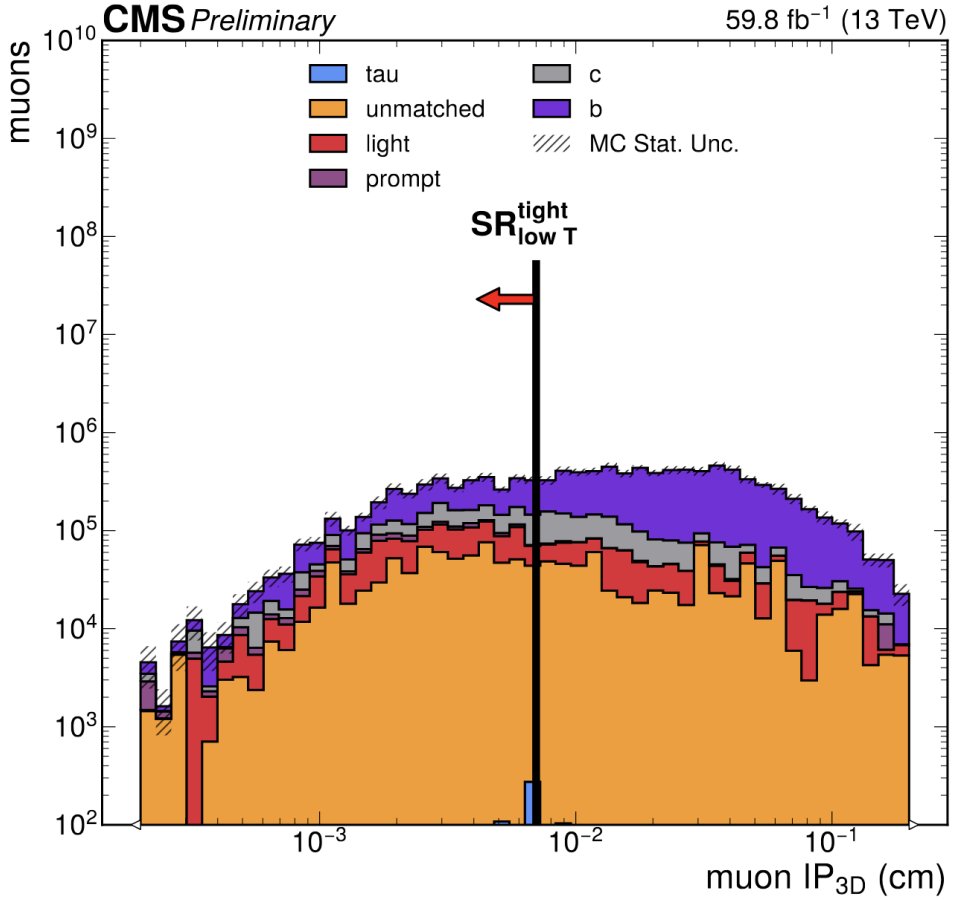

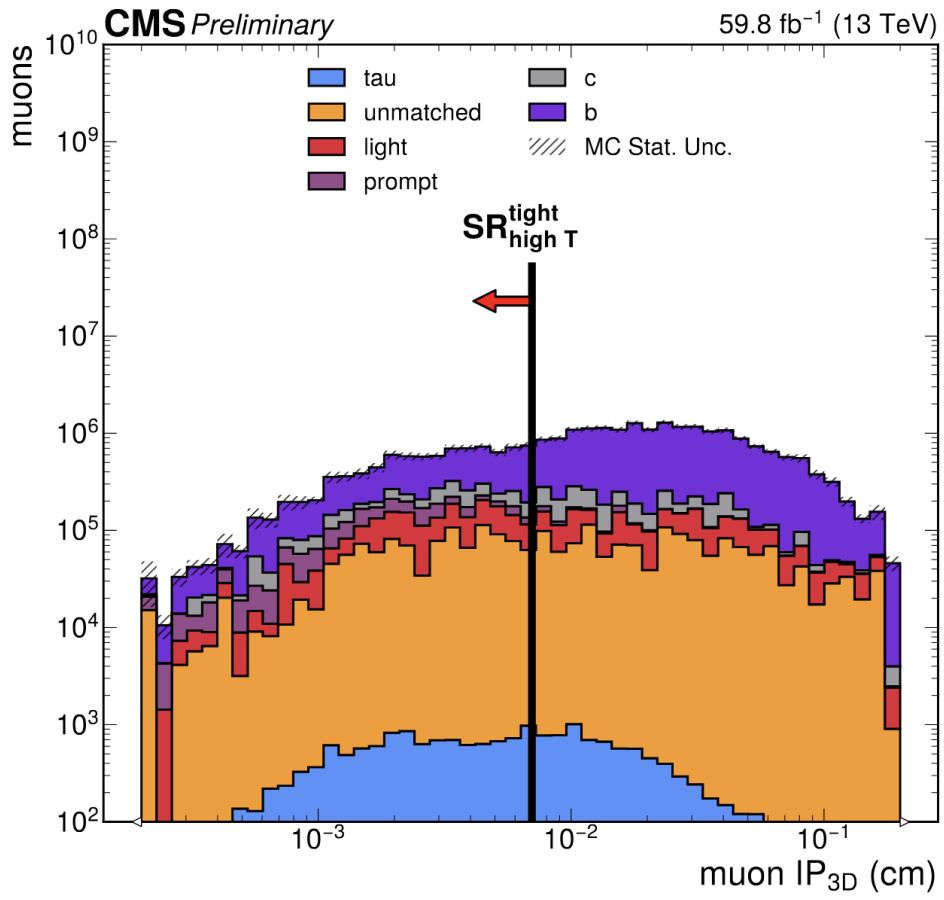

- The B meson decays dominate the non-isolated muons collection.
- D meson decays are next.
- Followed by prompt muons.

Control regions (Run 2)

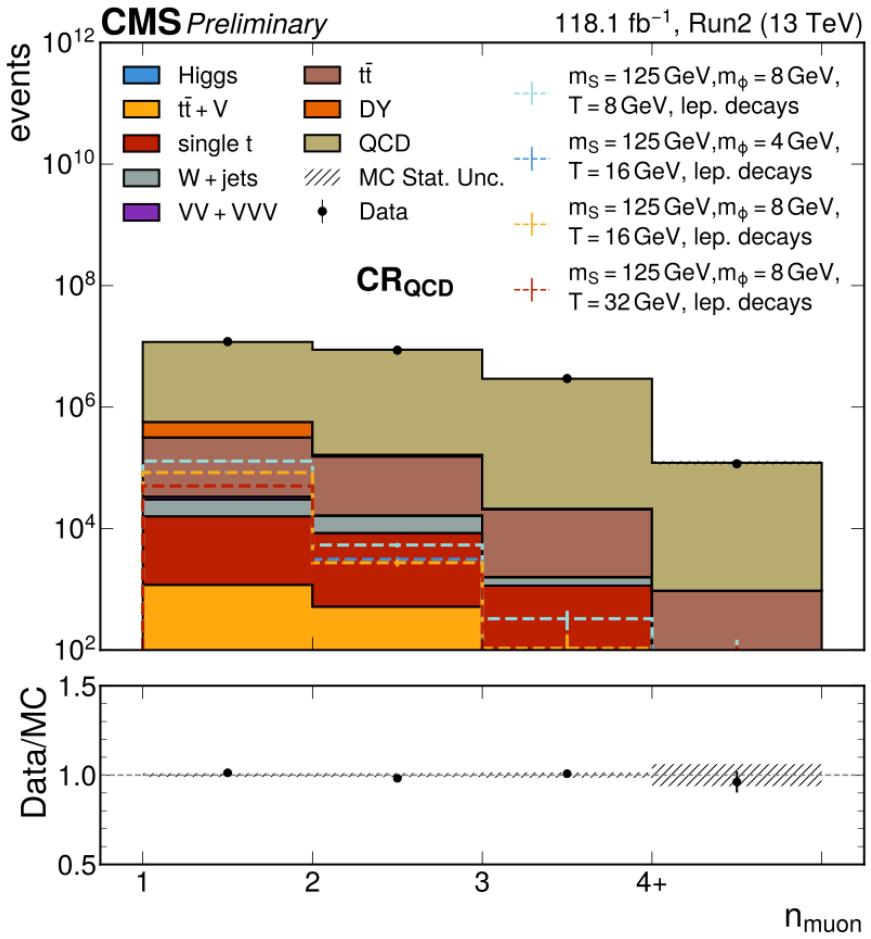

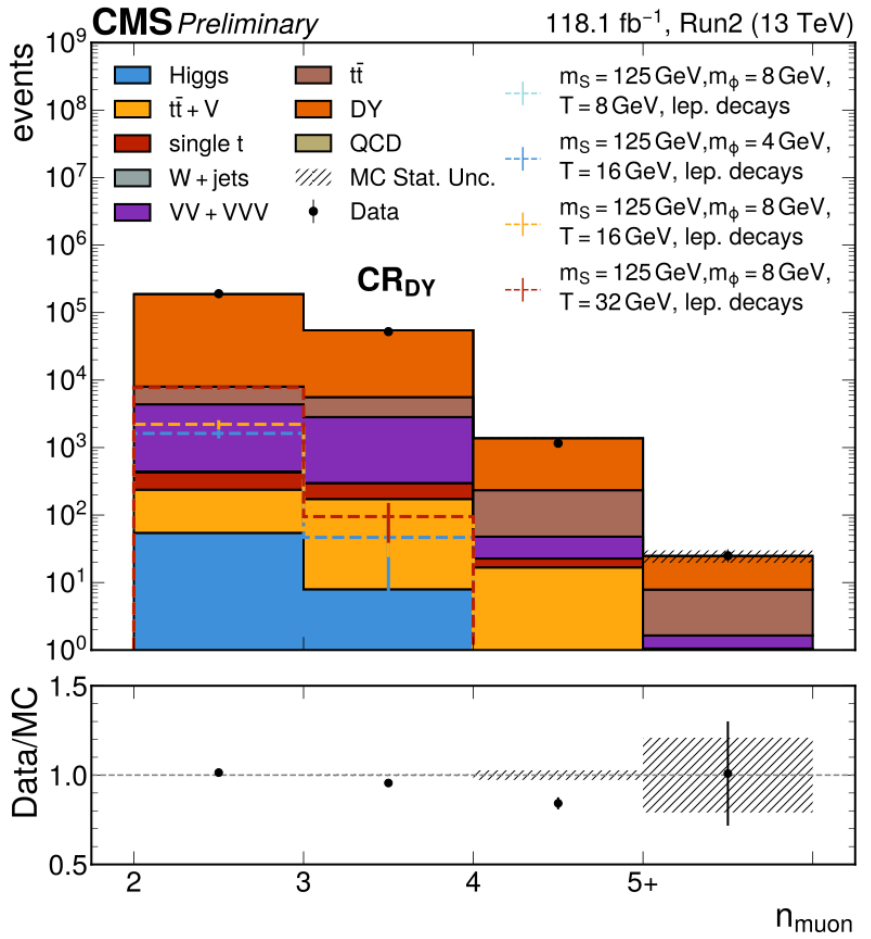

- These are used in Combine to normalize QCD and DY MC and constrain the systematics.

Note: k-factors have been applied to the MC in these plots to normalize them to data. The k-factors are derived by dividing the total yield of the dominant process by the total yield in data minus the total yield sum of all other MC.

Signal regions (Run 2)

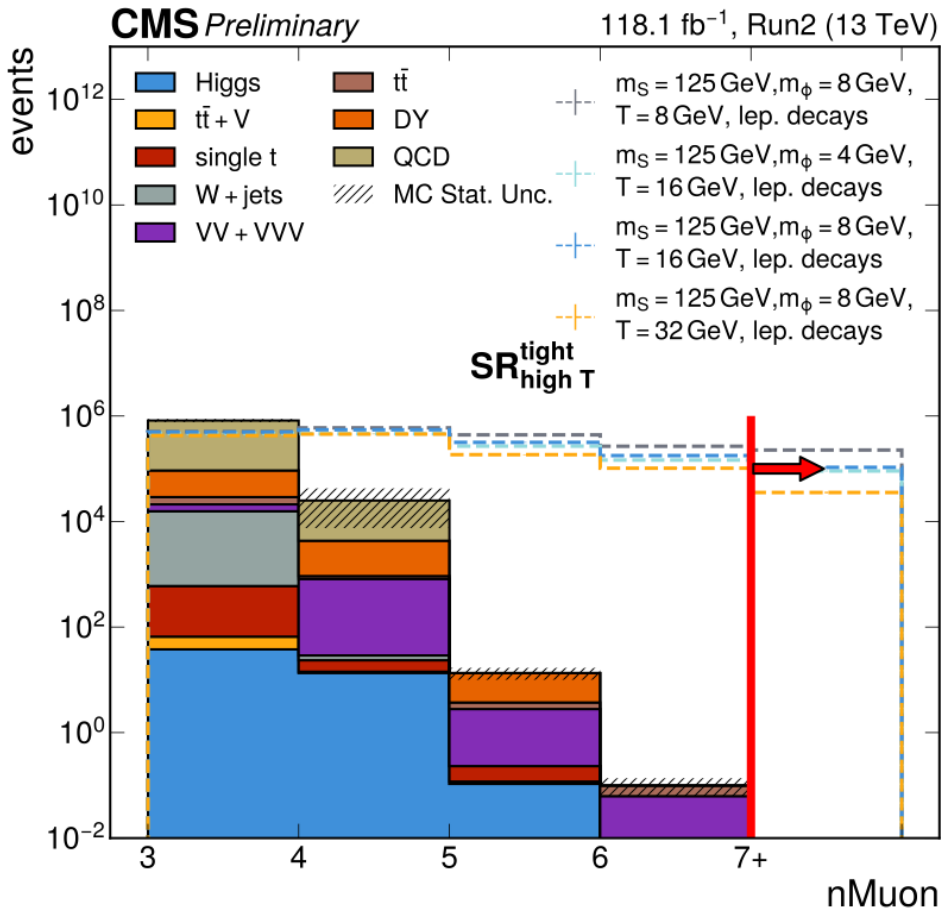

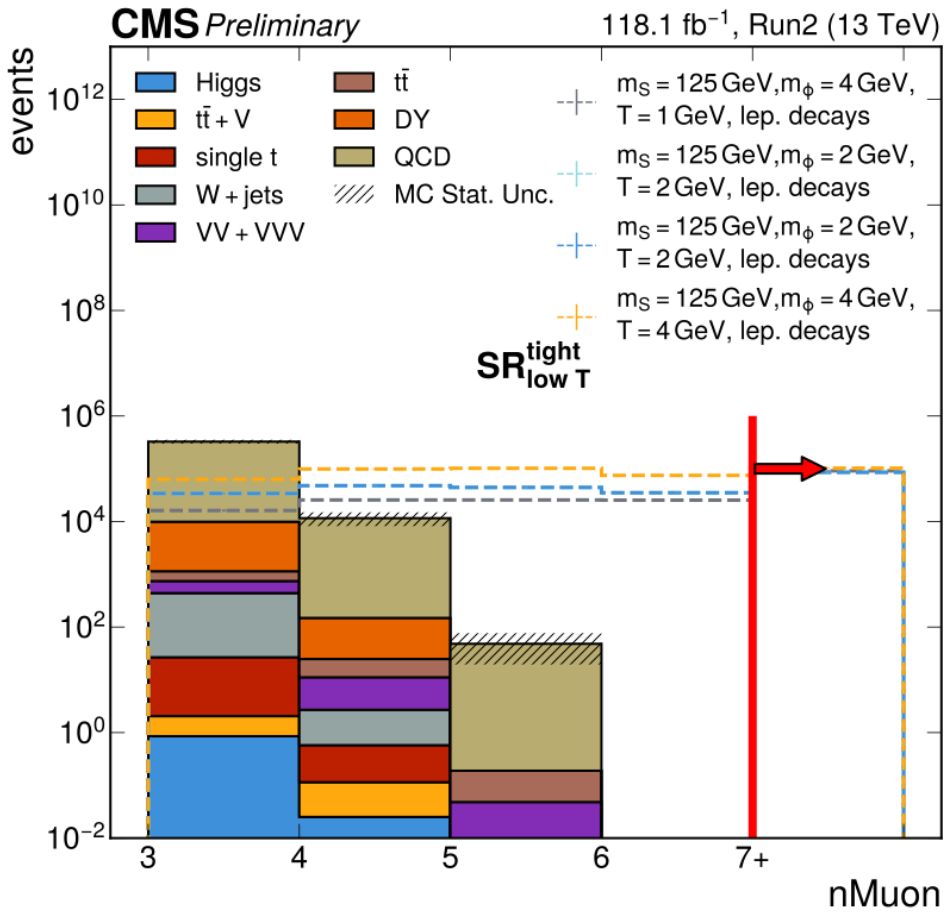

- Signal regions targeting **high & low T** SUEP models (left & right plots, respectively).
- The **discovery bins** are indicated with the red line & arrow, and they include events with **≥7 muons**.
- DY & QCD are the processes with the largest contributions, but they are statistically depleted for $n_{muon} \geq 5$.

SRs before extrapolation

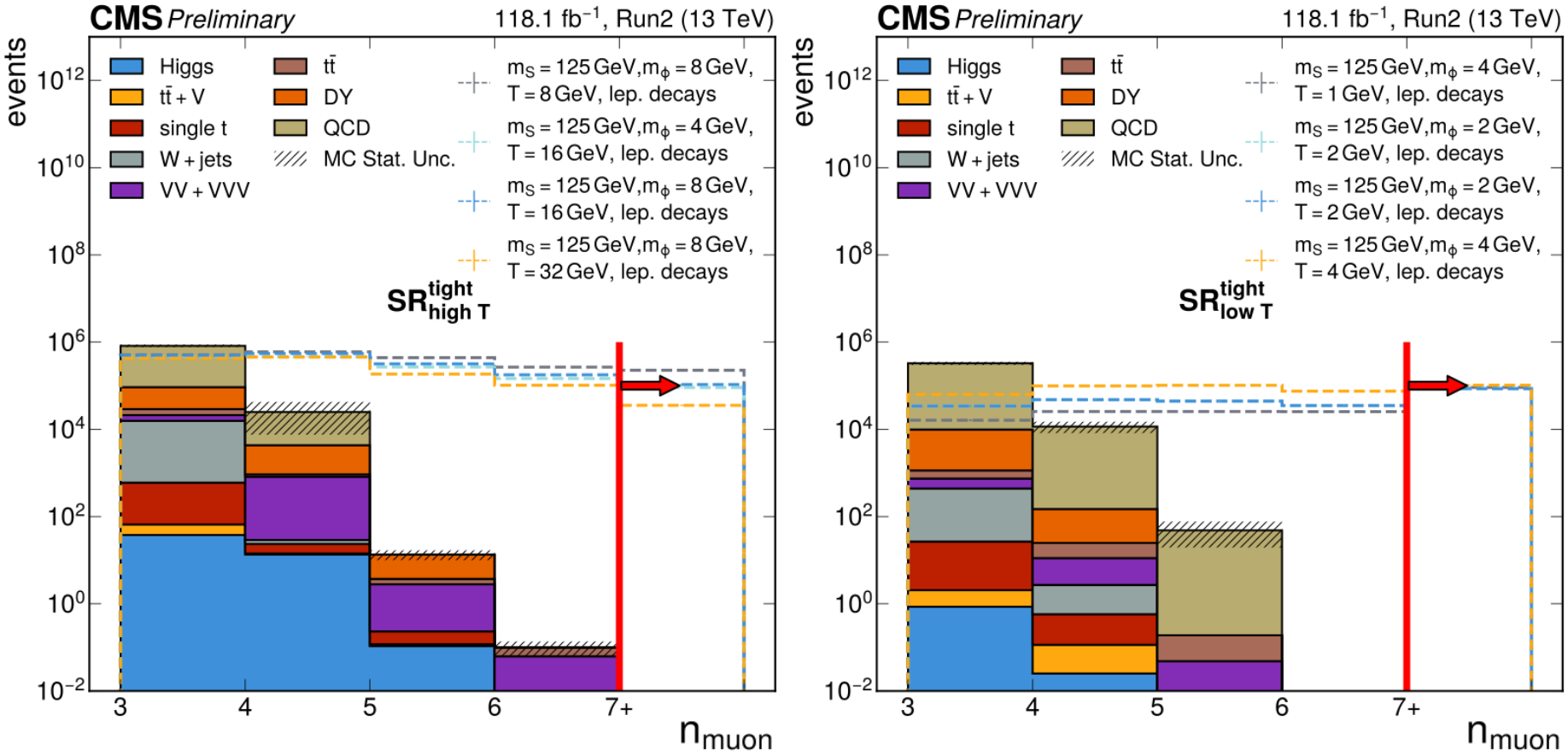

All MC processes have 0 yields in the discovery bins before the extrapolation.
The QCD and DY backgrounds have sudden drops to 0.

Background prediction

- MC bkg distributions in SRs have low statistics at high n_{muon} …
- Bkg muons come from meson decays (mostly B & D mesons).
- Smooth reduction is expected.
- Bkg estimation using data *not possible* because **all sidebands contain signal**.
- *Instead,* we utilize an
  → **extrapolation on the MC**
- Regions with good MC statistics can be used to derive it!

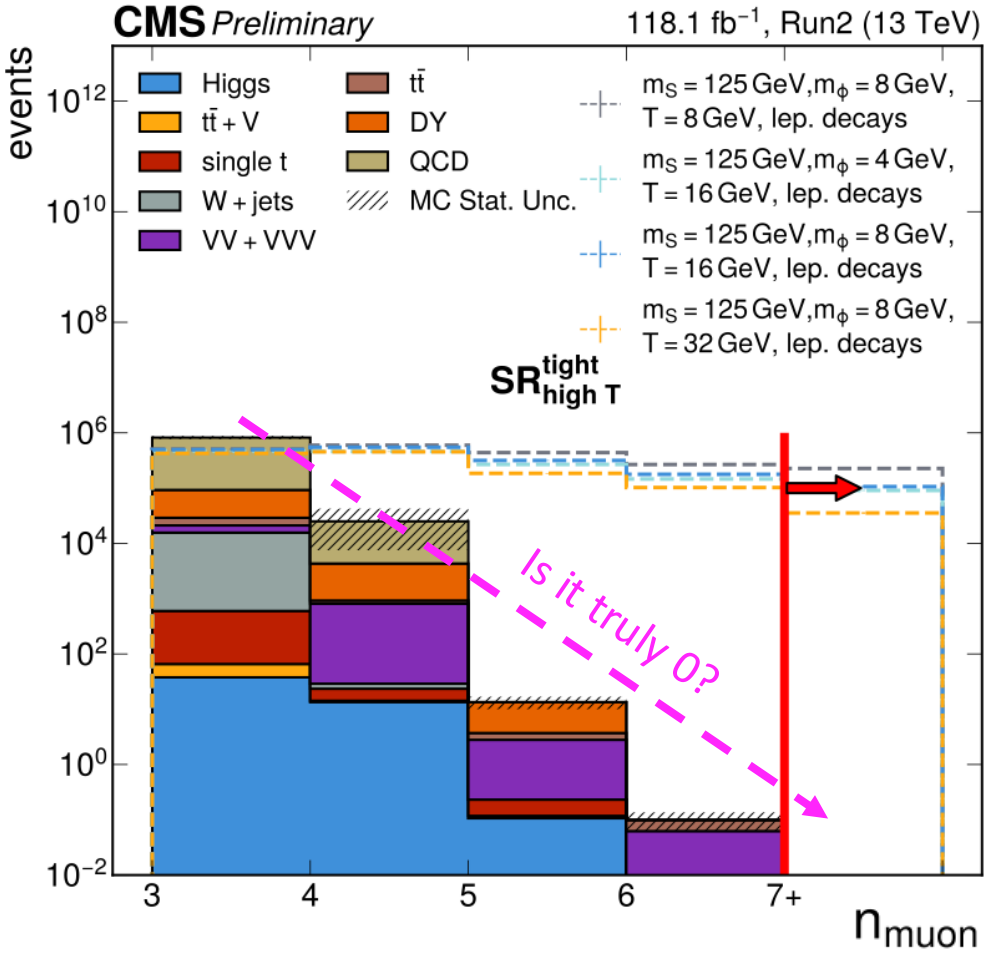

Background prediction

- Assumptions:
  1. the bkg in the SRs is assumed to follow a **power law**:
     $$f(n_{\text{muon}}) = A \cdot 10^{-B \cdot n_{muon}}$$
  2. the **slope** of the power law ($\log B$) is **the same** in the loose and tight regions.
- The loose region is populated with more events.
- Can be used to extract the slope of the power law function.
- In practice, a **simultaneous fit** is used for the two regions with:
  - **one shared slope parameter (B)** and
  - **two parameters for the normalizations (A_1, A_2)** of each region.
- The extrapolation is applied on QCD and DY MC since they are expected to be the leading sources of bkg.

Background strategy

- Background muons are either:
  - in QCD events *or*
  - overlaid on top of prompt muons from the hard process (e.g., DY).
- **MC statistics** for QCD are **not sufficient** for bkg estimation.
- One would normally use **data-based methods** for bkg estimation…
- *… however*, our **signal contaminates all side regions** because of high cross section and triggering efficiency.
- Focusing on **regions with very low total bkg (<1 event)** and using MC with an **extrapolation** for bkg prediction.
- **Non-negligible uncertainty** of the bkg prediction → **not as critical** *if* $B \ll 1$.

Common slope between tight and loose

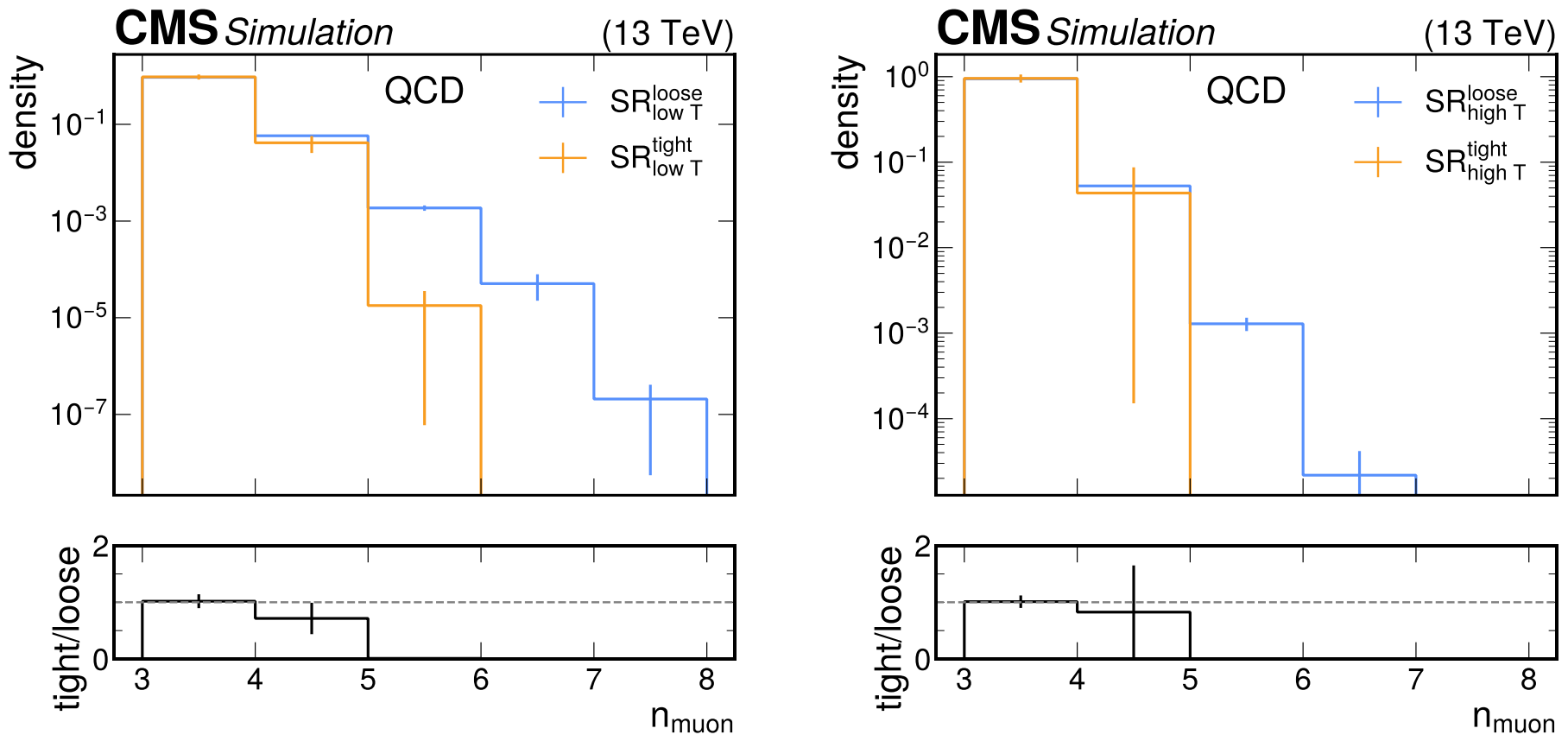

- Demonstrating the n_{muon} distribution densities for tight and loose regions for QCD.
- The statistics in the tight regions don't help but the assumption that they share a common slope looks reasonable.

Validation

- The method is validated using a **QCD-rich** and **signal-free** region.
- Using a **validation region (VR)**, split into **tight** and **loose regions**, to demonstrate the extrapolation.
- The VR is designed so that:
  1. is signal-free (checked all 289 signal points for contamination),
  2. has enough statistics, especially in the high n_{muon} bins.
- Loose cuts:
  - Muon pt > 5 GeV
  - Muon IP3D > 0.01 cm
  - Muon iso > 0.2
  - Lower limit on OS dimuon mass (> 10 GeV)
- Tight cuts (on top of loose cuts):
  - Muon IP3D > 0.02 cm
  - Muon iso > 0.4

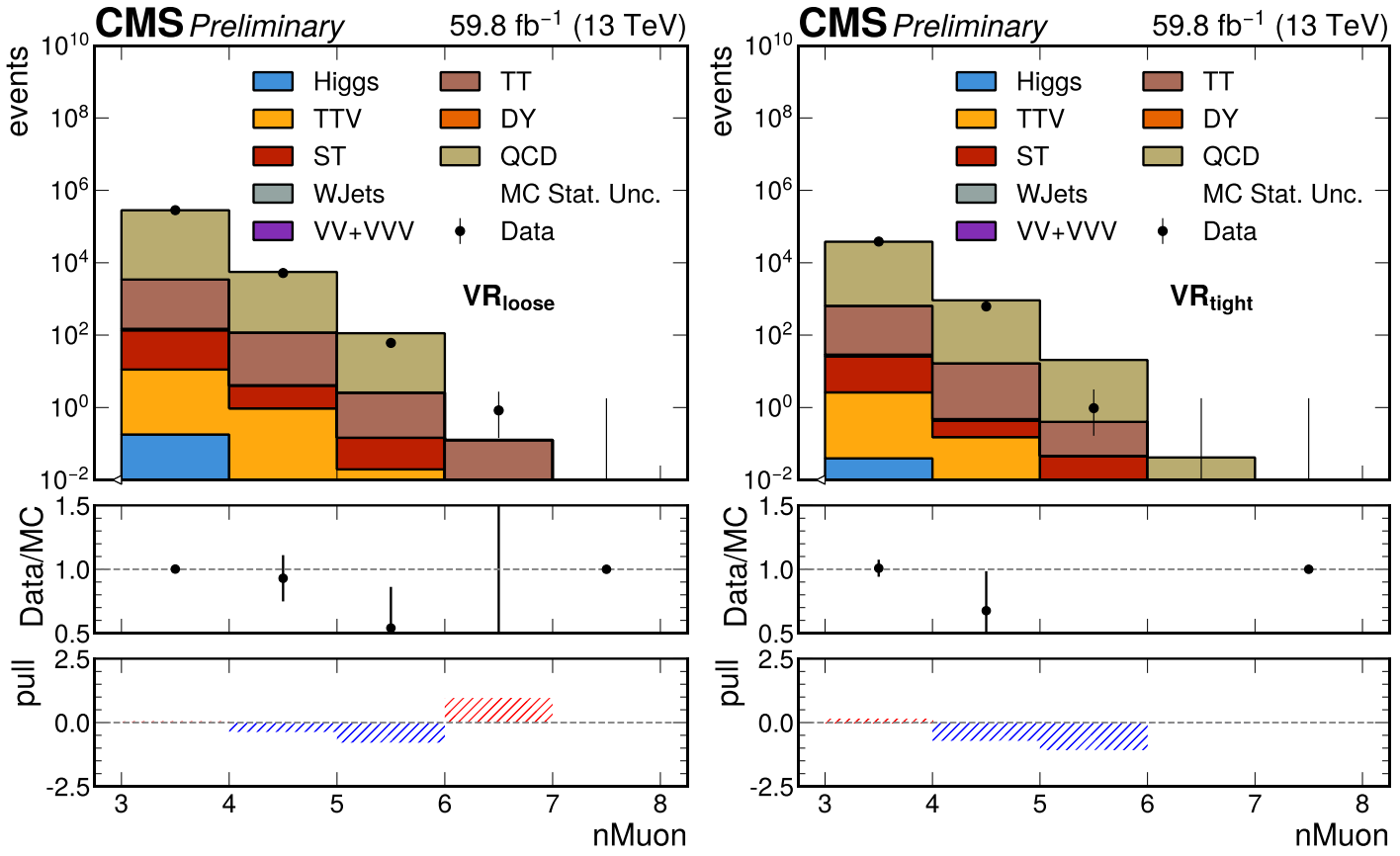

Validation – Fits

- Performing the fit *both* on QCD MC and data.
- Checking for **well-behaved & consistent fits**.
- In the next slides, will apply the method in the way that is performed in the SRs:
  - ✓ extrapolation on QCD MC and then comparison with the distribution in data.
- The extrapolation **improves** significantly the **agreement** between MC and data.

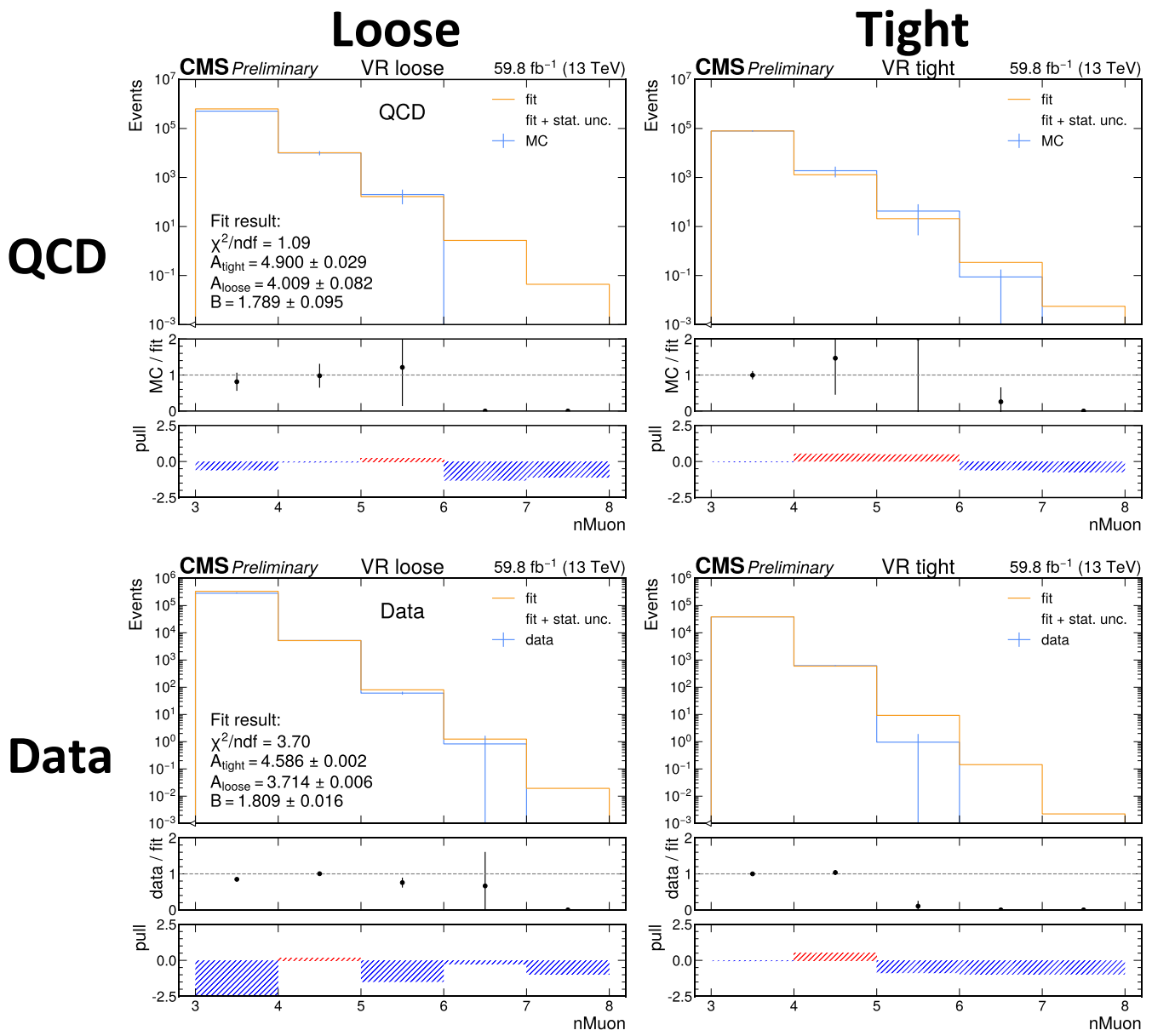

Validation

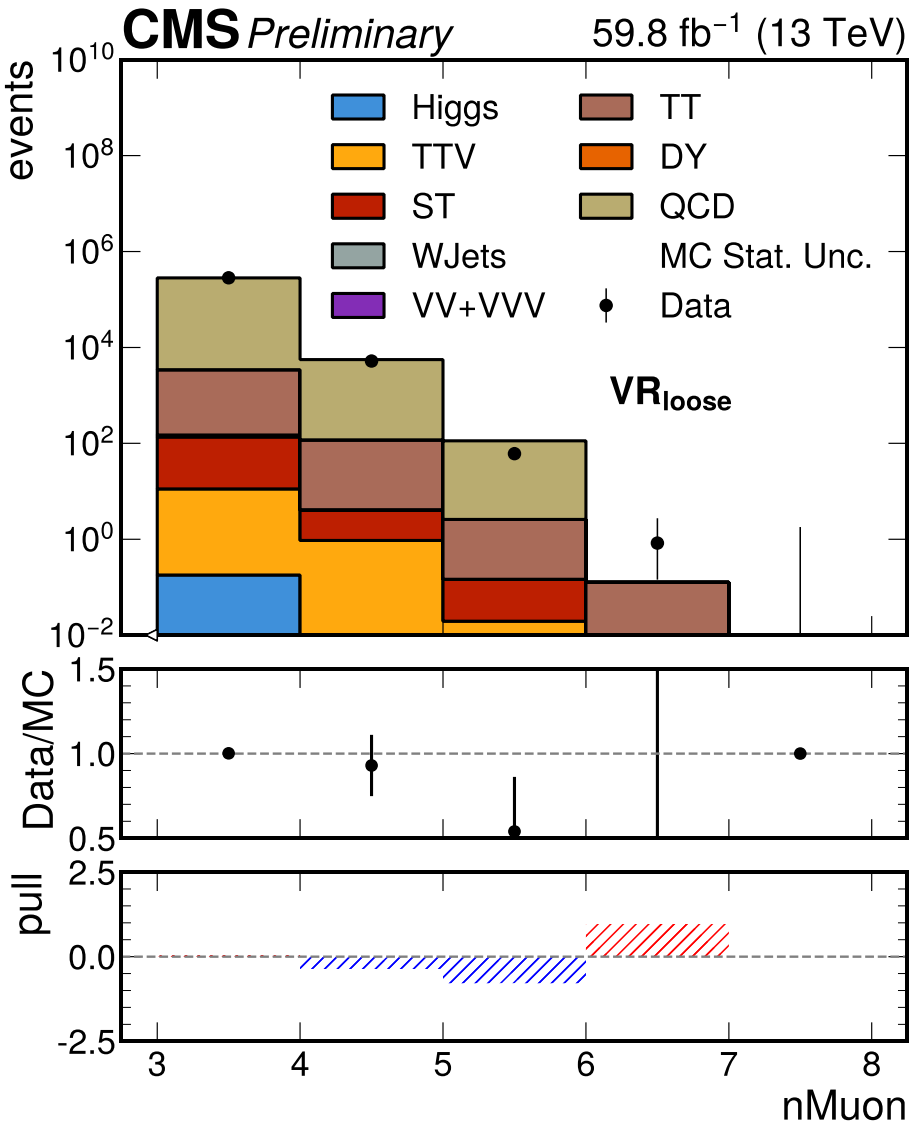
CMS Preliminary
59.8 fb^{-1} (13 TeV)
events
Higgs
TTV
ST
WJets
VV+VVV
TT
DY
QCD
MC Stat. Unc.
Data
VR$_{loose}$
Data/MC
pull
nMuon

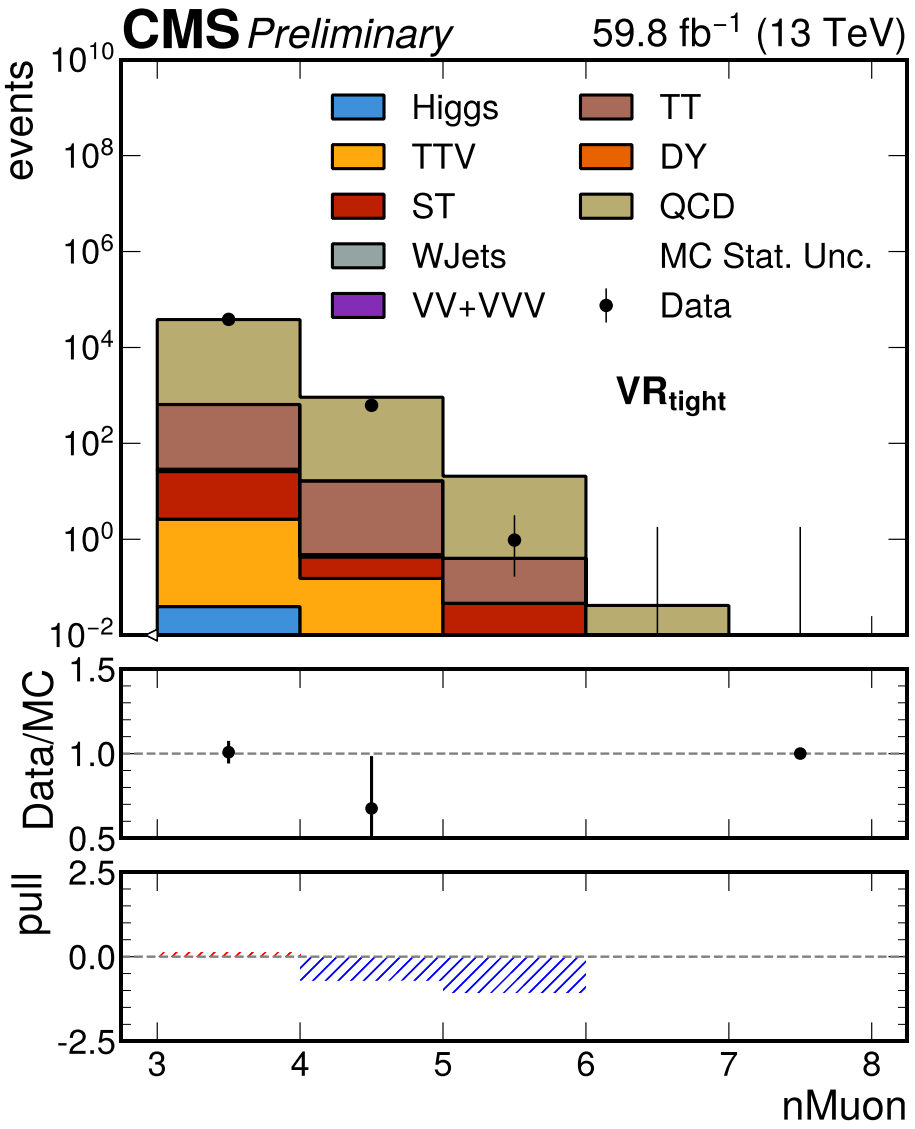
CMS Preliminary
59.8 fb^{-1} (13 TeV)
events
Higgs
TTV
ST
WJets
VV+VVV
TT
DY
QCD
MC Stat. Unc.
Data
VR$_{tight}$
Data/MC
pull
nMuon

Validation

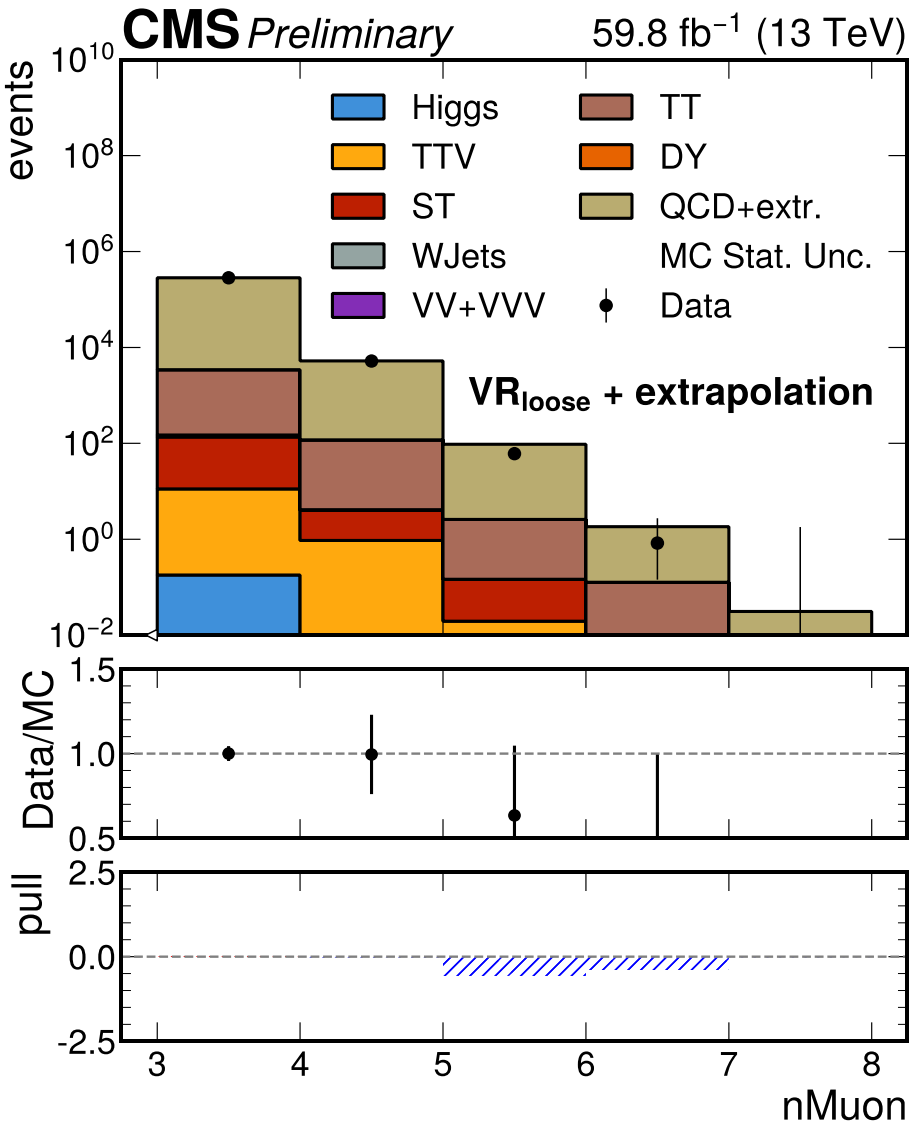
CMS Preliminary
59.8 fb^{-1} (13 TeV)
events
Higgs
TTV
ST
WJets
VV+VVV
TT
DY
QCD+extr.
MC Stat. Unc.
Data
VR$_{loose}$ + extrapolation
Data/MC
pull
nMuon

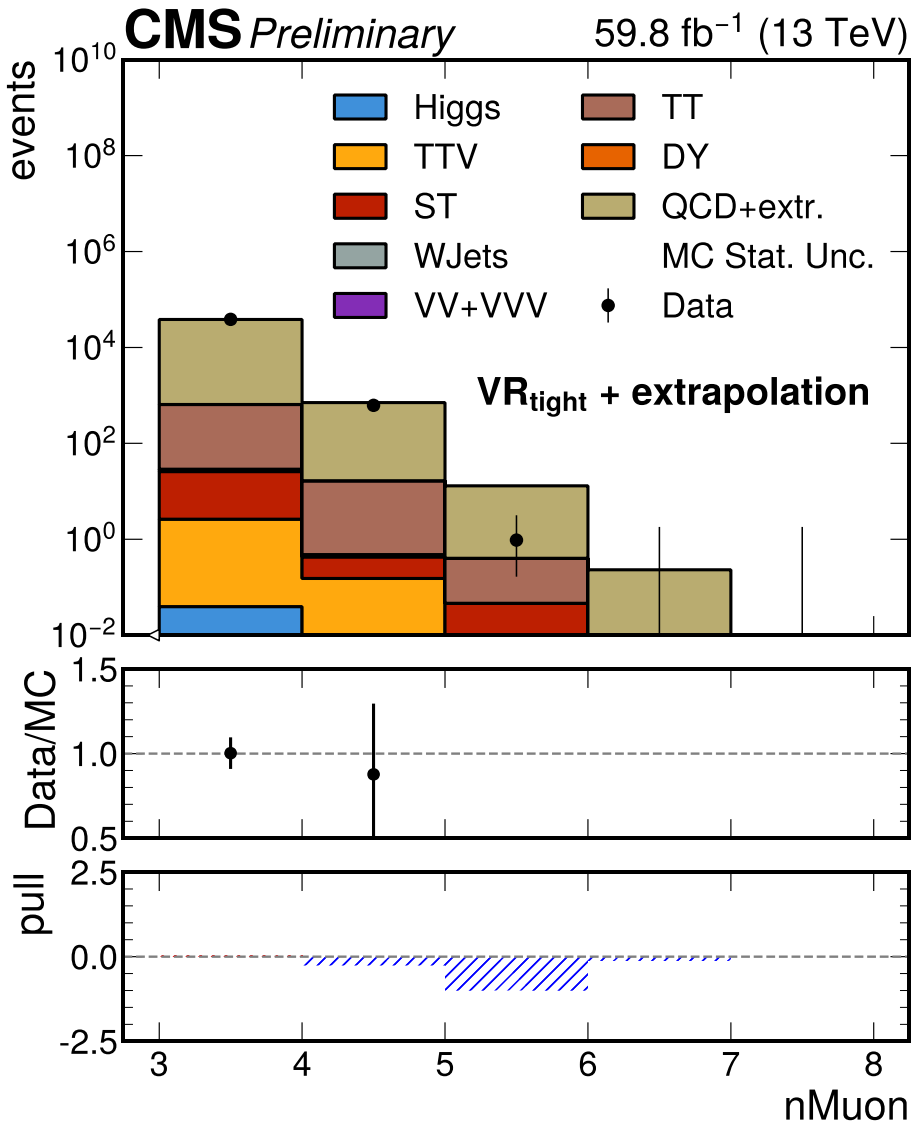
CMS Preliminary
59.8 fb^{-1} (13 TeV)
events
Higgs
TTV
ST
WJets
VV+VVV
TT
DY
QCD+extr.
MC Stat. Unc.
Data
VR$_{tight}$ + extrapolation
Data/MC
pull
nMuon

Common slope for DY MC

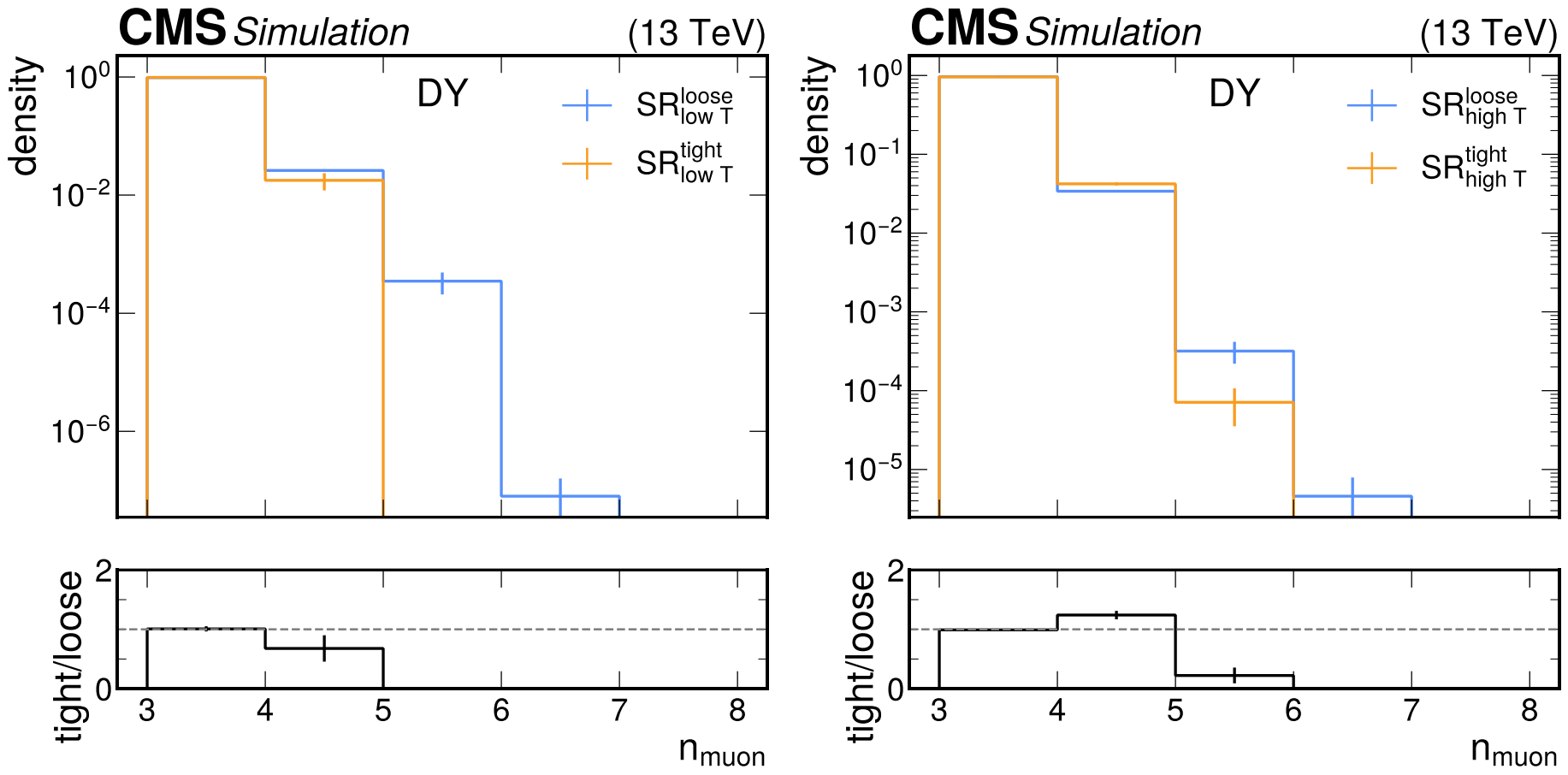

Fit for bkg extrapolation (DY)

Low temperature region

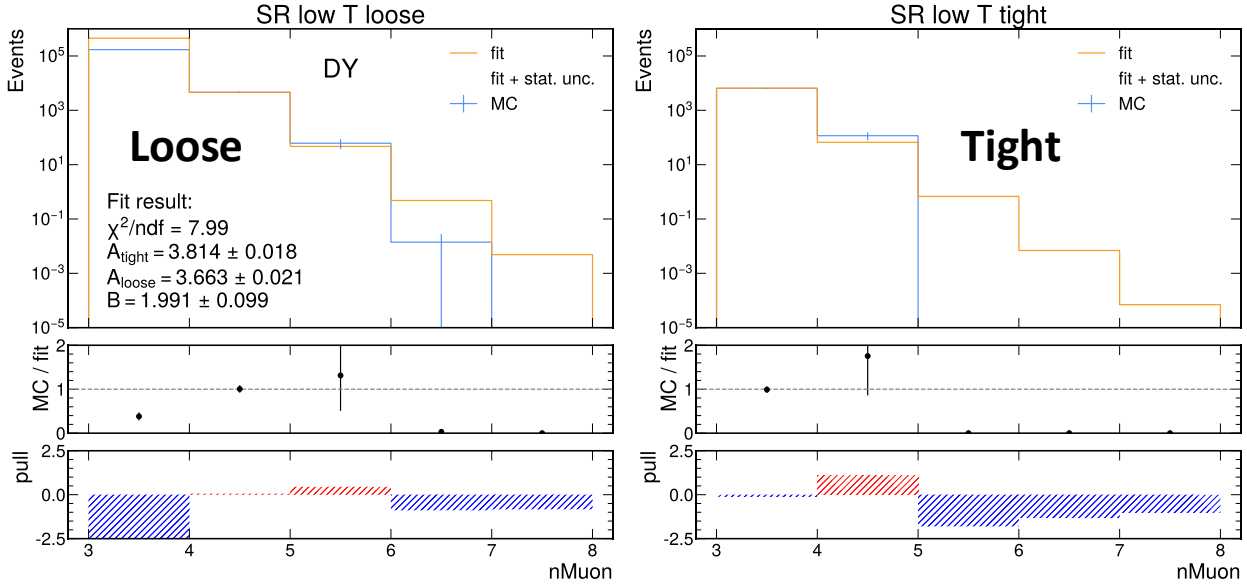

High temperature region

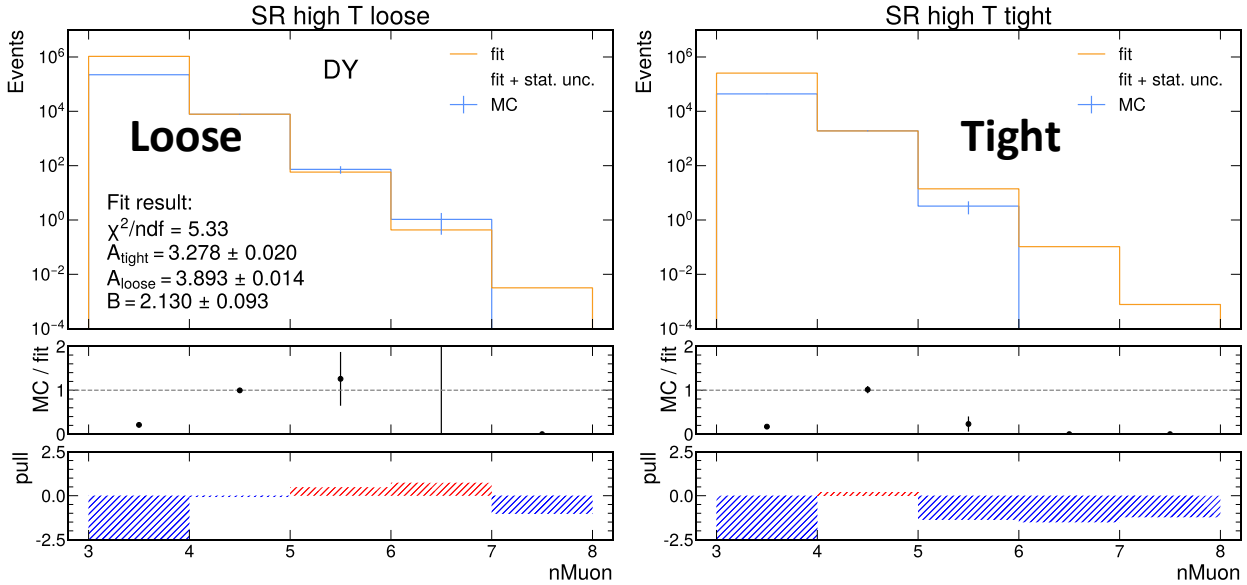

VR overlays

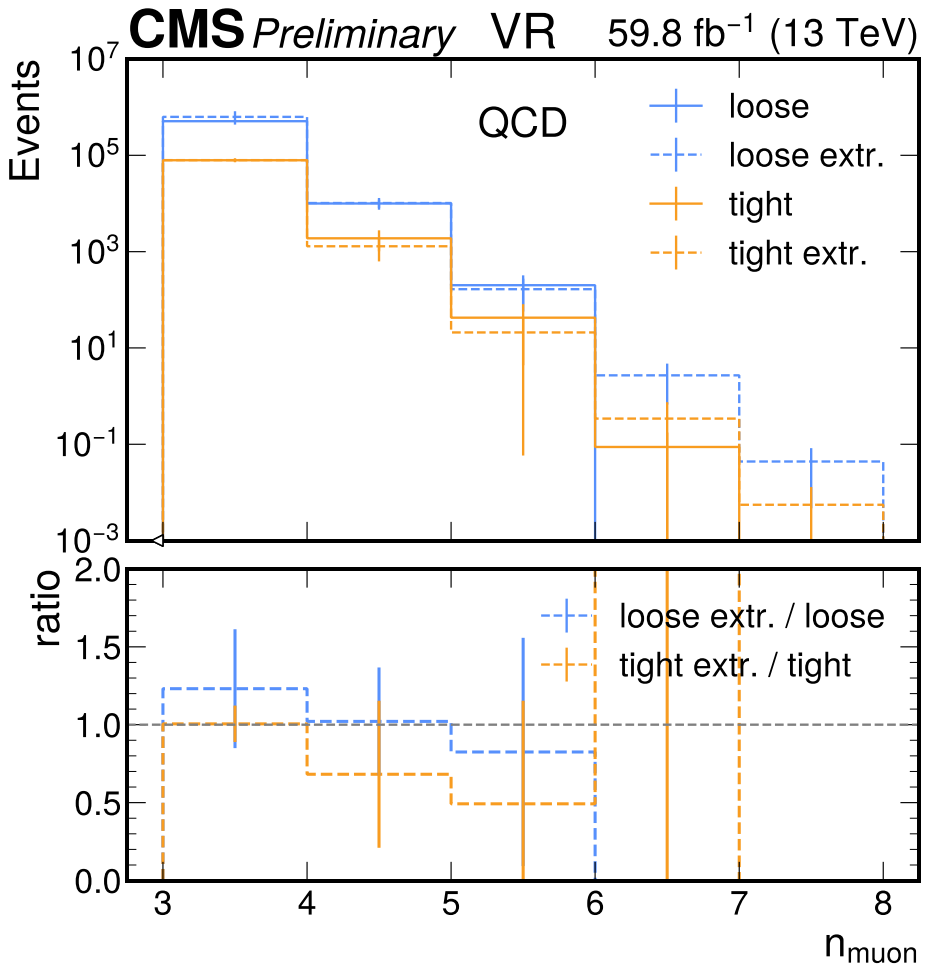

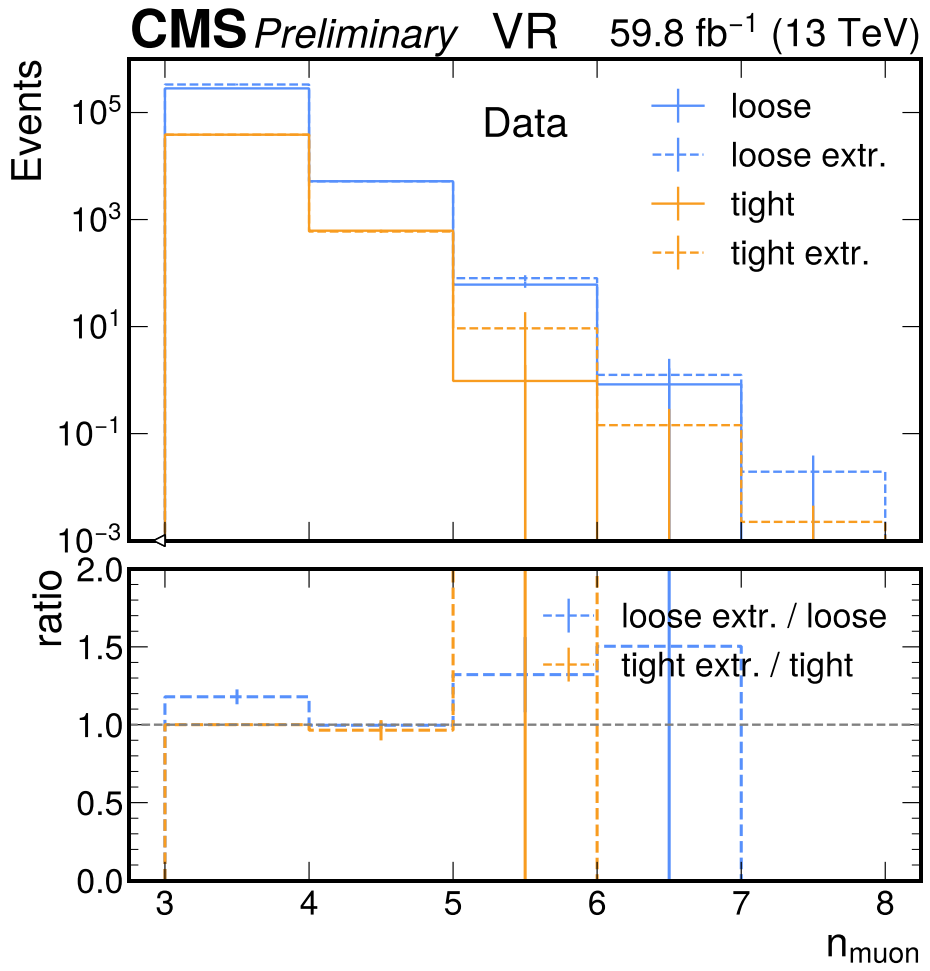

Extrapolation vs non extrapolation for loose & tight and for QCD and data.

SR overlays – QCD

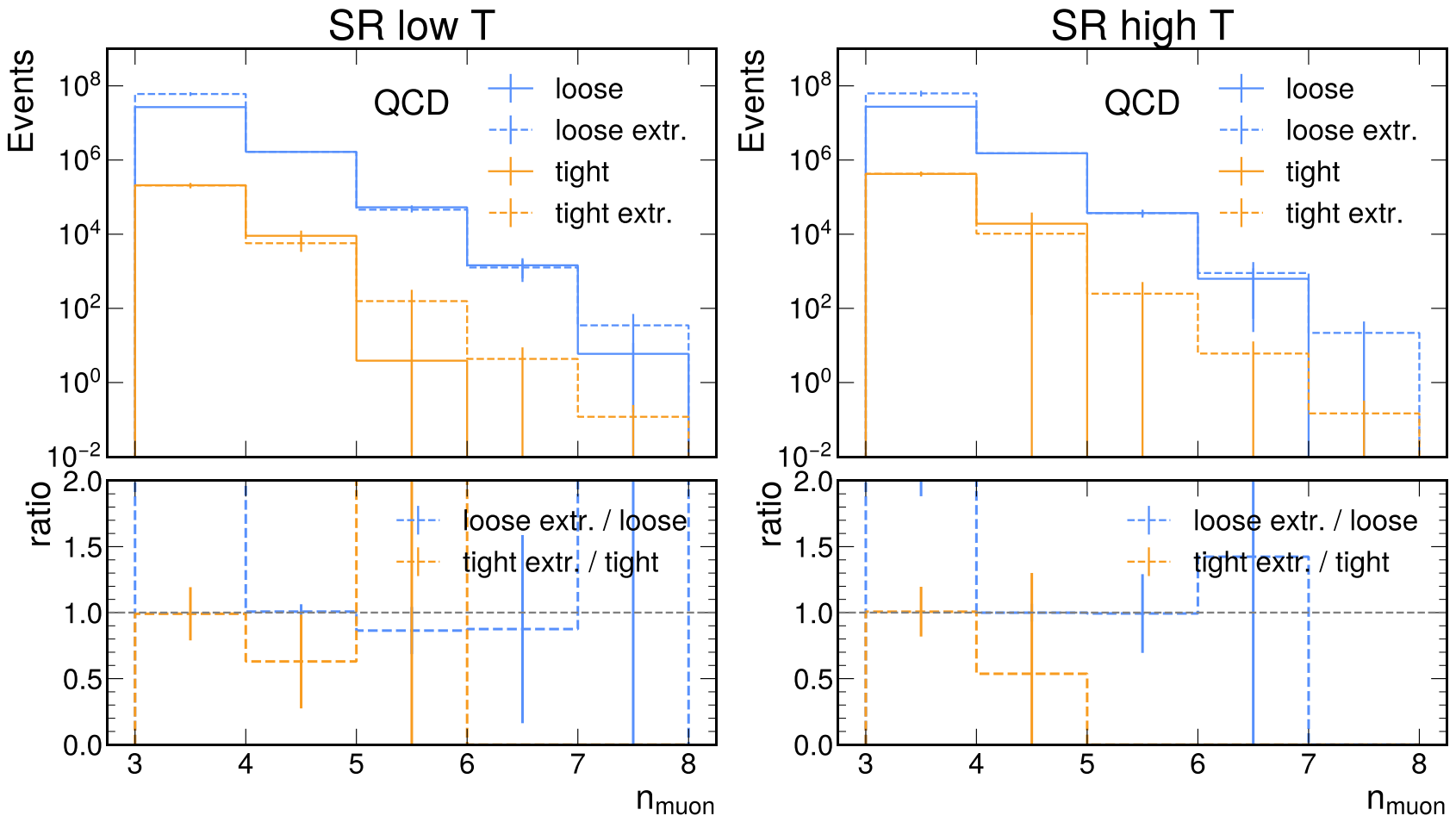

SR overlays – DY

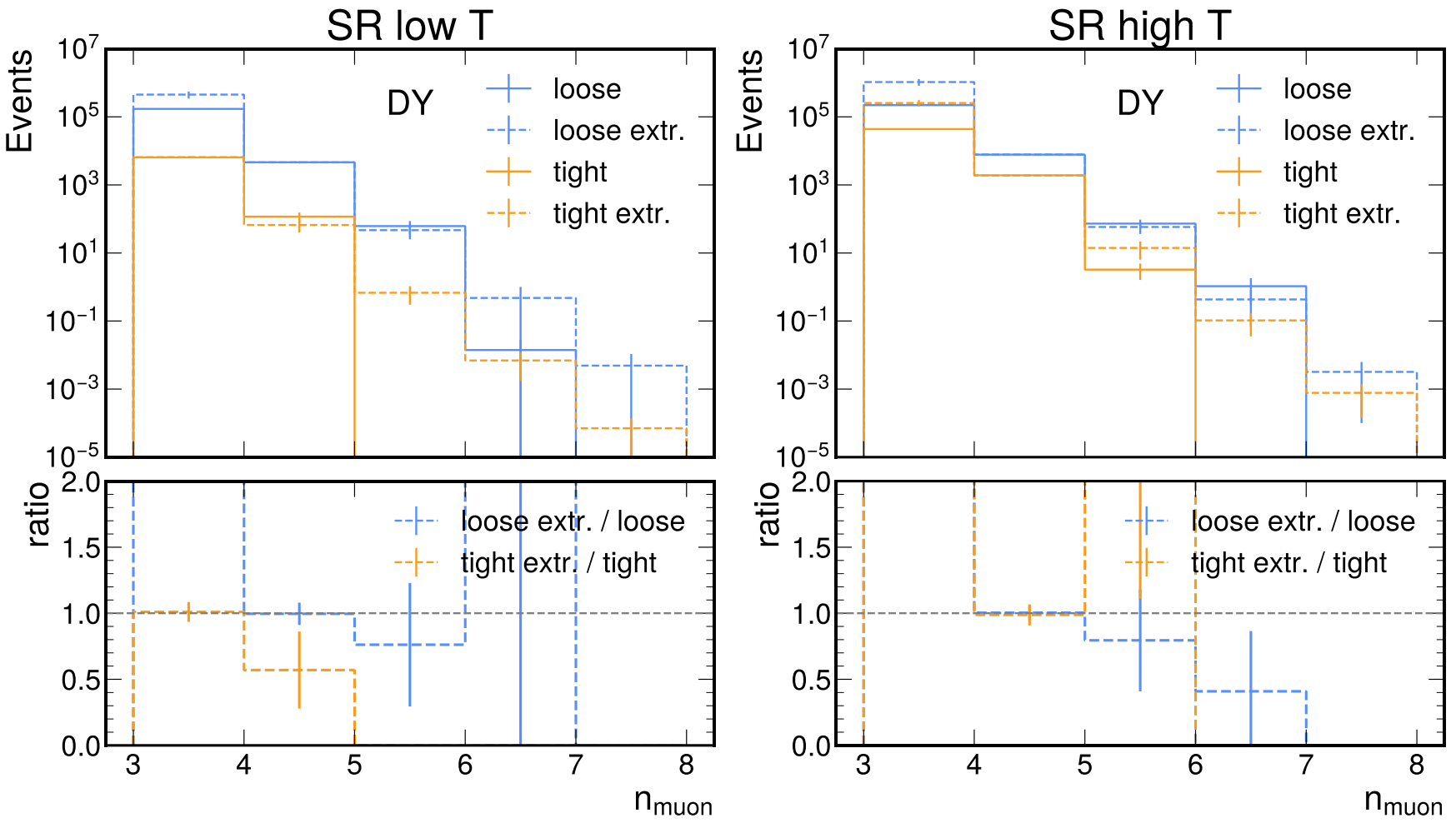

Choosing SRs

- The two SRs are not designed to be orthogonal.
- For each signal point, either one of them must be chosen.
- Since bkg is negligible in both, we decide using the higher signal yield.

SUEP model	$SR_{\text{high } T}$	$SR_{\text{low } T}$
$m_S = 500, m_\phi = 8, T = 16$, leptonic	**265207 ± 1230**	7562 ± 210
$m_S = 600, m_\phi = 8, T = 16$, leptonic	**142952 ± 642**	3116 ± 96
$m_S = 800, m_\phi = 8, T = 16$, leptonic	**42851 ± 187**	503 ± 20
$m_S = 1000, m_\phi = 8, T = 16$, leptonic	**14239 ± 82**	77.0 ± 6.1
$m_S = 125, m_\phi = 8, T = 16$, hadronic	**3317 ± 372**	187 ± 75

SUEP model	$SR_{\text{high } T}$	$SR_{\text{low } T}$
$m_S = 800, m_\phi = 1.4, T = 5.6$, hadronic	194 ± 12	**16259 ± 107**
$m_S = 1000, m_\phi = 1.4, T = 5.6$, hadronic	72.6 ± 4.7	**7433 ± 51**
$m_S = 125, m_\phi = 2, T = 2$, leptonic	20565 ± 975	**170865 ± 2850**
$m_S = 200, m_\phi = 2, T = 2$, leptonic	29994 ± 738	**160660 ± 1738**
$m_S = 300, m_\phi = 2, T = 2$, leptonic	32987 ± 586	**167138 ± 1359**

Bold color indicates larger total yield. This SR is chosen for the signal point.

Maximum likelihood fit

Likelihood function:

$$\mathcal{L}(data; r, \vec{\nu}) = \prod_{\text{years}} \prod_{\text{regions}} \prod_{\text{bins}} \text{Poiss}\left(n_{obs} \middle| n_{exp}(r, \vec{\nu})\right) \prod_{\text{nuisances}} p_e(\nu_e | \tilde{\nu}_e)$$

r: signal strength parameter

$\vec{\nu}$: nuisance parameters

Nuisances:

- strength of up & down variations of shape uncertainties
- strength of scaling uncertainties (constrained)
- free parameters
- Barlow-Beeston-lite nuisances for true MC yields

Likelihood ratio:

$$\Lambda(r) = \frac{\mathcal{L}\left(data; r, \hat{\hat{\vec{\nu}}}(r)\right)}{\mathcal{L}\left(data; \hat{r}, \hat{\hat{\vec{\nu}}}\right)}$$

Find maximum likelihood estimates $\hat{r}$ and $\hat{\hat{\vec{\nu}}}$, and then calculate likelihood ratio with profiled nuisances.

Test statistic:

$$t_r = -2 \ln \Lambda(r)$$

Upper limits:

$$CL_s = \frac{CL_{s+b}}{CL_b} > a$$

→ **Asymptotic approximation**
Cowan-Cranmer-Gross-Vitells.
arxiv:1007.1727

Corrections & Systematic uncertainties

- **Corrections**:
  - ✓L1 prefire
  - ✓PU reweighting

  } per event weights
  - ✓Muon scale factors for RECO, ID, ISO eff. → per muon weights
- **Systematic uncertainties**:
  - Theoretical uncertainties:
    - ✓Matrix element PDF uncertainty
    - ✓Matrix element scale variations (μ_R & μ_F)
    - ✓Parton shower variations (ISR & FSR) (not for QCD… 😢)
  - Experimental uncertainties:
    - ✓Luminosity (only scaling uncertainty)
    - ✓L1 prefire uncertainty
    - ✓PU reweighting uncertainty
    - ✓Muon scale factor uncertainty
    - ✓Track killing method for tracking efficiency.

All systematics have shape effect (except for lumi unc.)

⬇

Make up & down templates

⬇

For SRs, repeat extrapolation on up & down templates.

Fitting to data

Prefit

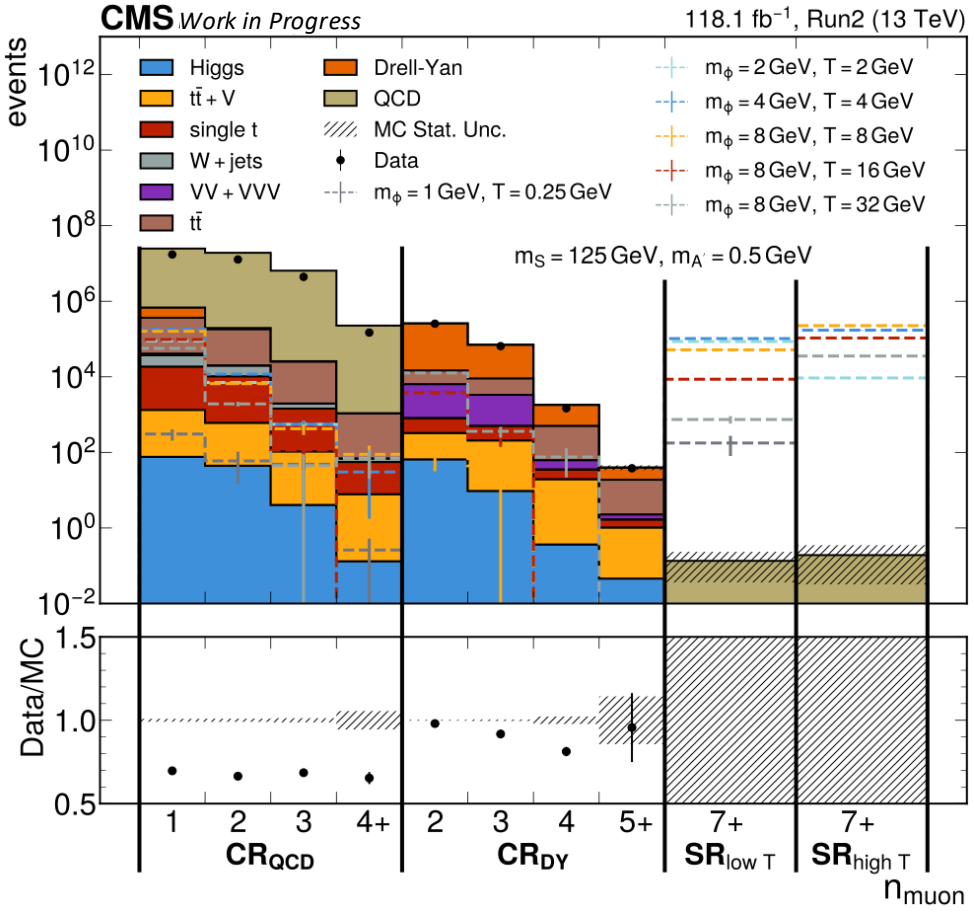

Postfit

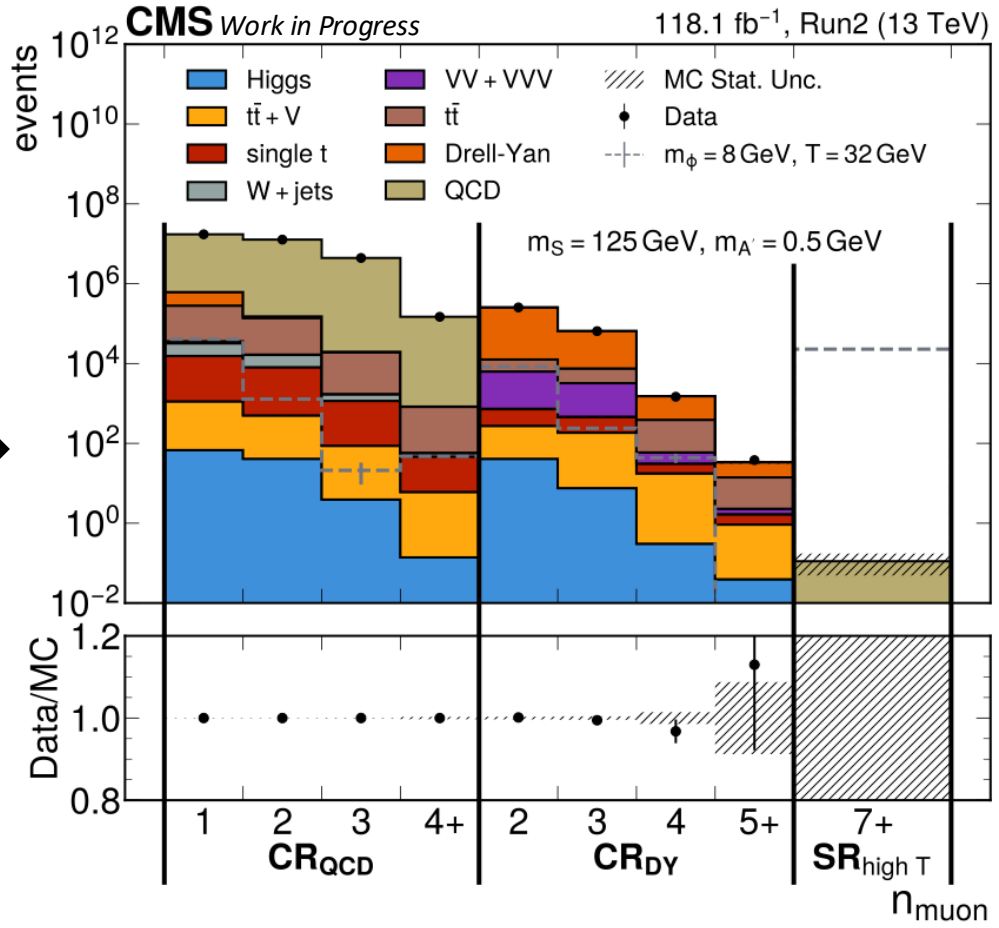

Reminder: Fitting separately each signal model and only using its corresponding SR.

That's why only one signal model & only SR$_{high\ T}$ are shown in the postfit plot.

*still blinded in the SR

95% CL upper limits

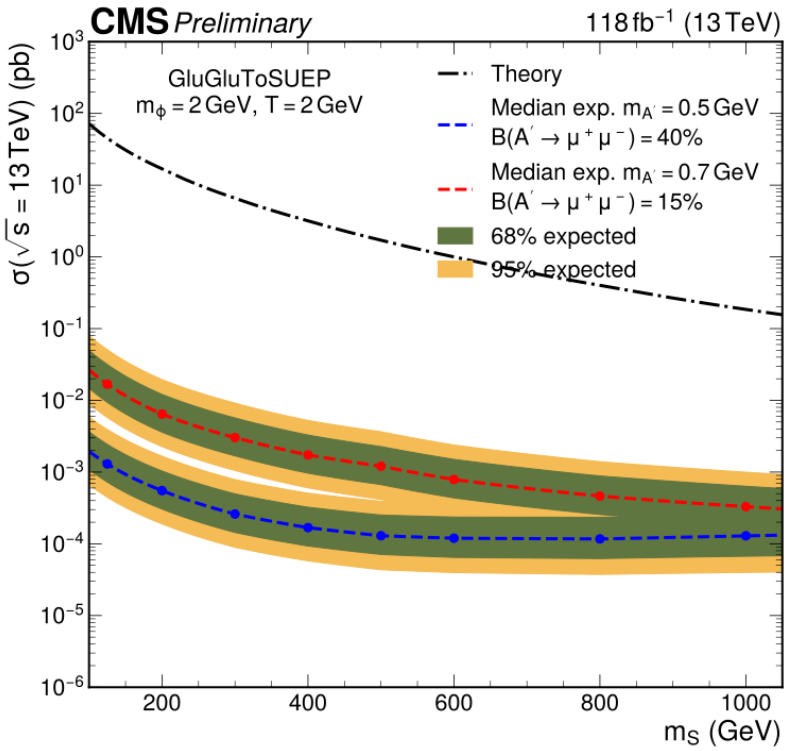

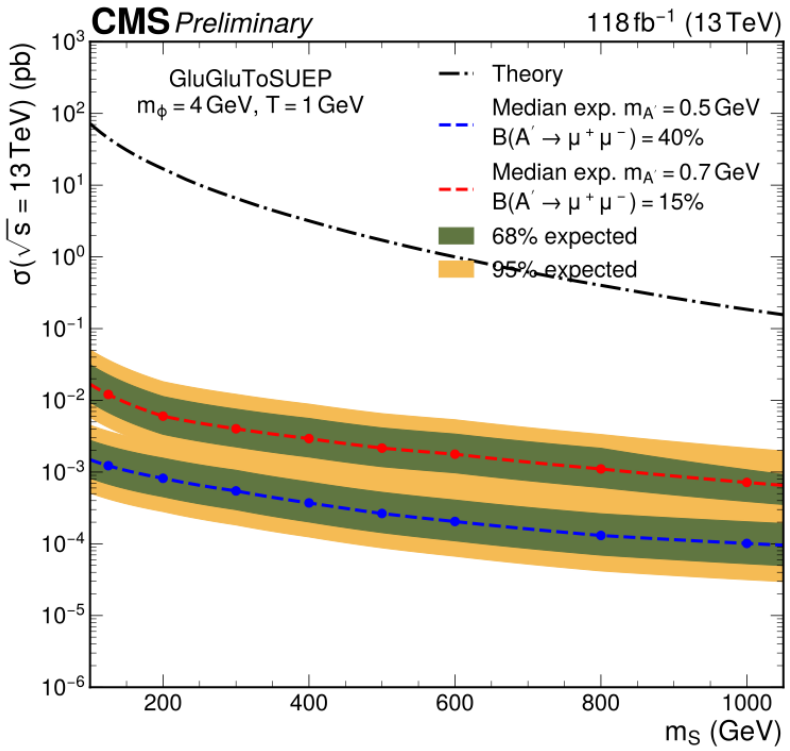

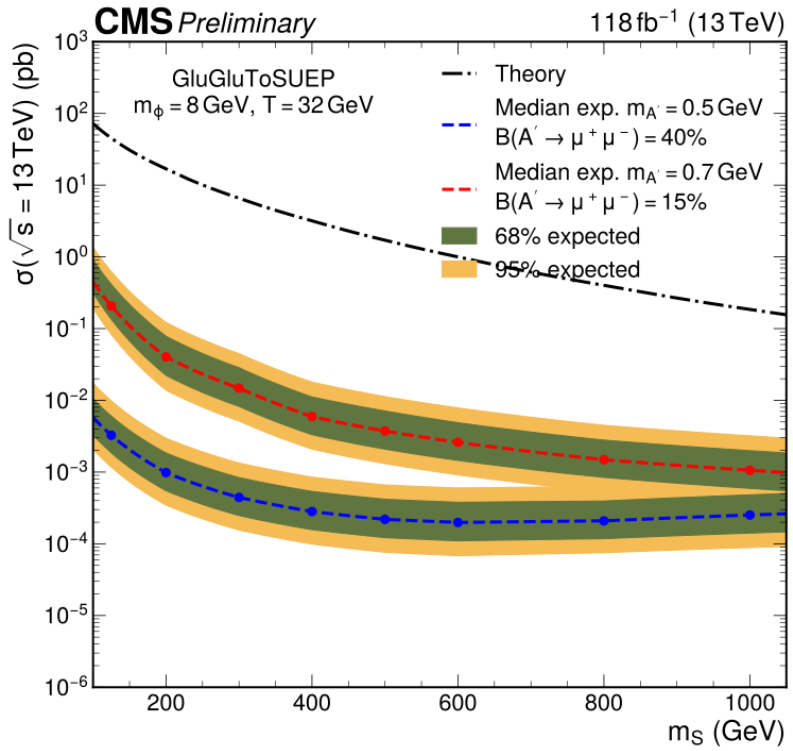

- **Very strong limits for entire m_S range. 3-4 orders of magnitude below theory σ.**
- Great improvement over existing CMS SUEP efforts for the **leptonic decay scenarios**.
- Existing searches cannot exclude most models with $T \geq 8$ GeV. We can exclude all these easily.
- Not trigger limited at low m_S.
- We don't have any of these problems!

Limits from offline & scouting

Screenshotted from paper for EXO-23-001:

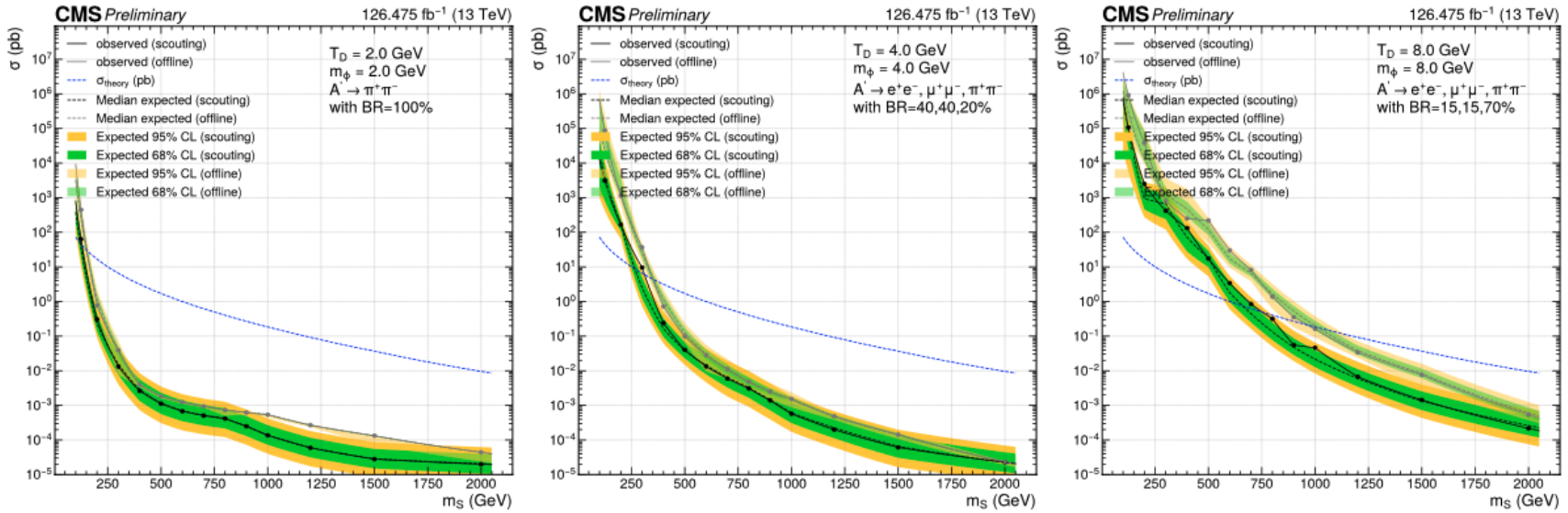

Figure 2: Expected and observed upper limits on the signal cross sections with respected to the mediator masses m_S this analysis with the data scouting strategy ("scouting") compared with the results of the offline analysis ("offline") [25]. Different values of the temperature, the dark hadron mass and dark photon mass are shown (left: $T_D = 2\,\text{GeV}$, $m_\phi = 2.0\,\text{GeV}$, $m_{A'} = 1\,\text{GeV}$; middle: $T_D = 4.0\,\text{GeV}$, $m_\phi = 4.0\,\text{GeV}$, $m_{A'} = 0.5\,\text{GeV}$; right: $T_D = 8.0\,\text{GeV}$, $m_\phi = 8.0\,\text{GeV}$, $m_{A'} = 0.7\,\text{GeV}$).

Limits from offline & scouting

Screenshotted from paper for EXO-23-001:

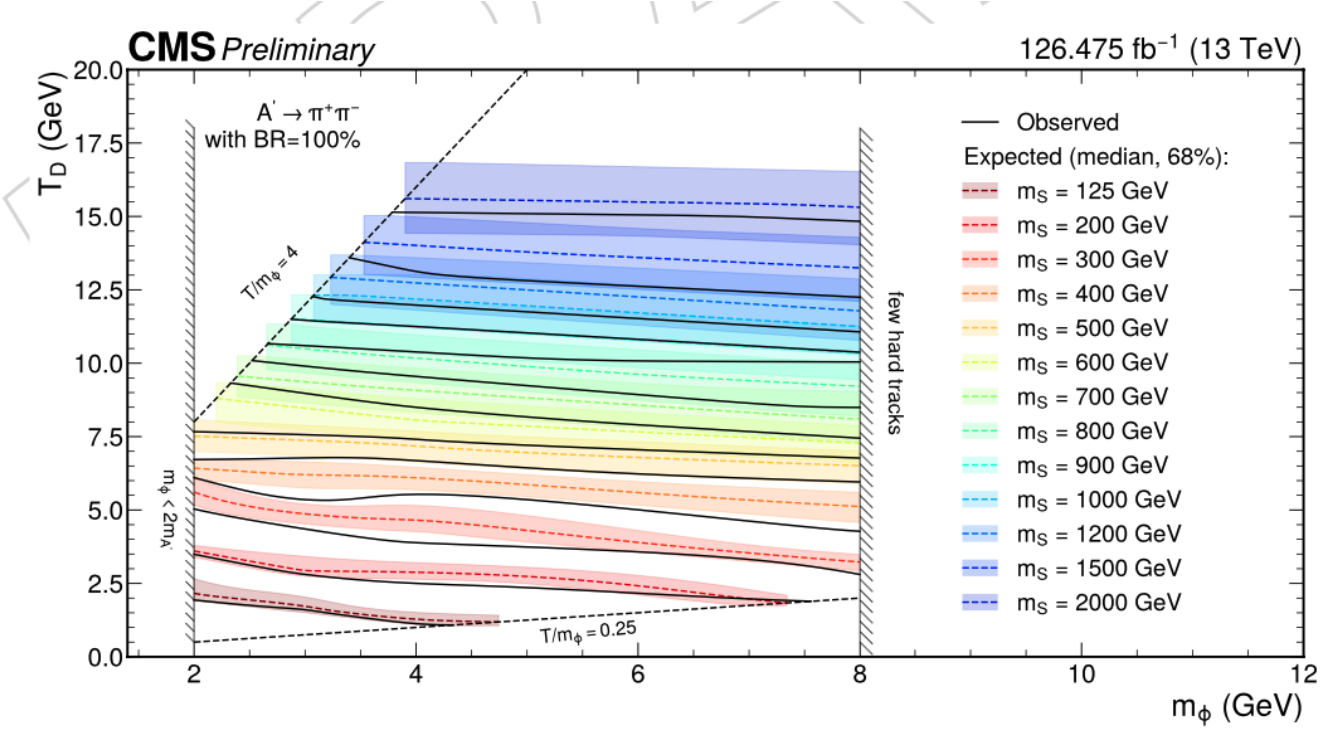

Figure 3: Expected and observed exclusions of signal parameters assuming the nominal S cross sections for the $m_{A'} = 1\,\text{GeV}$ signals with full hadronic decays as a function of T_D and m_ϕ for benchmark m_S models. The parameter space below the lines are excluded.

Phase-2 upgrades

- Working on QC testing of the HGCAL tileboards at Maryland over the last two months.
- Important and fun work!
- I would like to continue working on Phase-2 upgrade-related projects.
- Crucial to get the experiment ready in time for Run 4.